2

Electron Transfer Reactions With and Without Ion Transfer

A. J. Appleby

238 Wisenbaker Engineering Research Center
Texas A&M University, College Station, TX 77843-3402

I. INTRODUCTION

The most frequent molecular model used for electrolytic electron transfer since the 1930s is similar to the Franck-Condon (FC) principle[1] for spectral electronic transitions. Kinetic activation occurs until a rapid radiationless electronic transition becomes possible. Following FC and the equivalent Born-Oppenheimer approximation,[2] it is assumed that classical nuclear motion during the electronic transition is slow enough to be negligible. In condensed media, the potential energy of a reactant involves an extended number of nuclei and many degrees of freedom. To reconcile the energy requirements in condensed media with electron transfer has resulted in many ingenious mechanistic proposals. Charged molecules surrounded by rather tightly-bound solvent dipoles have potential energies different from vacuum values because of the presence of the surrounding dielectric solvent. These tightly-bound "Inner Sphere" solvent dipoles may or may not be free to move before rapid electron transfer of FC type.

Modern Aspects of Electrochemistry, Number 38, edited by B. E. Conway *et al.* Kluwer Academic/Plenum Publishers, New York, 2005.

Since the 1950s, the surrounding dielectric solvent has usually been considered to determine kinetics because of its assumed immobility during rapid electron transfer. Efforts to summarize reaction rate evidence in the 1970s[3,4] and more recently[5,6] have failed to leave the theory in a satisfactory state.

This chapter reviews electron transfer models, develops molecular models of the solvent surrounding ions of different types to provide a more complete picture of the orientational changes taking place, especially in cases where electron transfer is combined with atom transfer, where assembly of a solvation sphere is required during the process. Finally, the activation energies of some charge-transfer processes are given.

II. THE FRANCK-CONDON PRINCIPLE AND ELECTRON TRANSFER

1. Historical Development

The electrochemical FC principle can be traced to 1931 papers by Franck and Haber on photochemical electron transfer[7] and by Gurney on electrochemical hydrogen evolution.[8] Landau's publication on gaseous electron transfer followed in 1932.[9] The electron makes a single, rapid transition from a donor to an acceptor state in which all heavy particle motions are frozen in time. The electronic transition may be adiabatic, i.e., with a transition probability of unity with no tunneling through an energy barrier, or non-adiabatic, i.e., with tunneling. Transitions may take place with or without radiation or photon absorption. Gurney's model[8] for proton dissociation from the H_3O^+ ion[10] with simultaneous electron acceptance from a metal energy level introduced the concept, accounting for the overpotential[11], the Tafel equation[12] and its Butler-Volmer extension,[13,14] then recently confirmed by Bowden.[15] The H_3O^+ ion[10] was formalized as the oxonium or hydronium ion by Bernal and Fowler.[16]

Gurney[8] used Hund's molecular orbital model[10] for H_3O^+ to deduce that its dissociation energy was 8.3 eV, close to the 7.9 eV value estimated using a thermochemical cycle.[17] A thermally activated H_3O^+ ion[10] with one bond randomly stretched to a higher potential energy state was postulated to accept an electron from a metal electrode level and spontaneously "fly apart" (sic) to $H_2O + H$, since the force between a neutral hydrogen atom and a water molecule would always be

repulsive. The final state products would be in the same nuclear FC configuration as that of the activated initial state. For radiationless electron transfer, the potential energy difference between the initial and final states must be equal to that of the electron in the metal level. The probability of a given transition is given by the product of the (inverted) Fermi-Dirac distribution for electrons in the electrode multiplied by both the Boltzmann distribution for activated H_3O^+ ions and the electron tunneling probability through any energy barrier which may be present[18,19] Gurney linked the increased potential energy of the activated state of H_3O^+ (ΔU) to the energy difference between this excited state and that of the products in the same configuration (ΔE) by supposing that the potential energy-distance terms for the initial and final states were broadly linear, with similar positive and negative slopes for reactant bond-stretching and for product repulsion. Then $\Delta U \approx 0.5(\Delta E - E_o)$, where E_o is equal to the potential energy difference between the ground states of the reactants and products in the same nuclear configuration, giving an expression containing only the metal electron energy level. Integration over all metal energy levels gives a rate $\propto$ exp –0.5E/RT, where E is the reactant ground state energy. Gurney thereby accounted for what was later called the symmetry factor, approximately 0.5. The activation energy is therefore represented by the energy to reach the crossing point between the energy-distance curves for reactants and the products, after the difference between their absolute energies is removed by subtracting the potential energy of reaction. Bowden's earlier theory[15] supposed that adsorbed dipoles of a certain critical energy carrying a partial charge were laid down on the electrode surface. The Boltzmann distribution then gave an exponential expression between rate and voltage or overpotential, with a fractional term because of the partial charge. The first excited level for the proton vibration lies at +16.2kT[17] above the +24.3kT ground state for the symmetrical three-dimensional oscillator at 298 K, so in the absence of other interactions, H_2O–H^+ bond-stretching is very improbable. The ground state of the H_3O^+ ion must therefore carried on a classical thermally-excited translational-vibrational subsystem of neighboring water molecules, so the classical energy of the entire solvated H_3O^+ ion must be the excited state.

Later, Gurney pointed out the irreversibility of his model, since the transfer of electrons from hydrogen atoms to metal levels is improbable.[20] He also considered metal deposition[21] using Morse-function energy-distance diagrams for the reactants and products, so that the reaction energy pathway may be represented by "joining

together the curves" on their repulsive sides, giving a low barrier between reactants and products. This is analogous to the early Eyring and Polanyi reaction energy barriers derived from Morse functions,[22] which were followed by the 1935 Eyring absolute rate expression,[23] following Herzfeld.[24] In 1935, Horiuti and Polanyi considered the activation energy barrier for adsorbed atomic hydrogen to be the crossing point of the reactant and product energy states.[25] Butler[26] extended Gurney's 1931 theory to adsorbed hydrogen, implying that the electron makes an instantaneous FC transition, i.e., no time is allowed to form a true transition state.

Bates and Massey[27] extended Landau's work on gaseous systems in 1943. In 1952, Platzmann and Franck[28] applied similar concepts to the spectra of halide ions in solution. Randles[29] and Libby[30] respectively applied the FC principle to electrochemical reactions and homogeneous electron transfer between isotopic ions. Libby used the hydrogen molecule ion as a model, because its vacuum energy levels were known. He stressed that the FC principle would apply, since the velocity ratio for water molecule and electron motion would approximate the square root of their mass ratio, i.e., 200. Libby also introduced a "catalysis" concept for FC electron transfer by "complexing the exchanging ions in such a way that the complexes are symmetrical providing their geometries are identical to within the vibration amplitude involved in zero point motion." In other words, electron transfer is more likely if the initial and final state structures are identical. He considered that the electron wave function could only effectively penetrate the coordination shell of the ion if two reacting ions were bridged by an ion of opposite charge on closest approach. Assuming that the classical Born changing equation[31] could be applied to the ion energy, then the difference in free energy between the z and z + 1 states would be:

$$\Delta u = -[e^2z^2/2r\varepsilon_o - e^2(z+1)^2/2r\varepsilon_o] = e^2(2z+1)/2r\varepsilon_o \qquad (1)$$

where e is the electronic charge, ε_o is the static dielectric constant of the medium and r is the ion radius in both the initial and final states, following the FC principle. This expression would lead to a small energy barrier because of the high value of ε_o for water, so he postulated a much smaller ε_o value close to an ion. He also suggested that the effective dielectric constant to be used for high-frequency electron motion would be the optical infrared value, i.e., the square of the IR refractive index n, or about 1.8.

2. Inner and Outer Sphere Concepts

In 1954 Weiss[32] used Bernal and Fowler's simplified solvation model,[16] with an "Inner Sphere" of ionic coordination, i.e., a small spherical double layer around the ion of charge ze, followed by a sharp discontinuity at radius r_i, the edge of the "Outer Sphere" or "Dielectric Continuum." He used a simple electrostatic argument to determine the energy to remove an electron at optical frequency from the Inner Sphere:

$$\Delta u_i = cze\mu/\varepsilon_{opt}r_i^2 \tag{2}$$

where c is the coordination number of inner sphere water dipoles of dipole moment μ, and ε_{opt} is an optical frequency dielectric constant for the inner sphere, if this is physically meaningful. He used the Born charging equation was to estimate the energy change on both low frequency and optical frequency transfer of charge ze from the inner sphere to a vacuum at infinity:

$$\Delta u = -(z^2e^2/2r_i)(1 - 1/\varepsilon_o) \tag{3}$$

$$\Delta u_o = -(z^2e^2/2r_i)(1 - 1/n^2) \tag{4}$$

The difference between the two expressions would be the residual energy left in the dielectric continuum on transferring the charge at optical frequency under FC conditions, i.e., permanent dipoles remain in their original positions during charge transfer. Weiss noted that the expressions only apply in the region of bulk dielectric constant, beyond the "Debye sphere" immediately surrounding the solvated ion.[33] Debye estimated its radius as 11, 31, 57, and 88 Å for mono-, di-, tri- and tetravalent ions respectively.[16,33] As is discussed in Section III, the distances beyond which water reaches its bulk dielectric properties are in fact much less than these.

Weiss considered that the total energy on removing an electron from the central ion (of initial charge z + 1) at optical frequency to infinity should be on the order of:

$$\Delta u_a = -[cze\mu/\varepsilon_{opt}r_i^2 + (2z + 1)e^2/2r_i)(1/n^2 - 1/\varepsilon_o)] \tag{5}$$

The "Outer Sphere" part of this expression is similar to the functions used by Landau[34] and Mott and Gurney[35] for the polarization

due to displacement of a charge in a polar medium (c.f., Platzmann and Franck[28]). Weiss did not make use of this expression to estimate the height of the homogeneous electron exchange energy barrier which must be overcome by thermal vibrational-rotational energy. He assumed that the energy charge on discharging one ion and charging another in a homogeneous exchange reaction is equal to the algebraic sum of the optical frequency continuum terms for charge and discharge from the standard states (a vacuum at infinity), plus that of the Inner Sphere energy changes, plus the energy of assembly of the ions in the initial state. The latter is $e_i e_j/\varepsilon_o(r_i + r_j)$, where the e and r terms are the individual charges and radii. Weiss also said nothing about the crossing points of energy terms for reactants and products in or out of equilibrium, although he did point out that if weak interaction occurs, the probability of transition will be low and must be determined using the Landau-Zener adiabatic transition expression (see below). He also discussed electron tunneling, and was careful to distinguish between the transition of the reactant through the adiabatic "barrier" to the products, and electron tunneling through a Gamow energy barrier.[18,19]

Electron tunneling of Gamow type was discussed by (R. J.) Marcus, Zwolinski, and Eyring in 1954-55.[36] The rate was given by a transition state model with an activation energy term containing coulombic repulsion and reorganizational energy differences between reactants and products, multiplied by a frequency factor containing the tunneling coefficient. Somewhat similar approaches were taken by Laidler and coworkers.[37-39] Refs. 38 and 39 considered the possibility of some inner sphere rearrangement before electron transfer, with a change in solvation energy corresponding to a change in ion size. The concept of Inner Sphere and Outer Sphere reactions, depending on the type of activated state, was introduced by Taube.[40]

3. Dielectric Continuum Theory

The next developments of the FC approach were in papers by (R. A.) Marcus,[41-49] and a later series from the Soviet Union. About the same time Hush[50] introduced other concepts, to be discussed below. The early work of Marcus[41] considered the Inner Sphere to be invariant with frozen bonds and vibrational coordinates up to the time of electron transfer. The "classical subsystem" for ion activation has its ground state floating on a continuum of classical levels, i.e., vibrational-librational-hindered translational motions of solvent molecules in thermal equilibrium with the ground state of the "frozen" solvated ion.

The movement of a permanent or induced dipole changes the energy of the ion by Coulomb's law. The Inner Sphere dipoles are frozen, so only those in the outer sphere can move to change the potential energy of the central ion, reducing the system to the external electrolyte and the electron to be transferred. To avoid the difficulty of summing the energy changes imparted to the ground state of the ion due to dipole movements at progressively greater distances, the medium may be regarded as a dielectric continuum, and that the electron may be regarded as a charge distributed over the surface of a conducting spherical condenser of radius r, a non-physical adjustable parameter accounting for the ion solvation energy. The application of the FC principle results in a polarization of the environment of the charge on rapid electron transfer.

The early papers of Marcus[41,42] describe an activated state X* with the electronic configuration of the reactant(s) and the Outer Sphere atomic configuration of the activated product X. A collective displacement vector describes outer motions in a classical Hooke's law elastic medium. Microscopically, this would have Gibbs free energies of $e_{ind}^2/2\alpha_e$ for induced dipole charges (e_{ind}), where the electronic polarizability[51] α_e is $e^2/m_e(2\pi\nu_e)^2$ and m_e, ν_e are the electronic mass and frequency. The maximum energy of rotating permanent dipoles of moment μ at distance r from charge ze is $-ze\mu/\varepsilon_o r^2$. Marcus first looked at the medium macroscopically, regarding it as a dielectric with complete dielectric saturation in the Inner Sphere surrounding the ion.[41] He then considered partial saturation of the dielectric, with averaged dielectric constants.[42] A permanent dipole vector **u** cannot keep up with the sudden change of field under FC conditions, so it leaves a residual Gibbs energy in the medium $\mathbf{u}^2/2\alpha_u$[42,49] where α_u is the polarizability per unit volume. The classical induction equalities are $(\mathbf{P}.\mathbf{E})dV = (\mathbf{u}^2/2\alpha_u)dV = (\alpha_u E^2/2)dV$ integrated over the dielectric volume not occupied by the reactants, where **P** is the polarization vector dV or dipole moment **u** per unit volume, and **E** is the corresponding field. Two **P** and **E** terms are distinguished, according to their frequency response, $\mathbf{P}_u$, $\mathbf{E}_u$ for nuclear and molecular motions, and $\mathbf{P}_e$, $\mathbf{E}_e$ for electronic motions.[41,42] Later, a paniculate charge, rather than dipole description of the electrolyte was given, to account for a multipolar medium.[43]

The most probable X* and X were obtained by setting the differentials of the Gibbs energy of X* (δF^*) and the difference between those of X* and X $(\delta F^* - \delta F)$ equal to zero. The sum $\delta F^* +$

$m(\delta F^* - \delta F)$ is set equal to zero to define the crossing point for the X* and X electron states, where m is an undetermined Lagrangian multiplier. The (Gibbs) energy of activation (G_{act}) is the residual Gibbs energy barrier in the dielectric on FC charge transfer, after allowance for the Gibbs energy of reaction. The latter is $F^* - w^*$ at $\delta F^* = 0$, where w* is the Gibbs energy of the initial state, and is given by the volume integral:

$$G_{act} = F^* - w^* \qquad (6)$$
$$= (1/8\pi) \int [(\mathbf{E}^{*2}/\varepsilon_o) + m^2(\mathbf{E}^* - \mathbf{E})^2(1/n^2 - 1/\varepsilon_o)]dV$$
$$- e_i^2/2\varepsilon_o r_i - e_j^2/2\varepsilon_o r_j$$

where the final two terms are the Born charging equation expressions for the w*, the Gibbs energy of the components, with two initial components with charges e_i, e_j, and radii r_i, r_j. $\mathbf{E}^*$ is the volume-element dependent field vector due to the activated initial electronic state, and $\mathbf{E}$ is the value simultaneously present (in FC terms) in the final electronic state. It will be recognized that the integral of the first term inside the bracket is an energy of assembly under static dielectric conditions, whereas that of the second is the energy charge on going from reactants to products at optical frequency.

By conservation of energy, $F^* - F$ must be equal to $\Delta G^\circ - T\Delta S_e + w^{**}$, where ΔG° is the standard Gibbs energy of reaction, ΔS_e is any electronic entropy change on electron transfer, and w** is the work required to bring the activated reactants and activated products from infinity. The second minimizing condition, i.e., $\delta F^* - \delta F = 0$ gives:

$$F^* - F = (1/8\pi) \int \{ ([\mathbf{E}^{*2} - \mathbf{E}^2]/\varepsilon_o) - (2m - 1)(\mathbf{E}^* - \mathbf{E})^2(1/n^2 - 1/\varepsilon_o)\} dV \qquad (7)$$

The volume integrals were evaluated by substituting $dV = 4\pi r^2 dr$, using the Coulomb's law assumption that the $\mathbf{E}$ terms are given by the vector sum of the negative gradients of the potential due to each charge e_i at distance r_i, i.e, $-\sum\nabla(e_i/r_i)$ in the space outside of the reacting particles. Within the particles, the usual Born charging assumption for conducting spheres makes the $\mathbf{E}$ terms zero. The $\mathbf{E}^2$ terms contain $[e_i\nabla(1/r_i)]^2$ and $2e_ie_j\nabla(1/r_i)\nabla(1/r_j)$. The integral of the former from r_i to infinity is $4\pi e_i^2/r_i$, and that of the latter is $8\pi e_ie_j/R$, where $R = r_i + r_j$ at

closest approach. The first term inside the bracket in Eq. (6), after subtraction of the last two terms on the right, becomes $e_i e_j/\varepsilon_o R$, and the integral of $(\mathbf{E}^* - \mathbf{E})^2$ simplifies to $8\pi(\Delta e)^2(1/2e_i + 1/2e_j - 1/R)$. Multiplied by $(1/8\pi)m^2(1/n^2 - 1/\varepsilon_o)$, this is λ, the reorganizational energy. The multiplier m is calculated from Eq. (7), and substituted in Eq. (6). Libby's concept (c.f. Eq. 1) considered the energy charge on changing charge to be proportional to e.g., $z^2 - (z-1)^2$. However, all the z terms cancel in the Marcus equations, leaving only Δe, the amount of charge transferred in the forward and backward processes, i.e., by one electron unit so that the activation energy remains at the lowest level. The system is symmetrical, the electronic energy curves for the reactants and products being exactly similar and parabolic. This is because of the use of the expressions containing $\mathbf{mE}.\mathbf{mP} = m^2\mathbf{E}^2\alpha_u$ to give the continuum energy changes, i.e., m acts on the differential of the energy of a state, i.e., on its field, and not on its Gibbs energy. To quote Marcus, "in the absence of specific interactions, the (separate Born charging formulas for each reactant will hold at all separation values), since in the equation (for charging) each ion would merely see another charge, $-m\Delta e$, and the surrounding medium, in both the homogeneous and electrode cases".[44]

The reorganizational energy of the system, λ, was defined as the residual or inertial energy in the dielectric when the atomic configuration of the reactants (i.e, that in the Outer Sphere) is equal to that of the products. If the length of the many-dimensional reaction coordinate from the ground state of the reactants to that of the products is put equal to x, then $\lambda = kx^2$, where k is a constant. Ignoring the small $-T\Delta S_e + w^{**}$ terms, the similar parabolic terms for the reactants and products are vertically separated by ΔG°. The position of the crossing point, mx, along the reaction coordinate is given by a simple geometrical argument as $(\Delta G^\circ + \lambda)/2\lambda$. This gives a geometrical identity to the Marcus m. The Gibbs energy of activation ΔG^* is then equal to the energy at this crossing point, i.e.,

$$\Delta G^* = k(mx)^2 = (m^2)\lambda = (\Delta G^\circ + \lambda)^2/4\lambda \qquad (8)$$

The reorganizational energy λ was calculated using the Born charging formula energy differences for the ion with its primary solvation sheath under static and optical conditions, using the difference between the squares of the charges $(\Delta e)^2$. Thus, λ_{hom} for the

homogeneous electron transfer reaction between two ions of radii r_i and r_j at the closest approach distance $R = (r_i + r_j)$:

$$\lambda_{hom} = (\Delta e^2)(1/2r_i + 1/2r_j - 1/R)(1/n^2 - 1/\varepsilon_o) \quad (9)$$

The electrode case may also be thought of as involving two ions, one having infinite radius. However, Marcus considered that there was also an image charge situated at R', twice the distance of the reacting ion from the electrode.[44-46] Thus, λ_{elec} was given by:

$$\lambda_{elec} = (\Delta e^2)(1/2r_i - 1/2R')(1/n^2 - 1/\varepsilon_o) \quad (10)$$

We should note that for water, $1/\varepsilon_o$ is negligible, and the infrared value of $1/n^2$ is about 0.55. The overall rate is $\exp -m^2\lambda/kT$ multiplied by a frequency equal to the collision number and by the concentrations of the reactants.

Other Marcus papers correlated theory and experiment.[48,49] He discussed adiabatic and non-adiabatic homogeneous transfer, pointing out that the degree of broadening and splitting between the electron energy terms of reactants and products is related to the lifetime τ of each excited state via the uncertainty principle, i.e., $\Delta E\tau = h/4\pi$, where ΔE is the broadening, and $2\Delta E$ is the corresponding splitting, i.e., the overlap or interaction energy between reactants and products. The splitting $2\Delta E$ is about 0.6, 6.0, and 60 kJ/mole for electron transition times of 10^{-13}, 10^{-14}, and 10^{-15} s, so rapid electron transitions will greatly reduce the Gibbs energy of activation. The FC, i.e., Born-Oppenheimer) approximation for water dipoles will hold at least to 10^{-12} s, where the amount of splitting is negligible. Marcus indicated[47] that the calculated electron tunneling probability determined by modeling the solvent energy barrier between the reacting species[36] could be used to determine the amount of splitting, since the transition time is $1/\rho\nu$, where ρ is the tunneling probability and ν is the electron frequency in the reactant. Thus, $2\Delta E$ is approximately $h\nu\rho/2\pi$. This can be used in the Landau-Zener formula[9,52] or in more exact and general procedures[53] to determine the probability of non-adiabatic reactants to product transitions. Thus, the use of ρ as a prexponential term in the rate equation[36,39] is incorrect. The Marcus papers generally assume adiabaticity, unless proved otherwise. He pointed out[48] that no theory existed (indeed exists) for the large- to medium-overlap Landau-Zener transition at a metal electrode, because the multiplicity of levels

allows electrons to make unsuccessful transfers to one level, and successful ones to another during the cause of small fluctuations in space, energy, and time. Electrons would emerge at energies of ±2-3kT of the Fermi level, as Gurney had approximately demonstrated by integration.[8] A similar procedure to that of Gurney integrated to the band edge energy[54] was used by Gerischer for semiconductor electrodes.

4. Activation via the Dielectric Continuum

The Marcus theory used thermal activation via collisional interactions to overcome the electrostatic (or other) energy barriers. The Soviet school[55-59] used a similar dielectric continuum concept derived from work by Platzman and Franck[28] and Pekar[60] for radiationless transitions in polar crystals, and by Lax[61] in polyatomic molecules (see also Frohlich, Ref. 62). The work is most accessible in later review articles.[57-59] It used Pekar's Hamiltonian description of the energy of the medium derived from nonequilibrium thermodynamics, rather than the classical electrodynamics used by Marcus. Unlike Marcus, they regarded the dielectric continuum as capable of activating the discharging ion via coupled harmonic electrostatic motions. The Born-Oppenheimer approximation was used to separate the wave functions of low-frequency dipole vibrations from high-frequency electronic vibrations. Dipoles performing small oscillations around the discharging ion may each contribute one vibrational energy quantum (about 0.016kT at 298 K for a frequency of 10^{11} s^{-1}, or about 4×10^{-4} eV on a molar basis). Thus, 1300 dipoles are required for an activation energy of 0.5 eV, in a radius of 20 Å, corresponding to a large polaron.[58,59] The charge is transferred over a distance of about 6 Å, which is on the order of, and probably less than, the distance through which dielectric saturation occurs close to the discharging ion (the correlation radius of the dipole moments). The theory was considered valid at 20 Å, but was considered less so at 6 Å, because of vibrational frequency dispersion due to dielectric saturation at small distances[59] (c.f., Marcus[42]). However, the theory of small polarons[63,64] allowed estimates to be taken to smaller ions and charge and energy transfer distances.

The transition probability was calculated using the Landau-Zener equation for homogeneous adiabatic electron transfer, and for the electrode case with very weak coupling, for which an exact solution exists. In many cases, the rate was expressed with a non-calculable

preexponential interaction Hamiltonian for the overlap terms. The polaron approach differs from normal thermal activation. The latter may be regarded as via acoustic waves that result in collisions. The activation frequency is a collision number for Marcus, and the frequency of long-wave coupled dipole vibrations for the Soviet school. However, both are of the same order of magnitude at ordinary temperatures (about 10^{11} s^{-1}). One difference between the Marcus continuum theory and that of the Soviet school is the nature of the energy corresponding to the electron terms, which Marcus regarded as a Gibbs energy, because it uses the Born charging equation. However, $(1/n^2 - 1/\varepsilon_o)$ results from the difference between two Born charging equations and is largely temperature-independent,[59,65] so λ has the properties of potential energy.

5. Inner Sphere Rearrangement With "Flow of Charge"

Hush, followed by others[40,66] assumed that all rearrangement did not necessarily occur in the Dielectric Continuum. His early papers[50] appeared to take exception to the assumption of FC restrictions. He considered that adiabatic and non-adiabatic FC electron-transition processes of gas-phase type were not appropriate for electron-exchange reactions in solution at metal electrodes. The eigenfunction of the transferring electron might flow between reactants and products over a relatively long time, the behavior of the dielectric medium governing the course of the reaction. This implies a transition state of "normal" type with an energy col, where the electron density differs from that of the initial or final state by an amount equal to the symmetry factor. The slow change in charge density as the reaction proceeds implies an adiabatic process. The energy along the reaction coordinate would then only contain ion-solvent interactions, not electronic terms. These interactions were given simple forms, i.e., an energy of cavity formation in the solvent, which is largely independent of charge, the ion-dipole interaction depending linearly on charge, and a Born charging energy depending on the square of charge. No induced dipole effects (also depending on the square of charge) were considered. A further simplification assumed that energy changes resulting from the overall change of charge from reactants to products would overwhelm the differences resulting from the small changes in ligand-ion bond-length. Thus, the changing energy along the reaction coordinate due to ion-dipole interactions will be given by $e\mu q/r_d^2$, where μ is the dipole moment of water, q is the fraction of electronic charge at a given point

on the reaction coordinate, and r_d is the approximately constant ion-dipole distance. As charge flows in, the energy of the system at equilibrium must be corrected by an amount proportional to the change of charge.

The charge-transfer barrier due to ion-permanent dipole interactions was rather small, and since ion-induced dipole terms ($\propto z^2/r_d^4$)[16] were ignored, the only place to seek a charge-transfer barrier was in the Born charging energy. This varies as z^2/r_i, where r_i is again the Bernal and Fowler[16] Born ionic radius, approximately the radius of the solvated ion. To a first approximation, r_i, like r_d, may be considered constant, so that the (positive) change in energy on going from charge z to z – q is $(2qz - q^2)B$, where B is the Born continuum energy multiplier, equal to $e^2(1 - 1/\varepsilon_o)/2r_i$ (Eq. 3). To correct the energy after charge q has been transferred to the equilibrium value for the overall process $M^{z+} \rightarrow M^{(z-1)+}$, $[z^2 - (z - 1)^2]B$, the absolute (positive) energy difference between the initial and final states, must be multiplied by q and subtracted from $(2qz - q^2)B$, giving:

$$\Delta G^* = q(1 - q)e^2(1 - 1/\varepsilon_o)/2r_i \qquad (11)$$

which differentiation shows has a maximum at q* = 0.5, so that the Gibbs energy of activation under equilibrium conditions is $e^2(1 - 1/\varepsilon_o)/8r_i$. For r_i = 3.5 Å, this is about 49.6 kJ/mole, which is reasonable. Replacing $[z^2 - (z - 1)^2]B = C$ by $C + f\eta$, where f is F/RT adds the overpotential, η, to the expression. Differentiation now shows a maximum at $q^* = (C + f\eta)/2C$, so that $\Delta G^* = (C + f\eta)^2/4C$, which except for the multiplier $z^2 - (z - 1)^2$ is identical in form to the Marcus Eq. (8), with C equivalent to Marcus λ and $\Delta G^\circ = f\eta$. The electrochemical symmetry factor $(1/f)d\Delta G^*/d\eta$ is therefore equal to $(f/2)(C + \eta)/C$.

In a later paper,[67] Hush further developed his theory and compared it to that of Marcus. He took into account a change in ion-ligand distance in the inner sphere by adding a Mie repulsive energy cAr_d^{-n} to the ion-dipole electrostatic term $-cze\mu r_d^{-2}$, where A is constant, n is large (9-12), and c is the coordination number. By setting the derivative equal to zero and eliminating A (assumed to be constant along the reaction coordinate) from the equilibrium expressions for the states with charges z and z – q, we obtain:

$$r_{d,e,z-q} = r_{d,e,z}[z/(z - q)]^{1/(n-2)} \qquad (12)$$

where the $r_{d,e}$ values refer to equilibrium states, and q replaces Hush's λ to avoid confusion with the Marcus λ. Mie's equations of $Ar_d^{-n} - Br_d^{-m}$ type have an equilibrium energy equal to $-B(r_{d,e})^{-n}[1 - (m/n)]$. Again ignoring ion-induced dipole effects, the energy associated with the inner sphere ΔE_i is approximately given by the ion-dipole term, with m = 2 and B proportional to z. Using (12):

$$\Delta E_{i,z-q} = -[n - 2/n]B(z - q)(r_{d,e,z})^{-2}(1 - q/z)^{2/(n-2)} = \Delta E_{i,z}(1 - q/z)^{n/(n-2)} \quad (13)$$

As before, $-(\Delta E_{i,z} - \Delta E_{i,z-q}) + q(\Delta E_{i,z} - \Delta E_{i,z-1})$ can be expanded as far as the quadratic terms the energy change along the reaction coordinate above the ground states of the reactants and products in equilibrium. The first two binomial terms vanish, so:

$$\Delta E_i^* = -\Delta E_{i,z}[q(1 - q)][n/(n - 2)^2 z^2] \quad (14)$$

Again $q^* = 1/2$, so $\Delta E_i^* = -\Delta E_{i,z}[n/4(n - 2)^2 z^2]$ and is rather small (7-11 kJ/mole). Hush considered ΔE_i^* to be $\approx 50\%$ of the total activation energy, the remainder being Outer Continuum energy. Since it again contains q(1 – q), introduction of the overpotential as before again gives a symmetry factor $(C' + f\eta)/2C'$, where $C' = -\Delta H_{i,z}[m/4(m - 2)^2 z^2]$.

A complete model must include the induced dipole term. If it is initially assumed that $r_{d,e}$ is invariant, this is $-cz^2e^2(\alpha_e/2)(r_{d,e})^{-4}[1 - (4/n)]$. This has the same form and properties of the Born charging term, again giving a symmetry factor proportional to overpotential. Without the aid of further simplifying assumptions, it is not possible to obtain any exact expressions to show the behavior of the terms when $r_{d,e}$ is allowed to vary. Hush's expansion to the binomial quadratic term leads to a harmonic approximation. This suggests that the equilibrium force constants may be used to estimate the energy changes, since these will include the effect of the ion-dipole and ion-induced dipole terms in harmonic approximation. However, the way in which force constant change as z – q changes is unknown, although if z – q is identified with bond order,[68] the relationship between the force constant and this term may be linear. Another possibility is the use of a relationship between z and the enthalpy of solvation, $\Delta H_{i,z}$. Assuming the straight line log-log

relationship $\Delta H_{i,z} = -Kz^x$ for the Inner Sphere where K, x are constants, expansion of $z^x(1 - q/z)^x$ gives $q^* = 1/2 + f\eta/x(x - 1)Kz^{x-2}$, and:

$$\Delta H_i^* = C''[q(1 - q)] + qf\eta = C''/4 + (f\eta)^2/4C'' + f\eta/2 \qquad (15)$$

where $C'' = [x(x - 1)Kz^{x-2}]/2$. For ions of valence 1-4 in the same range of atomic weight, a good case may be made for the enthalpy of solvation being approximately proportional to z^2. If the inner sphere part follows the same relationship, the approximation in (14) becomes exact, with C" = K. The symmetry factor will again be of the form $(f/2)(C'' + f\eta)/C''$.

In his 1961 paper,[67] Hush modified his outer sphere energy equation by changing the $(1 - 1/\varepsilon_o)$ term to the Marcus expression $(1/n^2 - 1/\varepsilon_o)$ because the electron transition time, though longer than that under FC conditions, would still be short compared to solvent molecule motion. This proposition will be discussed later. The q value at the highest point of the energy surface (q*, Hush's $\lambda^{\neq}$) is then apparently formally identical to the Marcus m. The comparison of the Marcus and Hush crossing terms is indicated in Figure 1. Hush used similar expressions to those of Marcus for the continuum parts of the reorganizational energy in the homogeneous and heterogeneous electron transfer cases, but he correctly pointed out that R′ in Eq. (10) for the heterogeneous electrode reaction at infinite dilution should be left out in the real solutions which are normally studied.[67] Equation (9) would therefore somewhat understate the activation energy. Hush used the collision number $(kT/2\pi\mu^*)^{1/2}$ for the mean frequency for crossing the barrier, where μ^* is the reduced mass of the activated complex. He considered that reaction would be adiabatic, since the energy gap ΔE between the upper and lower electronic states at the crossing point should be about 0.03 eV or 2.75 kJ/mole, the order of magnitude of crystal interactions for transition metal ions. This is sufficient to give a transition probability close to unity.[67] This corresponds to a transition time $h/2\Delta E$ for the electron states on the order of 2×10^{-14} s, allowing a continuum energy expression containing $(1/n^2 - 1/\varepsilon_o)$. In a later paper,[69] Hush attempted to generalize his model, introducing some of the Soviet school ideas into the continuum description using the Kubo model for the small polaron.[70] He also discussed adiabatic cases. He treated all vibrations, in both the inner and outer spheres, as quadratic functions of frequency tensors operating on the vector differences between the equilibrium positions of the initial and final states.[69]

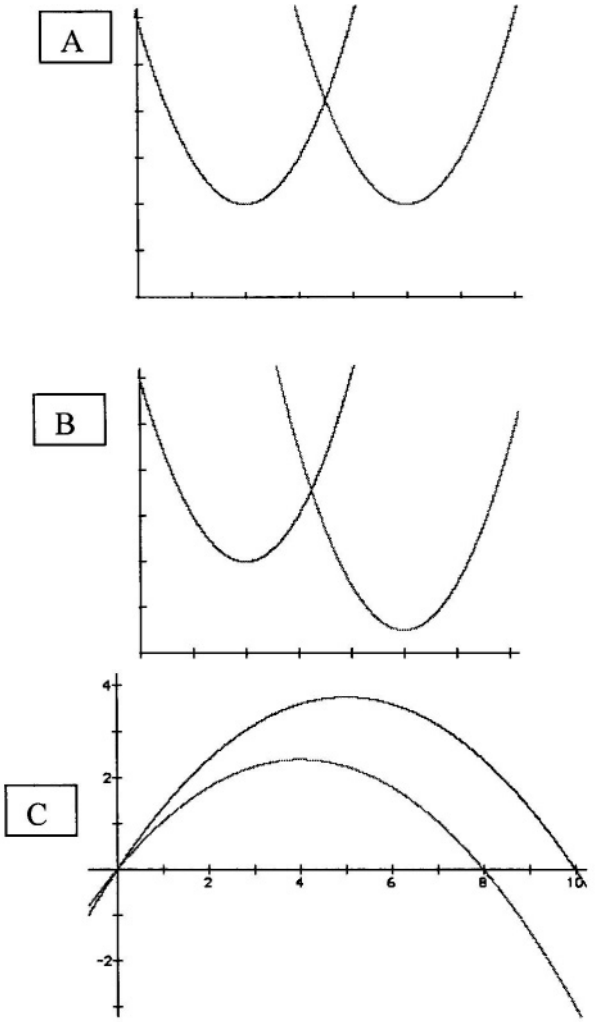

Figure 1. Two-dimensional potential energy surfaces in equilibrium (A) and out of equilibrium (B) for Marcus[41-49] Outer and Inner Sphere and Hush Outer Sphere;[67,69,176] (C) Hush Inner Sphere[50,67,176] in and out of equilibrium y-axes: Nominal energy x-axes: Nuclear configuration as a function of change of charge. C shows activation energies of 3.75 units at equilibrium (transition state charge 0.5), 2.4 units at –3.0 units energy displacement (transition state charge 0.4, mean symmetry factor 0.45).

Whether the electron transition time is $\approx h/2\Delta E$ is debatable. It corresponds to a single FC transition time, whereas the postulate of "flow of charge" to the inner sphere suggests a change in electron probability over time, i.e., a multiplicity of electron transfers between the donor and the acceptor, with the electron spending progressively larger amounts of time on the acceptor as the transitions proceed. Each of these may be regarded as a single radiationless FC electron transition. Between transitions, a small amount of bond-stretching occurs. Thus, a finite number of molecular vibrations of the reactant occurs as the charge changes from z to z – q and the ion-ligand bond lengthens. The symmetrical stretching frequencies[71] for typical 3+ and 2+ transition metal ions are about 390 and 490 cm^{-1}, corresponding to periods of 8.6×10^{-14} s and 6.8×10^{-14} s respectively. Thus, a reasonable minimum time for a flow of charge might be about 4×10^{-13} s, corresponding to about 5 vibrational periods. In the absence of a molecular energy model for the continuum (as distinct from the Born charging concept), it is difficult to give an opinion as to whether this time is sufficiently short for the polarization energy term containing $(1/n^2 - 1/\varepsilon_o)$ to apply. The relaxation time for distant continuum dipoles may be about 10^{-11} s.[57] The classical expression for $\cos\theta$, the limiting value of the Langevin function for small θ in fields of energy less than kT at some distance from an ion is $ze\mu/3\varepsilon_o r^2 kT$.[72,73] If ε_o has its bulk value at r = 10 Å (see Section III) the $\cos\theta$ values will be 0.03 and 0.02 for the transition z = 3 to z = 2, corresponding to a change in the angle of a water dipole to the field of 89° to 88°. To go from the torsional equilbrium position for a state z to a state z – 1 will require only a small fraction of a period. If this scenario is correct, the more distant continuum may always be in equilibrium with the changing field under Hush's "flow of charge" concept.

6. Inner Sphere Rearrangement and Force Constants

The first Inner Sphere treatment to use force constants to estimate energy changes between valency states in isotopic homogeneous electron exchange reactions under FC conditions was given by George and Griffith,[74] following Orgel.[75] The reactants (e.g. M^+ and M^{2+}) are considered to be at the distance of closest approach with excited inner spheres. If the difference in distance between the ion and the c identical ligands in the ground state is d, M^+ in its excited state has the ligand-ion bonds in compression through a portion of this distance, whereas M^{2+}

has its bonds stretched. For radiationless FC electron transfer, the sum of the potential energies of the two reactants above their ground states should be equal to that of the two (identical) products. The degree of harmonic compression of each of the n inner sphere bonds of force constant f in the M^+ reactant is x, and the degree of stretching of the n bonds of force constant f in M^{2+} is x'. On instantaneous conversion to the products, M^+ becomes M^{2+} with its bond stretched by the amount $d - x'$, and M^{2+} becomes M^+ compressed by $d - x$. The condition for radiationless transfer is therefore $1/2fx^2 + 1/2f'x'^2 = 1/2f'(d - x)^2 + 1/2f(d - x')^2$, which can only be true if $d = x + x'$, i.e., the excited system is symmetrical. Possible activation energies are each equal to the sum of the energies of the excited levels of the two reactants above their ground states. Using the symmetry condition, each must be equal to $1/2fx^2 + 1/2f'(d - x)^2$. The most probable is the minimum value at x_{min} where $x_{min}(f + f') = f'd$. Thus, the minimum value of the activation energy for a homogeneous redox exchange reaction (i.e., at a Gibbs energy of reaction equal to zero) will be given by the reduced force constant expression:

$$U^* = cd^2ff'/2(f + f') \tag{16}$$

Marcus generalized this reduced force constant expression to account for other cases, e.g., homogeneous reactions between different ions.[44,46] This harmonic approximation under FC conditions implies the reaction energy surface represented by the intersection of two parabolas, which are similar in the Marcus generalization. Thus, the relationship between Gibbs energy of inner sphere activation and the Gibbs energy of reaction is given by an equation of the same form as Eq. (16). As in the Hush approach, the inner and outer sphere energies at all stages of reaction are additive.

For the electrode case only one ion is involved, and it has been stated that U* would be half of the value given by Eq. (16).[76] When the electrode is a reactant, the electron energy is the Fermi Energy,[8] and there is only one activated reactant. In thermodynamic equilibrium, the Gibbs energy of the grounds states of the reduced and oxidized species are equal. Consider the harmonic portions of the energy-distance curves for the reactants and products as in Figure 2, in which the equilibrium ligand to ion distances are d_1 and d_2 respectively. Writing $d = d_1 - d_2$, as in the homogeneous case, solving for the point of intersection gives the activation energy under equilibrium conditions, i.e.,

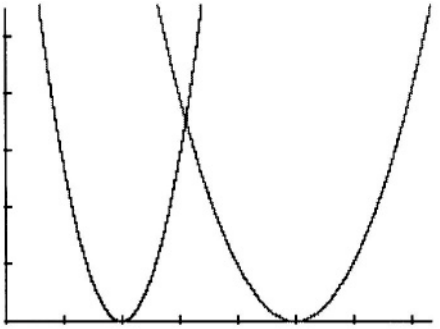

Figure 2. Two-dimensional potential energy surfaces in equilibrium for the heterogeneous (electrochemical) equivalent of the George and Griffith[74] homogeneous case involving Inner Sphere bond-stretching. y-axis: Nominal potential energy. x-axis: Nominal ion-water molecule distance. $d = d_1 - d_2$, where d_1, d_2 are the equilibrium distances of the initial and final states, giving a crossing point energy U* under equilibrium conditions of $cd^2ff'/2(f^{1/2} + f'^{1/2})^2$, where c is the coordination number and f, f' are the force constants of the initial and final states.

$$U^* = cd^2ff'/2(f^{1/2} + f'^{1/2})^2 \qquad (17)$$

For probable f, f' values (f = 2.8f', Sections IV-4, IV-9, VI-1), Eq. (17) is indeed about half of Eq. (16).

7. The Franck-Condon Approximation

The FC or Born-Oppenheimer approximation is physically clear if the activation energy barrier is in the Dielectric Continuum. The reacting ion is activated by some collisional or vibrational-librational means from the classical Boltzmann thermal pool, so that the rate of activation is equal to the rate of arrival of energy, which is equal to a characteristic classical electrolyte frequency. The electron transfers when its energy exceeds that of the barrier due to the inertia of the solvent permanent dipoles. Marcus[41-49] consistently supposed that the medium may be regarded as a dense gas phase with a collision frequency, which in its

simplest form for the heterogeneous case is given by $(kT/2\pi\mu^*)^{1/2}$ per unit area of electrode (c.f., Hush). For a typical transition metal ion coordinated by six water molecules, this is about 4.9×10^3 cm s^{-1}, or 10^{11} s^{-1} when divided by the width of the reaction zone (≈ 5 Å). It may be equally logical to regard a liquid as a mobile solid, with a range of classical frequencies to a Debye limit ν_m of *restrahlen* type, such that $\nu_m \approx c(9N_o/4\pi V)^{1/3}$, where c is the velocity of sound, N_o is Avogadro's number, and V is the molar volume.[77] This is equal to 4.3×10^{12} s^{-1} for water, which is close to kT/h (6.2×10^{12} s^{-1} at 298 K). After multiplication by a 5 Å reaction zone width, this corresponds to 3.1×10^5 cm-s^{-1}. Levich stated that there are two types of polarons in polar liquids, namely acoustic polarons and optical polarons, with molecular vibrations in the same and opposite directions, respectively. He only considered optical polarons as important for energy transfer. However, an equally good case could be made for acoustic polarons.

Another evident mechanism for energy transfer to activated ions may be by bimolecular collisions between water molecules and solvated ion reactants, for which the collision number is $n(r_1 + r_2)^2(8\pi kT/\mu')^{1/2}$, where n is the water molecule concentration, r_1 and r_2 are the radii of the solvated ion and water molecule of reduced mass μ'. With r_1, r_2 = 3.4 and 1.4 Å, this is 1.5×10^{13} s^{-1}. The Soviet theoreticians believed that the appropriate frequency should be for water dipole librations, which they took to be equal 10^{11} s^{-1}. This in fact corresponds to a frequency much lower than that of the classical continuum in water.[78] Under FC conditions, the net rate of formation of activated molecules (the rate of formation minus rate of deactivation) multiplied by the electron transmission coefficient under nonadiabatic transfer conditions, will determine the preexponential factor. If a one-electron redox reaction has an exchange current of 10^{-3} A/cm^2 at 1.0 M concentration, the extreme values of the frequency factors (10^6 and 4.9×10^3 cm^{-2} s^{-1}) correspond to activation energies of 62.6 and 49.4 kJ/mole respectively under equilibrium conditions for adiabatic FC electron transfer.

8. The Tafel Slope

Electrochemical kinetic measurements show that many reactions have a rather constant Tafel slope over a wide overpotential range. This is true for both redox[79] and combined electron- and atom-transfer reactions, particularly proton transfer.[3,80] None of the approaches discussed above account for the experimental facts. References 41-50, 55-59, and 67 all

give a curved Tafel slope in which the symmetry factor depends linearly on overpotential. In the Marcus and Soviet FC approaches, this results from the intersection of two similar parabolas as electron energy terms in molecular configuration space. For the (apparently) non-FC Hush inner sphere expressions, it may result from the binomial square-term approximations used. Introduction of $f\eta$ into the harmonic force constant expression given in Eq. (17) gives a rather complex expression corresponding to the intersection of two dissimilar parabolas, giving a curved Tafel plot.

Further problems occur with combined electron- and atom-transfer. Marcus[81] modified his electrostatic theory for bond-breaking and forming cases by using Johnston's semi-empirical bond-energy-bond-order (BEBO) model.[68] This does not significantly straighten the log current density-overpotential dependence.[3] The first Soviet evaluation of bond-breaking was applied to proton transfer[82]. The first difficulty is the energy gap between the n = 0 and n = 1 vibration states for protons in the $O\text{--}H^{\delta+}$ bond in solvated H_3O^+ of 16.2kT at 298 K, so the probability of the proton occupying higher vibrational states and the proton vibrational partition function are small. Thus, Ref. 82 considered the proton to undergo FC reaction in its ground state, which floats on the classical levels of the electrolyte thermal bath, which are continuous from 60 cm^{-1} to ca. 3444 cm^{-1} (2×10^{12} to 10^{14} s^{-1}).[78] As discussed earlier, thermal activation was considered to be via coupled librations, not modified gas-phase collisions. The proton could move from its initial to final state over a short distance (0.5 Å) by tunneling. The exact mechanism releasing it from its "cage" of water molecules was not addressed. In heavy particle transfers, e.g., chlorine evolution from chloride ion, a tunneling transition could not occur, so the corresponding theory required ingenious modifications.[83] The use of the FC expressions resulted in the same curved log $i - \eta$ plot as that for redox reactions. These approaches were criticized on the grounds that rotational-librational-vibrational exchange may be enough to give a sufficient number of excited proton states to sustain the reaction, and because the energy fluctuations resulting from coordinated dipole reorientation in the continuum would be too small to allow activation[4a].

Later publications of the Soviet group attempted to straighten the log $i - \eta$ plot, starting by postulating straight electron energy terms.[59] Later proposals included transitions from excited proton states, and a dynamic ionic atmosphere which could modulate the charge on the proton, abandoning strict FC conditions.[80,84] A semiclassical treatment of the inner sphere was introduced for redox processes.[85] The hydrogen

evolution process was regarded as a supermolecule reaction, in which the introduction of anharmonicity could result in linear Tafel behavior.[86] Later papers[80] and reviews of proton[87] and heavy particle discharge[88,89] regarded the system in a similar way. A recent review[90] regards redox processes (simple electrochemical electron transfer or ECET reactions) as FC Outer Sphere transfers, whereas for reactions involving ion-atom electron transfer (electrochemical ion transfer, ECIT), e.g., iodide/iodine,[91] it proposes that the FC condition should be relaxed.

The theory of charge transfer is apparently still in an unsatisfactory state. Few developments have occurred over the past twenty years, and theories are still not in good accord with experiment, particularly for the Tafel slope. It is claimed that introduction of anharmonicity into the intersecting terms under FC conditions can result in straight Tafel lines,[79,86] but no molecular calculations substantiate this. A problem in developing an improved theory are the fact that the energy of interaction of ions with the Dielectric Continuum is restricted to Born charging, which has no molecular basis. The second problem is the fact that simple models of the Inner Sphere, even if they include ion-dipole, ion-induced dipole, and dipole-dipole repulsion terms,[16,92,93] still result in bond lengths and force constants which do not agree with experimental values.[71] EXAFS results show an inner sphere coordination number of 6 for typical transition metal ions, and the inner sphere ion-ligand bond is rather short, i.e., 2.0-2.1 Å.[94] Addition of quadrupole terms[95] is not enough to correct the simple theoretical models (see Appendix). Although solvation energy can be represented as a nominal power series to include the change of dielectric constant with field strength,[96] this is not helpful in understanding the physics of solvation.

III. INTERACTION OF IONS WITH POLAR MEDIA TO DIELECTRIC SATURATION

1. The "Electrostatic Continuum"

The model used for ion solvation energies since the work of Bernal and Fowler[16] has considered simple electrostatic interactions between the ion and the permanent and induced charges on solvent molecules, plus a term for estimating the work involved in importing the ionic charge

from its standard state at infinity to the neighborhood of the ion situated in the Electrostatic or Dielectric Continuum. The Born charging equation[31] for the Continuum treats the ion as a Gaussian sphere with a solid metallized surface (i.e., a spherical condenser) of nominal radius r_o to which small elements of electronic charge are slowly and reversibly transported from infinity. The sphere has a minute initial charge, and work is done in bringing up each succeeding element. The resulting integration in a medium of static dielectric constant ε_o gives a Gibbs energy of $-z^2e^2/2\varepsilon_o r_o$. If the Gibbs energy of the ion *in vacuo* at infinity is arbitrarily zero, then the value in the medium of static dielectric constant ε_o is $-(1 - 1/\varepsilon_o)z^2e^2/2r_o$. The assumption of infinitesimally slow, reversible charging is hardly appropriate for a change in unit electronic charge in a time period of ca. 10^{-14} seconds. The application of Born charging to electron transfer has been recently reviewed.[97] Objections have been raised to the validity of the calculation, particularly in regard to the indivisibility of the electronic charge.* [93,98] If the same argument were applied to an electron, the charging energy and the corresponding relativistic mass would be impossibly large.[97] The equation also does not take into account partial or complete dielectric saturation near the ion, whose effective Born radius cannot in any case cannot be considered as a perfectly conducting sphere. It also does not take into account the differences in experimental Gibbs energies between positive and negative ions of similar radius.[98,99] It has been claimed that the expression for the "self-energy" of an ion interacting with the Continuum is free the above objections.[42] This is $(\varepsilon_o \mathbf{E}_A.\mathbf{E}_A/8\pi)dV$ integrated from nominal ionic radius r_o to ∞, where $\mathbf{E}_A$ is the field in volume element dV of state A. This integral gives $z^2e^2/2\varepsilon_o r_o$, which when subtracted from the *in vacuo* value gives the same expression as Eq. (3).[100] The Born charging energy and the self-energy expressions are formally identical, and both derive from the work of charging a molecular spherical condenser with fractional multiples of electronic charge. Thus the use of "self-energy" instead of Born charging[42] still depends on the validity of the Born charging assumptions. Born charging will be replaced here by a molecular model for the continuum interaction. In it, the standard state

---

* "If an ion can be treated as a conducting or non-conducting sphere, of radius r_i, and the solvent as a uniform medium of unvarying dielectric constant D, electrostatic theory can provide an explanation of the energy and entropy of the ions. The first supposition is possibly, and the second certainly, false..." (Ref. 17b, p. 881).

of the solvent dipoles is for the liquid state at infinity and for the ion it is its vacuum value. The model may be regarded as one in which dipoles are transported from infinity and assembled around the ion.

2. The Electrostatic Gibbs Energy in a Continuous Polar Medium

The equilibrium electrostatic Gibbs energy ΔG_A of an isolated volume element dV of a state A *in vacuo* containing a polarization vector $\mathbf{P}_A dV$ is $(\mathbf{P}_A.\mathbf{A}_A)dV$, where $\mathbf{A}_A$ is the electric displacement vector, assumed constant within dV, and $\mathbf{P}_A$ is the dipole moment per unit volume induced by the local field. In a real medium, a multiplicity of polarization elements are present, all of which contribute to a polarization field $\mathbf{E}_{p,A}$. In addition, the imaginary cavity containing a reference dipole contributes a cavity field, $\mathbf{E}_c$, which locally decreases $\mathbf{E}_{p,A}$. Hence, there is an internal field $\mathbf{F}_A$ in dV, whose value is $\mathbf{A}_A + (\mathbf{E}_{p,A} + \mathbf{E}_c)$. The polarization element $\mathbf{P}_A$ interacts with this field, which results from the vector sums of the polarizations induced in other volume elements. The energy $\mathbf{P}_A.(\mathbf{E}_{p,A} + \mathbf{E}_c)$ summed over all volume elements is equal to the sums of the individual interactions of the polarization in one unit with that of the polarizations in all other elements. Hence, the $\mathbf{P}_A.(\mathbf{E}_{p,A} + \mathbf{E}_c)$ energies are associated with each pair of units, and therefore each must be divided by 2 to avoid double counting.

The local internal field $\mathbf{F}_A$ is produced by an external field $\mathbf{E}_A$. To account for the Onsager cavity[101] in the medium (see below), the ratio of $\mathbf{F}_A$ to $\mathbf{E}_A$ is q_A for the sake of generality. By definition, $\mathbf{A}_A/\mathbf{E}_A = \varepsilon_A$, the *microscopic* or *local* static dielectric constant in element dV, which may be a function of the (external or internal) field. Since $\mathbf{E}_{p,A} + \mathbf{E}_c = \mathbf{F}_A - \mathbf{A}_A$, the total electrostatic energy in the volume element dV is given by:

$$\begin{aligned} d\Delta G_A &= (-)[\mathbf{P}_A.\mathbf{A}_A + \mathbf{P}_A.(\mathbf{E}_{p,A} + \mathbf{E}_c)/2 - W_A]dV \\ &= (-)(\mathbf{P}_A.\mathbf{A}_A/2 + \mathbf{P}_A.\mathbf{F}_A/2 - W_A)dV \\ &= (-)(\mathbf{P}_A.\mathbf{A}_A/2 + q_A\mathbf{P}_A.\mathbf{E}_A/2 - W_A)dV \\ &= (-)(\mathbf{P}_A.\mathbf{A}_A/2 + q_A\mathbf{P}_A.\mathbf{A}_A/2\varepsilon_A - W_A)dV \end{aligned} \qquad (18)$$

where (–) represents the overall sign of the term, W_A is the (+) work required to create the polarization $\mathbf{P}_A$ when the external field $\mathbf{E}_A$ is applied, i.e., when the electric displacement $\mathbf{A}_A$ is switched on. This work is usually expressed as the integral of the charge e associated with

the dipole $\mathbf{P}_A$ multiplied by the Onsager cavity field $\mathbf{F}_A$ and by the element of distance $d\mathbf{l}$ through which the charge e is extracted by the field, i.e., the expression $-\int_0^{\mathbf{l}} e\mathbf{F}_A\, d\mathbf{l}$.[102] While $\mathbf{P}_A$ is produced by and reacts with the *internal* field, its value is conventionally given in terms of the measurable external field. If the molecular polarization $\mathbf{P}_A$ is proportional to the internal field $\mathbf{F}_A$, so that $\mathbf{P}_A = e\mathbf{l} = n_o\alpha_{T,A}\mathbf{E}_A = n_o\alpha_{T,A}\mathbf{F}_A/q_A$, where n_o is the number of solvent dipoles per unit volume and $\alpha_{T,A}$ is the molecular polarizability of the medium in dV, this integral becomes $+q_A(e\mathbf{l})^2/2n_o\alpha_{T,A} = +q_A(\mathbf{P}_A)^2/2n_o\alpha_{T,A} = +\mathbf{P}_A.\mathbf{F}_A/2 = (+)q_A\mathbf{P}_A.\mathbf{E}_A/2$. So, provided $\mathbf{P}_A$ is proportional to the external field, i.e., $\alpha_{T,A}$ is constant, W_A will be exactly equal to $+\mathbf{P}_A.\mathbf{F}_A/2$. This will certainly be true for solids, in which permanent dipoles in fixed positions realign themselves along the field. In liquids, essentially free rotation of dipoles is assumed,[72,73] but the creation of polarization in each volume element by an applied field to give a time-averaged realignment still requires extraction of charge along the field vector, i.e., work to create the polarization. The total electrostatic energy in dV with constant $\alpha_{T,A}$ is therefore $(-)(\mathbf{P}_A.\mathbf{A}_A/2)dV$, i.e., $(-)[n_o\alpha_{T,A}(\mathbf{A}_A)^2/2\varepsilon_A]dV$. This shows that the induction is reduced by ε_A from the vacuum value, not by ε_A^2, as implied in derivations putting the interaction energy equal to $(-)[n_o\alpha_{T,A}(\mathbf{E}_A)^2/2]dV$.[99,100]

The local field consists of the difference between $\mathbf{A}_A$ and the vector sum of the displacement vectors $\mathbf{A}_A'$ from all charges in the system acting in the same direction as $\mathbf{A}_A$. The definition of the *macroscopic* dielectric constant ε_A is $\mathbf{A}_A/\mathbf{E}_A$. This corresponds to the definition from Gauss's theorem for parallel fields $\mathbf{E}_A = 4\pi\rho/\varepsilon_A$, where ρ is the charge density on a surface. Comparison of the capacities of a generalized parallel-plate condenser *in vacuo* and filled with a medium of dielectric constant ε_A shows that $\mathbf{A}_A = 4\pi\rho$; $\mathbf{E}_{p,A} = -4\pi\mathbf{P}_A$; and $\mathbf{E}_A = 4\pi(\rho - \mathbf{P}_A)$,[100] where $4\pi\mathbf{P}_A$ is the counterfield induced by the applied external field $\mathbf{E}_A$; $\mathbf{P}_A = n_o(\alpha_e\mathbf{E}_A + \mu\cos\theta)$ is the induced moment per unit volume; n_o is the number of molecular dipoles of individual moment μ per unit volume; α_e is their electronic polarizability; $\cos\theta$ is the Langevin function; and $d\mathbf{P}_A/d\mathbf{E}_A = \alpha_{T,A}$, the total optical frequency and molecular (inertial) polarization in element A. Because $\varepsilon_A = \mathbf{A}_A/\mathbf{E}_A = \mathbf{A}_A/(\mathbf{A}_A - 4\pi\mathbf{P}_A)$ and $\mathbf{P}_A = n_o\alpha_{T,A}\mathbf{E}_A = n_o\alpha_{T,A}\mathbf{A}_A/\varepsilon_A$, it follows that ε_A must be generally equal to $1 + 4\pi\mathbf{P}_A/\mathbf{E}_A$, i.e., $1 + 4\pi n_o\alpha_{T,A}$, since the derivation does not depend

on any particular model for the condenser. If $\alpha_{T,A}$ is constant in dV, then ε_A must also be constant. This expression for ε_A is valid for a uniform parallel field and for a spherically uniform charge density and field distribution. It is at least approximately correct for a spherical distribution in which the charges (dipoles around an ion) are not continuous (see Appendix). We shall now use three simple assumptions: (i) The center of the sphere is occupied by an ion of charge ze, e being the electronic charge; (ii) the electrostatic energy in dV, $(-)n_o\alpha_{T,A}(\mathbf{A}_A.\mathbf{A}_A)/2\varepsilon_A]dV = (-)[(\varepsilon_A - 1)(\mathbf{A}_A.\mathbf{A}_A)/8\pi\varepsilon_A]dV$, may be summed from a_o to infinity to give the total energy present in the medium outside a sphere of radius a_o; (iii) $\alpha_{T,A} = \alpha_T$ and $\varepsilon_A = \varepsilon_o$ are constant throughout the medium. The validity of (ii) and (iii) will be examined below.

Since $\mathbf{A}_A = ze/a^2$ for both a point charge and for a charge uniformly distributed over a surface, and dV is $4\pi a^2 da$, where a is the ion-dipole center distance, the electrostatic energy due to the presence of an ion in the surrounding dielectric continuum of dielectric constant ε_o may be approximated by the integral:

$$\begin{aligned}\Delta G'_{cont} &= \int(\mathbf{P}_A \cdot \mathbf{A}_A/2)dV \\ &= -\int_{a_o}^{\infty} \alpha_T n_0(\mathbf{A}_A.\mathbf{A}_A)/2\varepsilon_0]dV \\ &= -(1-1/\varepsilon_o)\int_{a_0}^{\infty}(z^2e^2/2a^2)da \\ &= -(1-1/\varepsilon_o)(z^2e^2/2a_1)\end{aligned} \tag{19}$$

i.e., it is numerically equal to the Born charging energy of the ion regarded as a spherical condenser of radius a_o compared with the corresponding value *in vacuo*. It is therefore either a Gibbs or Helmholtz free energy, since liquids have very small isothermal compressibilities. However, the "Continuum" is no longer continuous, but molecular, and the distance a_1, defining the energy of interaction of the charge ze with the Dielectric Continuum is now clearly defined. It is not the radius of a "hard" solvation sphere treated as a hypothetical metallic spherical condenser, but the distance from the ion to the dipole centers of the first layer of solvent molecules for which the solvent has bulk values of $\alpha_{T,A}$ (= α_T), and ε_A (= ε_o). Integration will be inaccurate when a_o and da are of similar order of magnitude and the total energy

decreases in large finite steps with increasing a. Other inaccuracies may result from the approximation $dV = 4\pi a^2 da$ for the volume element, the effect of multipole terms, and from the approach to dielectric saturation. By substituting the exact expression $4\pi(a_{n+1}^3 - a_n^3)/3$ for dV in Eq. (19), putting the radii a_n, a_{n+1} of the inner edges of the nth and (n + 1)th shells equal to 2r(s + n – 1/2) and 2r(s + n + 1/2) respectively, where r is the effective solvent molecule radius, and s is constant, we obtain:

$$\Delta G_{cont} = -\left(1 - \frac{1}{\varepsilon_o}\right)\left(\frac{z^2 e^2}{2r}\right)\sum_{n=1}^{n=\infty}\left[\frac{1}{(s+n)^2} + \frac{1}{12(s+n)^4}\right] \qquad (20)$$

The theory of the dielectric constant of liquid water considers it to consist of rather freely rotating approximately tetrahedral superdipole groups.[72,73] Its radial distribution function[103] shows closest neighbors at the hydrogen-bond distance of 2.9 Å, and second nearest neighbors at about the tetrahedral diagonal distance, i.e., 4.74 Å, with no defined structure beyond. If we assume the superdipoles to be close-packed, the volume of each five-molecule group from the bulk density of water will be 1.11×10^{-22} cm^3, i.e., their effective radius will be 2.98 Å. Allowing for, e.g., 8% defects suggests that 2.9 Å is a reasonable effective radius, so that the dipole center of a time-averaged water molecule may be considered to be located at the center of the shell of thickness 2r = 5.8 Å.

The series was summed to 20 terms, then extrapolated to infinity using the integral, which is a good approximation for the small residual energy. Values of s in the range 0.08 to 0.3 were selected, corresponding to superdipole center distances varying from 6.30 Å to 7.55 Å. As discussed in Section IV-8, these values lie around a reasonable range for encountering free water superdipoles from a central ion, the shorter ones being distance from a small tetrahedral 1+ ion, and the longer one for 3+ ions. The calculations showed that putting a_o in Eq. (19) equal to a_1 in Eq. (20) understates the interaction calculated by the integral compared with the summation, whereas putting a_o equal to 2r(s + 1 – 1/2), i.e., the first shell edge, overstates it. The relation a_o (Å) $= 0.94a_1 - 1.96$ reconciles the two. At s = 0.09, 61% of the interaction is in the first shell, and 77% is in the first and second shell. At s = 0.18 and 0.3, the values are 58%, 75%, and 55%,72%.

Since Bernal and Fowler,[16] the charging radius r_o in the Born equation has been put equal to the Inner Sphere radius, or approximately the ion to water molecule center distance plus 1.4 Å. At least for 1+ ions, this gives a fairly good approximation to the Gibbs energy of interaction of the ion with the outer Dielectric Continuum if α_T and ε_o are constant throughout the medium. High-valency ions are discussed in Section IV.

We note that ΔH_{cont}, ΔS_{cont} contain initial multipliers $-[1 - (1 - LT)/\varepsilon_o]$, and $-L/\varepsilon_o$, where $-L$ is $(\partial \ln \varepsilon_o/\partial T)_P$.[98] For water at 298.2 K, the ratio $\Delta H_{cont}/\Delta G_{cont}$ is 1.023.

3. The Approach To Dielectric Saturation

When $\alpha_{T,A}$ varies with the ion field as dielectric saturation is approached, $\mathbf{A}_A/\mathbf{E}_A$ and $\mathbf{P}_A/\mathbf{E}_A$ become nonlinear:

$$\varepsilon_A = 1 + 4\pi n_o \alpha_{T,A} = 1 + 4\pi n_o(\mathbf{P}_A/\mathbf{E}_A);\ \varepsilon_A \mathbf{E}_A = \mathbf{A}_A = \mathbf{E}_A + 4\pi n_o \mathbf{P}_A \quad (21)$$

Here, ε_A is the *integral* dielectric constant, i.e., the value corresponding to the measured values of $\mathbf{A}_A$ and $\mathbf{E}_A$. When ε_A is not constant, the work to create $\mathbf{P}_A$ may not be equal to $(\mathbf{P}_A.\mathbf{F}_A/2).dV$. When $\partial \mathbf{P}_A/\partial \mathbf{E}_A$ is a function of $\mathbf{E}_A$, we require a means of calculating both $\mathbf{P}_A$ and W_A. We use the integral $(-)\int_0^{\mathbf{F}_A} \mathbf{P}_A \, d\mathbf{F}_A = XA$.[42] Testing with various $\mathbf{P}_A.\mathbf{F}_A$ functions verifies that this gives the *net* energy of interaction of $\mathbf{P}_A$ with $\mathbf{E}_A$, i.e.,

$$W_A = X_A + |\mathbf{P}_A.\mathbf{F}_A| = (-)\int_0^{\mathbf{F}_A} \mathbf{P}_A \, d\mathbf{F}_A + |\mathbf{P}_A.\mathbf{F}_A| \quad (22)$$

where W_A, X_A are always positive and negative, respectively. Thus, in general:

$$d\Delta G_A = (-)(\mathbf{P}_A.\mathbf{A}_A/2 - \mathbf{P}_A.\mathbf{F}_A/2 - X_A)dV \quad (23)$$

4. Polarization

In the Marcus nomenclature,[41,42] the polarization in polar liquids is u- or e-type. The u-type is due to reorientation of molecular dipoles by an

applied field. Its time constant is comparatively long ($\approx 10^{-12} - 10^{-11}$ s, depending on the type of motion and the degree of molecular association). In water, maximum absorption occurs in the broad Debye bands of frequencies $5x10^{9} - 5x10^{11}$ s^{-1}, followed by thermal infrared resonance absorption corresponding to restricted dipole rotations or librations at 10^{12}–10^{12} s^{-1}. This is followed by small infra-red bands for intermolecular vibrations to $\approx 10^{14}$ s^{-1}. The e-type results from high-frequency distortion of electronic orbitals by the applied field in the range $5x10^{14}$ to beyond 10^{15} s^{-1} (Dogonadze and Kornyshev[104]). The assumption that all nuclear motions are a single u-type is an oversimplification, but the e-type has special properties. Its polarization vector is always considered proportional to the field at accessible field strengths, and it always lies along the field vector. In general:

$$\mathbf{P}_A = \mathbf{P}_{u,A} + \mathbf{P}_{e,A} = n_0\alpha_{T,A}\mathbf{F}_A/q_A = n_0\alpha_{u,A}\mathbf{E}_A + n_0\alpha_e\mathbf{E}_A \qquad (24)$$

where $\alpha_{u,A}$ is a function of $\mathbf{F}_A$, but the electronic or optical polarizability $\alpha_e = 1 + 4\pi n_0 n^2$ is not, with limitations to be discussed later. $\mathbf{P}_{u,A}$ may be subdivided into two types of molecular displacement polarizations, namely free or hindered rotations, $\mathbf{P}_{ul,A}$, and translational or electrostrictive motions, $\mathbf{P}_{ut,A}$. In a uniform applied field, only the first is significant. However, in the non-uniform field near an ion, both types will occur, since the dipole will move up-field to maximize its interaction energy until the coulombic force is opposed by non-electrostatic contact forces. In a uniform field, non-polar molecules show no rotation since α_e is always parallel to the field. In a non-uniform field, electronic induction will cause translation of non-polar molecules, giving ut-type polarization.

Only $\mathbf{P}_{ul,A}$ has been generally considered in the literature. It may be written $\mu_{eff}\cos\theta_A$, where μ_{eff} is the effective value of the permanent dipole moment of a molecule in the polar medium, lying at a time-averaged angle θ_A to the internal field $\mathbf{F}_A$. Because of electronic polarization due to the fields of neighboring permanent dipoles, μ_{eff} differs from the vacuum value, μ_v. In the absence of a field, the permanent dipoles perform thermal motions around positions determined by their attractive and repulsive forces. The *net* electrostatic forces averaged over all polar solvent dipoles are always attractive, whereas the non-electrostatic contact forces are always

repulsive.[105] The classical statistical mechanical distribution of $\cos\theta_A$ values is given by the Langevin function, $\mathbf{L}(x_A)$,[106] i.e.,

$$\mathbf{L}(x_A) = \cos\theta_A = (\coth \mathbf{F}_A\mu'/kT) - kT/\mathbf{F}_A\mu' \qquad (25)$$

where $x_A = \mathbf{F}_A\mu'/kT$, and μ' is a further effective dipole moment value which depends on the structure of the polar solvent, i.e., the attractive and repulsive forces between individual dipoles. It is the moment of the smallest average pseudo-freely-rotating spherical specimen of the polar medium, containing μ_{eff} at its center.[72] Equation (25) should be rigorous provided that the structure of the polar medium is everywhere uniform, there are sufficient dipoles in each population for Stirling's factorial formula to reasonably apply, and the energy levels of the dipoles are classical and continuous, permitting an integration to obtain the partition function.

The molecular ul-polarization induced in dV by the external field $\mathbf{E}_A$ in a polar solvent is given by:

$$\mathbf{P}_{ul,A}dV = \alpha_{ul,A}\mathbf{E}_A dV = \mu_{eff}\cos\theta_A dV = \mu_{eff}\mathbf{L}(x_A)dV \qquad (26)$$

From Eq. (25), for small x, $\mathbf{F}_A\mu' < kT$, and $\mathbf{L}(x_A) \approx x/3$. Under these conditions:

$$\alpha_{ul,A} = \mathbf{P}_{ul,A}/\mathbf{E}_A = (n_o :_{eff}/\mathbf{E}_A)\cdot(\mathbf{F}_A \cdot :'/3kT) = n_o q_A :_{eff} \cdot :'/3kT \qquad (27)$$

Thus, from Eqs. (24) and (27):

$$\begin{aligned} \varepsilon_o - 1 &= 4\pi n_o q(\alpha_e + :_{eff} \cdot :'/3kT) \\ n^2 - 1 &= 4\pi n_o q\alpha_e \\ \varepsilon_o &= n^2 + 4\pi n_o q(:_{eff} \cdot :')/3kT \end{aligned} \qquad (28)$$

where q is a generalized value of q_A. The last expression is the Kirkwood equation[72] for the static dielectric constant of associated polar liquids. From Eq. (26), in general:

$$\varepsilon_A = n^2 + 4\pi n_o \mu_{eff}\mathbf{L}(x_A)/\mathbf{E}_A \qquad (29)$$

These equations were first derived by Debye,[33,107] with the assumption that the relationship between $\mathbf{F}_A$ and $\mathbf{E}_A$ was for a Lorentz cavity containing a medium with the macroscopic dielectric constant and no

permanent dipole, when $\mathbf{F}_A = \mathbf{E}_A + 4\pi\mathbf{P}_A/3$. By elimination of $\mathbf{P}_A$ with $\mathbf{E}_A = \mathbf{A}_A - 4\pi\mathbf{P}_A = \varepsilon_A\mathbf{E}_A - 4\pi\mathbf{P}_A$, q_A for this cavity is $(\varepsilon_A + 2)/3$. Moving the $(\varepsilon_A + 2)$ term to the denominator of the left side of the first part of Eq. (28) gives the Clausius-Mossotti equation. Onsager[101] showed that this theory was incorrect for media containing permanent dipoles, and that q_A was $3\varepsilon_A/(2\varepsilon_A + 1)$ if the imaginary cavity containing the dipole has a dielectric constant of unity. Before the hypothetical introduction of its dipole, but with the field switched on, opposite walls of the cavity were already polarized by the opposing charges of neighboring liquid dipoles, partly aligned along the direction of the field. Thus, the cavity already contained a virtual dipole before introduction of real dipole, increasing both its net value and that of the cavity field. The corresponding factor[101] for a dipole bathed in a medium of dielectric constant n^2, i.e., the electron cloud surrounding the permanent dipole) is $3\varepsilon_A/(2\varepsilon_A + n^2)$. Frölich[108] considered that if μ_{eff} is a *point* dipole in the center of a relatively large (in molecular terms) Lorentz cavity with a dielectric constant n^2, then its field within the Onsager cavity will be $(n^2 + 2)/3$ times the vacuum value, i.e., $\mu_{eff} = (n^2 + 2)\mu_A/3$. This expression is limited by the dimensional constraints of the Onsager and Lorentz cavities,[108] and will fail in non-uniform radial fields near an ion. For water $(n^2 + 2)/3 \approx 1.25$, and the practical value of μ_{eff} can be adjusted to agree with that of ε_o.

The total local field $\mathbf{F}_A'$ is equal to the vector sum of the Onsager cavity field $\mathbf{F}_A$, and the Onsager reaction field.[101] The latter is independent of $\mathbf{E}_A$, and results from the dipoles' own fields.[101] In the medium of dielectric constant n^2, $\mathbf{F}_A'$ is:

$$\mathbf{F}_A' = [3\varepsilon_A/(2\varepsilon_A + n^2)]\mathbf{E}_A + [2(\varepsilon_A - 1)/(n^2r^3)(2\varepsilon_A + n^2)]:_{eff} \qquad (30)$$

where the terms are respectively the cavity and reaction fields, where r is the dipolar molecule radius.[101,108a] Frölich[108a] showed that only the first term is important for permanent dipoles, since the second only changes the absolute value of the dipole moment, which may be regarded as an adjustable parameter.

5. The Static Dielectric Constant of Water

The effective value of $:_{eff}:'$ in Eq. (28) may be calculated using various assumptions. Kirkwood[72] proposed that $:_{eff}:'$ for associated liquids is $\mu_A^2(1 + n_o f_V)$, where f_V is the electrostatic radial distribution function

summed over the selected molecule and its partners in space. He substituted $z\langle\cos\gamma\rangle_{av}$ for $n_0 f_V$, where z is the number of closest neighbors whose moments are an angle γ, and $\langle\cos\gamma\rangle_{av}$ is the $\cos\gamma$ value averaged over all possible orientations. Neglecting second-nearest neighbors and multipole effects, he assumed a quasi-tetrahedral structure for water with 4 nearest neighbors,[16] each dipole being at the O–H bond angle, taken as $\approx 50°$ (in reality, 52.25°[*]). Each hydrogen bond on the central water dipole is directed towards the π-orbitals of the oxygen on the neighboring molecule, which are also at an angle to the dipole, and perpendicular to the O-H bond plane. Assuming that free rotation[109] of the hydrogen bond, the effective moment of the neighboring water dipole along the axis of rotation is $\mu_{eff}\cos 52.25$, which is in turn at 52.25° to the dipole axis of the central water molecule. Hence, the effective value of $\mu_{eff}\cdot\mu'$ in Eq. (28) for torsion of the tetrahedral four-molecule water cluster is $\mu_{eff}^2(1 + 4\cos^2 52.25)$. Simple electrostatics[99] shows that the averaged vector sum of the fields of the 4 nearest neighbors along the axis of μ_{eff} is $(8\cos^2 52.25)\mu'/a^3$, where a is the distance between dipole centers. This increases the value of the vacuum moment μ_V due to the dipole field electronic polarization, i.e., $\mu_{eff} = \mu_v + (8\cos^2 52.25)\alpha_e\mu'/a^2$, hence:

$$:_{eff}\cdot:' = \mu_v^2(1 + 4\cos^2 52.25)/[1 - (8\cos^2 52.25)\alpha_e/a^3)]^2 = Q\mu_v^2 \quad (31)$$

where a is the effective hydrogen bond length of 2.9 Å at 298 K,[103] which Kirkwood took as 2.75 Å. From Eqs. (28) and (31), we obtain:

$$(\varepsilon_o - 1)(2\varepsilon_o + 1)/3\varepsilon_o = 4\pi n_o(\alpha_e + Q\mu_v^2/3kT) \quad (32)$$

For water, with $\alpha_e = 1.444 \times 10^{-24}$ cm^3/molecule, Kirkwood's original assumptions (Q = 4.47) give an excellent ε_o value (78.0 at 298 K). However, the use of the more realistic 52.25° and 2.9 Å (Q = 3.44) gives 63.9.

The radial distribution function was obtained by Pople,[103] c.f., Harris and Alder,[110] Haggis, Hasted, and Buchanan.[111] Pople showed that Kirkwood's assumption of complete hydrogen bonding in the first shell with none in the second was oversimplified. The first shell dipoles are bonded to the second via bent hydrogen bonds of bending

[*] Discussed in Ref. 99, pp. 10-12.

force constant g, so that the Kirkwood expression $\mu' = \mu_{eff}(1 + 4\cos^2 52.25)$ should be summed over all shells and replaced by $\mu' = \mu_{eff}[1 + \Sigma n_i \langle\cos\theta_i\rangle_{av}]$, where n_i is the number of dipoles in the ith shell, which lie at angle $\cos^{-1}\theta_i$ to the central dipole. For the first shell, $\langle\cos\theta_i\rangle_{av}$ is $(\cos 52.25 L\exp + g/kT)^2$. The second shell has one repulsive and two attractive orientations with $\cos^{-1}\theta_2 = (1/3)(\cos 52.25 L\exp + g/kT)$,[4] the general attractive orientation being $\cos^{-1}\theta_l = 3^{3\ i}(\cos 52.25 L\exp + g/kT)^{2i}$. Pople found the effect of each shell on the static dielectric constant using the n_i values from the radial distribution function. With g/kT = 10 at 273 K, the relative contributions of the first, second, and third shells were found to be 1.20, 0.33, and 0.07, and the temperature dependence of the dielectric constant showed good agreement between theory and experiment.[103]

6. The Dielectric Constant at High Field Strengths

Approaching dielectric saturation, $\mathbf{P}_{ul,A}$ is no longer proportional to $\mathbf{E}_A$, and we require a usable expression for $\alpha_{ul,A}$ as a function of $\mathbf{E}_A$. Malsch[112] showed that ε_A appeared to be proportional to $-E_A^2$ for $E_A < 3 \times 10^5$ V/cm (1000 esu-cm^2). The interaction of such fields with dipole moments of $\approx$2.0 D will result in interaction energies of less than 0.1 kT, far from the saturation requirement $\mathbf{F}_A\mu' > kT$. Several equations have been suggested to relate ε_A and E_A[114-117] (see Ref. 113) Theories of the dielectric constant in high fields by Debye,[33,107] Sack,[118] and Webb[119] using the obsolete Lorentz cavity approach are only of historical interest. They show a much slower recovery from dielectric saturation with distance from an ion[120] than those based on the Onsager cavity.* The first attempt to extend the Onsager-Kirkwood theory to high fields was by Ritson and Hasted,[122] who used empirical

---

* Grahame[117] and Conway, Bockris and Ammar[120] used the normal Poisson distribution between potential ϕ_A and charge density ρ_A, i.e., $\nabla^2\phi_A = -4\pi\rho/\varepsilon_A$, under conditions of a field-dependent dielectric constant. Buckingham[121] showed that this is incomplete if there is a gradient of $\mathbf{E}_A$ and ε_A. The Maxwell relation $\mathbf{div}\mathbf{A}_A = 4\pi\rho/\varepsilon_A$ is $\varepsilon_A \mathbf{div}\mathbf{E}_A + \mathbf{E}_A.\mathbf{grad}\ \varepsilon_A$, the second term arising from the differential. Hence, the complete Poisson equation becomes $\nabla^2\phi_A = -4\pi\rho/\varepsilon_A + \mathbf{E}_A.\mathbf{grad}|\mathbf{E}_A|(d\ln\varepsilon_A/d\mathbf{E}_A)$.

expressions similar to Eq. (29)** to calculate ε_A parallel and perpendicular to the radius vector of a (univalent) ion as a function of the field $\mathbf{E}_A$ and distance. They did not discuss the validity of their approach, but they used $4\pi\partial\mathbf{P}_A/\partial\mathbf{E}_A$ to obtain the dielectric constant. Since $\mathbf{E}_A\varepsilon_A = \mathbf{A}_A = n^2\mathbf{E}_A + 4\pi\mathbf{P}_A$ by definition, their expressions are identical to the *differential dielectric constant* $\partial\mathbf{A}_A/\partial\mathbf{E}_A$[108b]. The results show a very rapid fall in $\partial\mathbf{A}_A/\partial\mathbf{E}_A$ at distances less than $\approx$3.5 Å from a univalent ion, the fall being more rapid along the radius than perpendicular to it.

Booth[73] used Frölich's[108] modification of the Onsager expressions[101] for the cavity field in non-associated polar liquids, and corresponding modifications of Kirkwood's equation for associated polar media. Booth's assumptions in deriving Eq. (28) for the Kirkwood case are important to determine the validity of his final expressions. He used the Onsager-Frölich cavity field ratio $3\varepsilon_A/(2\varepsilon_A + n^2)$ as the value for $q_A = \mathbf{F}_A/\mathbf{E}_A$ in the Langevin function, pointing out that the cavity field expression would be exact only if $\varepsilon_A = \varepsilon_o$, i.e., $\mathbf{E}_A$ is everywhere small and constant. To make the calculation tractable, he assumed the validity of Eq. (30), and that $\varepsilon_A \gg n^2$, so that Eq. (30) became:

$$\mathbf{F}_A' = 3/2(\mathbf{E}_A + \mu_{eff}/n^2r^3) \tag{33}$$

The reaction field is small and independent of $\mathbf{E}_A$ and $\mathbf{F}_A'$, so he put $\mathbf{F}_A' \approx \mathbf{F}_A = q_A\mathbf{E}_A = (3/2)\mathbf{F}_A$ for simplicity. Using Frölich's Lorentz cavity with the dipole in an n^2 medium[108]:

$$\mu_{eff} \approx A\mu_v(n^2 + 2)/3; \quad \mu' \approx B\mu_v(n^2 + 2)/3 \tag{34}$$

where A and B are structure-dependent constants, both unity for a non-associated (Onsager) liquid. For water, Booth[73] used a tetrahedral model, first indicating that $B = (5 + 8\ \cos\gamma\rangle_{av} + 12\ \cos\gamma'\rangle_{av})^{0.5}$, and $A = (1 + 4\ \cos\gamma\rangle_{av})/B = X/B$, where γ is the angle between the axes of nearest neighbor moments, and γ' is the angle between the axes of the nearest neighbors of a given molecule. He used 1/3 for $\langle\cos\gamma\rangle$, i.e., he

** Their equations for the Onsager theory put μ^2 in the Langevin function, instead of one μ inside and one outside. However, the error is not serious since the calculations and graphs are correct.

took γ to be 180-109.47°, and $\langle\cos\gamma'\rangle$ 1/27, the approximate value for [90°–(109.47°–104.5°)], where 104.5° is the angle subtended by the protons in the water molecule. Hence $B = (\sqrt{73})/3 = 2.848$ and $A = 7/(\sqrt{73}) = 0.819$. Booth's equations[73] for ε_A (high fields) and ε_o (low fields) are:

$$\varepsilon_A = n^2 + 4\pi n_o A[\mu_v(n^2 + 2)/3E_A]L\{1.5BE_A[\mu_v(n^2 + 2)/3]/kT\} \quad (35)$$

$$\varepsilon_o = n^2 + 4\pi n_o(1.5)X[\mu_v(n^2 + 2)/3]^2/3kT \quad (36)$$

where $X = AB = (1 + 4\cos\gamma_{av}) = 7/3$. Making the same assumptions as Booth's, Kirkwood's expression for ε_{eff} $= 3.443\mu_v^2[(n^2 + 2)/3]^2$ would give:

$$\varepsilon_o = n^2 + 4\pi n_o(1.5)(3.443)[\mu_v(n^2 + 2)/3]^2/3kT \quad (37)$$

From the Clausius-Mosotti equation, with $n_o = 3.33 \times 10^{22}$ molecules-cm^{-3} and with $\alpha_e = 1.444 \times 10^{-24}$ cm^3-molecule at 298 K, n^2 can be taken as 1.76. Using $\varepsilon_o = 78.5$, Eq. (36) gives 2.03×10^{-18} esu-cm (2.03 D, Debye units) for μ_v, or 2.04 D if the correct (1.484), rather than the approximate (1.5), value of q is used. In contrast, with the correct value of q_A, Eq. (37) gives 1.92 D. The value of μ_{eff} using Booth's preliminary model[73] is $A\mu_v(n^2 + 2)/3$, i.e., 2.09 D, assuming that $\varepsilon_o - n^2 = 76.7$ is used to calculate the value of μ_v from Eq. (36).

Calculations by Coulson and Eisenberg[123] from the charge distribution of water molecules suggest a value of about 2.42 D at 298 K due to induction by the fields of surrounding dipoles. In an erratum[124] to Ref. 73, Booth used a statistical analysis to derive more generalized values of A and B, with a value of $X = AB = (1 + 4\cos\gamma_{av}) = 7/3$ to give the correct result for ε_o in Eq. (36). This reduced the value of B from $(\sqrt{73})/3$ to 7/3, giving A = 1, which increases μ_{eff} to 2.54 D. Kirkwood suggested that μ_{eff} should be that for the moment of the central water molecule, whereas the torsional term in the Langevin function should be that for the group of associated molecules preventing the rotation of the central dipole. Hence Booth's result for B $= (1 + 4\cos\gamma_{av}) \approx 7/3$ seems reasonable, at least for low fields, provided that longer-range effects are ignored, and the cavity field assumptions hold. Booth's final calculation[125] increased the value of B by 10% to 1.1(7/3), by reducing the value of A from 1,0 to 0.909 to

account for the effect of distortion of the Onsager cavity field when the field is non-uniform close to an ion, therefore no longer parallel within the cavity. This results in a value of μ_{eff} equal to 2.31 D. Booth also thought that the reaction field (Eq. 31) might also influence the value of ε_A in intense fields, and proposed a small correction in the opposite direction to account for this. A further effect maintaining the value of the dielectric constant as the field increases may result from electrostriction, which should locally increase n_o.[125] In view of the uncertainties in Booth's assumptions and calculations, a nominal value of 2.02 D is initially used here. This may be regarded as the local value of the dipole moment when the effect of the Lorentz-Frölich expression cavity expression containing n^2 has broken down due to dimensional constraints. The dipole moment value will be modified as necessary to enable a best fit to experimental bond-lengths for the inner sphere.

If the Langevin function in Eq. (35) is expanded* to the second term, we obtain:

$$\varepsilon_A = n^2 + 4\pi n_o q_A X[\mu_v(n^2 + 2)/3]^2\{1 - [q_A B\mathbf{E}_A\mu_v(n^2 + 2)/3kT]^2/15\}/3kT \quad (38)$$

This is only valid for $B\mathbf{E}_A\mu_v(n^2 + 2)/2kT < 1$, but owing to the form of the series, it is a good approximation for values < 1.2. The change in ε_A in field $\mathbf{E}_A$ from that at limitingly low fields, i.e., $\Delta\varepsilon_A$, may be written by reintroducing the Onsager-Frölich cavity field, instead of the factor $q_A = 1.5$, using Eq. (38) and the general relation:*

$$f(\varepsilon_A) = f(\varepsilon_o) + \Delta\varepsilon_A[\partial f(\varepsilon_A)/\partial\varepsilon_A]\varepsilon_A = \varepsilon_o \quad (39)$$

where $f(\varepsilon_A)$ from rearranged Eq. (38) is $(\varepsilon_A - n^2)(2\varepsilon_A + n^2)/3\varepsilon_A$. After differentiation and solving for $\Delta\varepsilon_A$, we obtain:

$$\Delta\varepsilon_A/\varepsilon_o = -3(4\pi n_o\varepsilon_o XB^2)[\mu_v(n^2 + 2)/3]^4\mathbf{A}_A^2/[5(kT)^3(2\varepsilon_o^2 + n^4)(2\varepsilon_o + n^2)^2] \quad (40)$$

---

*The expansion of L(x) is $x/3[1 - x^2/15 + 2x^4/315 - x^6/1575....+ (-1)^{n+1}(3)(2^{2n})[B_{2n}/(2n)!]x^{2n-2}]$, where B_{2n} is the (2n)th Bernouilli number. The three terms to x^4 give quite accurate results to x = 1.5 (for x = 1.5 or L(x) = 0.4381, its value is 0.4411). For large x (x > 1.5), $1 + 2e^{-2x} + 2e^{-4x} - 1/x$ gives accurate results (0.4379 at x = 1.5). Thus, from Equations 35 and 36, $\varepsilon_A = n^2 + (\varepsilon_o - n^2)p$, where p is the even term power series in the square brackets.

$$= -3(\varepsilon_o - n^2)\mu'^2 A_A^2/5(kT)^2(2\varepsilon_o^2 + n^2) \quad (41)$$

which is a generalized form of the Van Vleck,[114] Böttcher,[115] and Schellman[116] equations, which are applicable to weak fields ($E_A\mu_v/kT < 1$). The g_2 term in Schellman's Eq. (19)[116] is equal to XB^2.

7. Inadequacies of the Booth Theory

Although Booth separated the electronic and permanent dipole polarization, Buckingham[121] contended that omitting polarization energy from the potential energy function may affect ε_A. The interactions between pseudo-freely-rotating superdipole groups of effective moment $\mu' = 7\mu_{eff}/3$ [124] may be estimated using Pople's geometry[103] for the first to third, and second to fourth neighbors at minus and plus the tetrahedral angle to each other, which results in a third nearest neighbor distance of a = 7.35 Å with a nearest neighbor distance of 2.92 Å. The maximum displacement at this distance due to a rotating superdipole is 24,000 esu-cm^{-2}, which will result in only a small change in ε_A from the vacuum value (Eq. 35). Ignoring the Lorentz $(n^2 + 2)/3$ cavity term for closest-neighbor groups, and taking the mean interaction between each pair[103] as $-2\alpha_T\mu'^2/3\varepsilon_A a^6$, with $\alpha_T = (\varepsilon_A - n^2)/4\pi n_o$, we find it to be –0.008kT, far less than the free rotation requirement. For this, the thermal energy per rotational axis should exceed twice the electrostatic interaction energy per axis. Essentially free rotation coupled to partial hydrogen bonding of the larger groups therefore can occur, whereas the individual dipoles are not free. The specific heats at constant volume for liquids are explained by supposing that hindered rotations or librations with an energy barrier $\approx kT$ occur.[126] Similarly, the large change in the static dielectric constant on melting in polar media, going from a small temperature-independent value to a large value proportional to the Langevin polarizability 1/T suggests very different of solid and liquid dipoles (c.f., nitromethane[127]).

Buckingham objected to calculating ε_A via the averaging (i.e., Langevin) function, since this assumes a simple solution before the problem is fully stated. However, this seems to be the only realistic method of handling the problem. Pople's modified treatment of Kirkwood's dipole clusters[103] in which the internal field distorts hydrogen bonding between shells outside of the first cluster, has been

discussed in Section III-4. Pople did not consider that work must be done to bend the hydrogen bonds when the field is applied. This is because hydrogen bonds are continuously making and breaking, so that the bent bond is the statistical average, and no net work is required to go from one configuration to the next. This will be true until the field becomes sufficiently great to orient, then twist, and finally to completely line up the individual dipoles in a superdipole group, resulting in a breakdown of the local water structure.

A further objection by Buckingham was Booth's use of the rigid dipole in a Lorentz cavity containing a medium of refractive index n^2, which will certainly break down at short distances. Booth also assumed that n^2 is field-independent, which will not be true in intense fields. Buckingham and Pople[128] showed that the induced dipole was in fact a power series in the odd terms of $\mathbf{E}_A$, and could not contain the even terms, which would have no directionality. The permanent dipole value is also a series, with weak field and strong field terms.[128] Following Debye,[129] Buckingham[121] showed that the electronic polarizability may be anisotropic. Hence, the dielectric constant $\varepsilon_A = \mathbf{A}_A/\mathbf{E}_A$ is also a power series, this time with even terms in $\mathbf{E}_A$ for an isotropic material to avoid directionality (c.f., the expansion of the Langevin function, footnote under Eq. 38). However, Booth had pointed out the even power series would not be valid in intense fields, which would themselves introduce anisotropic effects.[125] Thus, the expression for the dielectric constant as a function of the field becomes completely nominal. Buckingham also showed that $\partial\mathbf{A}_A/\partial\mathbf{E}_A$ (c.f., Ritson and Hasted[122]), which he called the *incremental dielectric constant,* was also a power series of even $\mathbf{E}_A^{2n}$ terms, each in the series for ε_A being multiplied by n + 1. This is easily verified by differentiation.

8. The Dielectric Constant as a Function of Displacement

The best-known empirical expression for ε_A as a function of E_A^2 is Grahame's.[117,130] Its differential form with vector notation dropped, an with n^2 isotropic and constant is:

$$\partial A_A/\partial E_A = n^2 + \{(\varepsilon_o - n^2)/[1 + (b/m)E_A^2]^m\} \qquad (42)$$

where b and m are constants, the latter considered by Grahame to lie between 0.5 and 2.[117] Here $\partial A_A/\partial E_A$ was defined by Grahame as the *differential dielectric constant* or *dielectric coefficient,*[44,108b,122] i.e.,

Buckingham's *incremental dielectric constant.* The corresponding *integral* dielectric constant $\varepsilon_A = A_A/E_A$ given by Booth's equation[124] is the integral of Eq. (42) between the limits 0 and E_A, divided by E_A. Its value depends on the value of m, and is:

$$\varepsilon_A = n^2 + (\varepsilon_o - n^2)(bE_A^2)^{-1/2} \tan^{-1}(b^{1/2}E_A) \qquad (43)$$

$$\varepsilon_A = n^2 + (\varepsilon_o - n^2)(2bE_A^2)^{-1/2} \ln\{(2b)^{1/2}E_A + (1 + 2bE_A^2]^{1/2}\} \qquad (44)$$

for m = 1 and m = 0.5, respectively. It has been stated[39,99] that Eq. (42) was based on the theoretical ideas of Booth,[73,124,125] but this does not appear to be the case, since it predates Booth's work. Grahame[130] compared these expressions with Booth's after his first publications,[73,124] using b^* = 1.08×10^{-8} esu^{-2}–cm^4 derived from Malsch's results.[112] He showed a rather good correspondence between the two expressions, particularly for m = 1. For m = 0.5, Grahame's integral predicts slightly lower ε_A values for moderate fields (e.g., 73.3 compared with 73.5 for Booth's expression for E_A = 4,600 esu-cm^{-2}, corresponding to 3.75 Å from a univalent ion). At very high fields, Eq. (44) predicts higher values than Booth's expression (e.g., 19.4 compared with Booth's 11.9 for $E_A = 10^5$ esu-cm^{-2}). However, Booth's value corresponds to a distance of only 2.0 Å from a univalent ion. Values at such high displacements are irrelevant, since Booth's assumptions concerning water structure break down as x_A approaches 3, i.e., for fields greater than about 4,600 esu-cm^{-2}. This is discussed later in this Section. Equation (43) (m = 1) was used by Laidler and coworkers[37,131] with $b = 1.08 \times 10^{-8}$ esu^{-2}–cm^4 to examine the dielectric behavior of water near ions and their electrostatic repulsions.

The relationship of Eq. (42) to Booth's is of interest. For $E_A^2[B\mu_v(n^2 + 2)/2kT]^2/15 \ll 1$, Eq. (38) may be written:

$$\varepsilon_A = n^2 + (\varepsilon_o - n^2)/\{1 + E_A^2[B\mu_v(n^2 + 2)/2kT]^2/15\} \qquad (45)$$

Equation (45) has the same form as Eq. (42) with m = 1, but it represents the integral dielectric constant. The value of $[B\mu_V(n^2 + 2)/2kT]^2/15$ is 3.110×10^{-9} esu^{-2}–cm^4 with $\mu_v(n^2 + 2)/3 = 2.540 \times 10^{-18}$, calculated from Eq. (36) using the experimental value of

---

* Units of b are E_A^{-2}. For units of E_A, 1.0 V–m^{-1} = 0.01 V–cm^{-1} = 3.33×10^{-5} esu-cm^{-2}.

$(\varepsilon_o - n^2)$. This we may put equal to b'/m, where m is unknown. The quantity b' is analogous to Grahame's b, but is an integral quantity derived from the experimental $\varepsilon_o - n^2$, rather than a differential quantity derived from Malsch's experiments with fields up to 833 $esu\text{-}cm^{-2}$ (2.5×10^5 $V\text{-}cm^{-2}$).[112] The correctness of Malsch's data has in any case been questioned, since he did not allow for adiabatic heating.[132] As Grahame pointed out,[117] m does not enter into the E_A^2 term in the binomial expansion of Eq. (42). We can infer the value of m by comparing the coefficients of these and the E_A^4 term in expansions of Eqs. (35) (see Eq. 38 footnote) and 42, i.e., $x^2/15 = bE_A^2$, and $2x^4/315 = (b/m)^2$, giving m = 7/13 = 0.538. This approximate fitting using the first two terms provides a starting point to give a simple and convenient function mimicking Booth's. As might be expected, the error is least at small to relatively large fields (at 10^4 $esu\text{-}cm^{-2}$, $\varepsilon_A = 61.17$ vs. 61.18 for Booth, a difference of –0.8%). It becomes greater as fields increase, e.g., at 10^5 $esu\text{-}cm^{-2}$, it is 10.3, vs. 11.9 for Booth, a difference of–15%. All things considered, representing Eq. (42) as an expression for the *integral,* rather than the *differential* dielectric constant, using a slightly adjusted $b = 3.15 \times 10^{-9}$ $esu^{-2}\text{–}cm^4$, with m = 0.5 in Eq. (42), gives a very good fit with Eq. (35), as Figure 3 shows. At 10^4 $esu\text{-}cm^{-2}$, the error is –0.05% compared with Booth, with –5.8% at 10^5 $esu\text{-}cm^{-2}$. This use of smaller m values can further improve accuracy in very high fields (e.g., m = 0.485, –1.0% at 10^5 $esu\text{-}cm^{-2}$) but small changes then occur at lower fields (+0.09% at 10^4 $esu\text{-}cm^{-2}$).

Why this equation fits so well is clear from the expansion of Eqs. (42) and (35). In weak fields $(b/m)E_A^2 < 1$, and Eq. (42) becomes $\varepsilon_A = n^2 + \{(\varepsilon_o - n^2)(1 - bE_A^2)$, which corresponds to Eq. (41), whereas Eq. (35) may be written:

$$\varepsilon_A = n^2 + (\varepsilon_o - n^2)(5bE_A^2/3)^{-1/2}\mathbf{L}(x_A) = n^2 + (\varepsilon_o - n^2)(3/x)\mathbf{L}(x_A) \qquad (46)$$

In intense fields, $\mathbf{L}(x_A)$ approaches $(1 - 1/x_A)$, and it is easily verified by calculation that $(3/x_A)(1 - 1/x_A)$ in Eq. (46) coincides closely with $(1 + 2x_A^2/15) = (1 + 2bE_A^2)^{-1/2}$ from Eq. (42) for $x_A > 2.5\text{-}3.0$. Thus Grahame's Eq. (42) with m = 0.5 may act as an excellent replacement for Booth's expression (Eq. 35) for the *integral* dielectric constant to simplify calculation, if necessary. It also suggests a function which may be used to mimic $\mathbf{L}(x_A)$:

$$\mathbf{L}(x_A) = (5b/3)^{1/2}E_A/(1 + 2bE_A^2)^{1/2} \qquad (47)$$

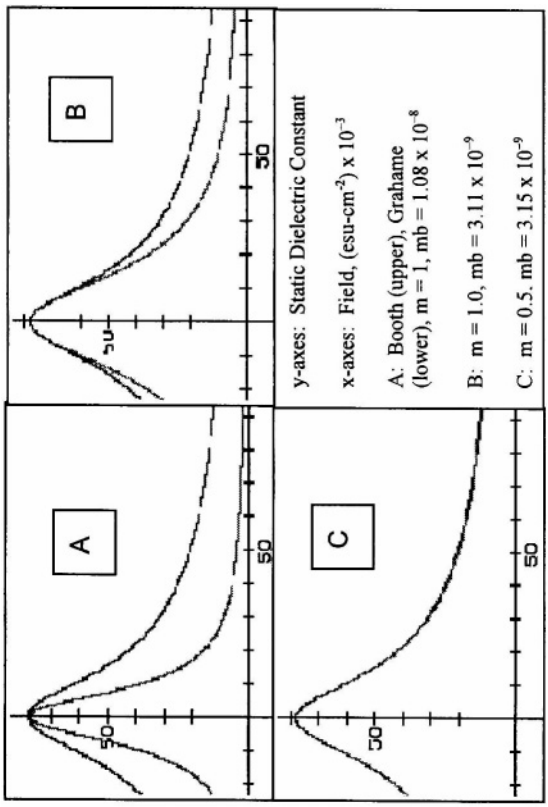

Figure 3. Grahame's equation[117, 130] $\partial A_A/\partial E_A = n^2 + \{(\varepsilon_o - n^2)/[1 + (b/m)E_A^{2|m|}\}$ (Eq. 42) for the *differential* dielectric constant, plotted as an *integral* dielectric constant ε_A with m = 0.5, b = 3.15 x 10^{-9} esu^{-2}-cm^4 along with Booth's equation (Eq. 35) for ε_A as a function of field E_A with A = 1, B = 7/3[124], μ_v = 2.027 D. Ordinate: ε_A (dimensionless units). Abcissa: E_A, esu-cm^{-2} x 10^{-3}.

Further progress requires an expression for ε_A as a function of $\mathbf{A}_A$, i.e., as a function of distance from an ion. From Eqs. (35) and (36), the Booth expression for ε_A in terms of ε_o is:

$$\varepsilon_A = n^2 + (\varepsilon_o - n^2)(3/x_A)\mathbf{L}(x_A) \tag{48}$$

This expression may determine the relationship between ε_A as a function of $\mathbf{A}_A$ in intense fields, e.g., for $x > 3$, when the approximation $\mathbf{L}(x)_A = 1 - 1/x_A$ applies. However, it assumes classical statistics, so it will require a quantum correction for x values in this range, assuming that the Langevin function is still applicable. For smaller values of x_A, Eq. (48) may be solved graphically. A more transparent expression for small x_A values would be useful. Equation (42) with m = 1/2 leads to a quartic equation in ε_A which may be simplified by expansion to a cubic expression. A solution is the use of Booth's approximation ε_A and $\varepsilon_o \gg n^2$, with substitution of Eq. (47) into Eq. (42). This gives a simple and useful approximation:

$$\varepsilon_A = (\varepsilon_o^2 - 2bA_A^2)^{1/2} \tag{49}$$

with $b = 3.15 \times 10^{-9}$ esu^{-2}-cm^4, which is rather accurate for $x_A < 2.5$, above which the classical theory may in any case not be applicable. The value of both ε_o and b will depend on temperature and solution composition and concentration.

How the polarization opposes the displacement in intense fields can be shown by using the approximate expression for $\mathbf{L}(x_A)$ derived from Eqs. (45) and (49):

$$\mathbf{L}(x_A) = (5b/3)^{1/2}\mathbf{A}_A/\varepsilon_o = a_{ul,o}\mathbf{A}_A/\mu_{eff}\varepsilon_o = (1 - n^2/\varepsilon_o)\mathbf{A}_A/4\pi\mu_{eff}n_o \tag{50}$$

Since $(1 - n^2/\varepsilon_o)$ is close to unity for associated polar liquids, $\mathbf{L}(x_A)$ only depends strongly on the value of the electric displacement. From Eq. (50), to a good approximation up to x = 2.5:

$$\mathbf{P}_{ul,A}.\mathbf{A}_A/2 = -\mu_{eff}(\mathbf{A}_A.\mathbf{A}_A)8\pi n_o \tag{51}$$

So long as $\mathbf{P}_{ul,A}$ and $\mathbf{L}(x_A)$ are proportional to $\mathbf{A}_A$, the polarization produced can oppose the displacement. When $\mathbf{L}(x_A)$ tends to its high-

field value of 1 – 1/x starting at about x = 3 $[L(x_A) = 0.67)]$, the polarization can no longer oppose the displacement, so ε_A falls rapidly.

For $x_A = 3$, Eq. (35) gives $\varepsilon_A = 53.2$ at $A_A = 7.39 \times 10^5$ esu-cm^{-2}, whereas Eq. (42) with m = 0.5, and Eq. (49), both with $b = 3.15 \times 10^{-9}$, give $\varepsilon_A = 52.0$ and 53.2 at the same displacement, corresponding to distances of 2.55 Å, 3.60 Å, and 4.41 Å from ions with z = 1, 2, and 3 respectively. In this range of x_A and A_A, the Booth expression may be in error as the structure of water begins to break down in high fields. At smaller values of A_A the error would much less, e.g., for x = 1, the values are 73.6 and 73.5, respectively at $A_A \approx 3.41 \times 10^5$, i.e., distances of 3.75, 5.31, and 6.50 Å for z = 1, 2, 3. For x = 2 the corresponding values would be 63.5 and 64.0, with $A_A \approx 5.88 \times 10^5$, and 2.86, 4.04, and 4.95 Å. The extent of structure-breaking at x = 3 (i.e., when the interaction energy between the librating or rotating dipole and the cavity field is 3kT) is indicated by the fact that the average angle of the superdipole to the field is then $\cos^{-1}L(3) = \cos^{-1}0.672 = 47.8°$. This limiting value of A_A should cover all requirements for calculations involving the outer solvation sphere and corresponds to a upper limiting value of x and $L(x)_A$ which may be reasonably consistent with Booth's simplifying assumptions. This is further discussed in Section III-12.

So far the mean Gibbs energy of interaction between an ion and a single dipole (Eq. 18) has been ignored. This should not be confused with the effective potential energy to describe the dynamics of superdipoles of effective moment $\mu' = 1.5B\mu_v(n^2 + 2)/3$. The moment μ_{eff} of the central dipole of each superdipole group is $A\mu_v(n^2 + 2)/3$. The latter, multiplied by the field and $L(x_A) = L\{1.5BE_A[\mu_v(n^2 + 2)/3]/kT\} = \cos\theta$ is the potential energy required to torque the central dipole to a thermally-averaged angle θ to the internal field. The Gibbs energy of interaction between an ion and a single dipole (from Eq. 18) at low to moderate fields is $-\mathbf{P}_A\cdot\mathbf{A}_A/2n_o = -\mu_{eff}L(x_A)A_A/2$, while the Langevin potential energy is $-\mu' A_A/\varepsilon_A$, i.e., their ratio is $(A/3B)L(x_A)\varepsilon_A$, where A and B are from Eq. (35). From Eq. (49), this becomes $(A/3B)L(x_A)(\varepsilon_o^2 - 2bA_A^2)^{1/2}$. At $x_A = 0.3$, when the Booth theory predicts $\varepsilon_A = 77.9$ at an A_A value of 1.08×10^5 (6.7, 9.4, and 11.5 Å from ions with z = 1, 2, and 3), the Gibbs energy of interaction is already 0.33kT. At $x_A = 1$, it has become 3.3kT, and at $x_A = 2$, 9.6kT. This approaches the strength of hydrogen bonds, so water molecules will become successively stripped from the tetrahedral super-dipole, and the associated Kirkwood-Booth structure will finally approach that of a non-associated Onsager liquid. The tetrahedral group will first line

up with the three nearest dipoles and the central dipole towards the ion, giving a B value > 4*. The initial increase in B, i.e., increase in x, will result in an approximately 30% decrease in ε_A, but both of these are more than compensated by the increase in B in the expression for energy of interaction. As B decreases to the Onsager value of 1.0, the interaction energy becomes slightly more negative, but the dielectric constant will show an increase of ca 25% over the original value, since x becomes smaller. Whether these changes are significant is difficult to tell, since they should be approximately compensated by the fact that Booth's assumptions regarding the Onsager-Frölich cavity field for $\mathbf{F}_A$ and the Lorentz cavity for n^2 will begin to fail. As stated earlier, the Langevin derivation assumes free rotation. The transition from free rotation to vibration occurs at $x_A > 0.25$ per degree of freedom. At energies above the limit, the fraction of molecules still capable of rotation will drop rapidly. Most molecules will be vibrating in alignment with the field. Thus, the mean angle to the field will drop more rapidly than predicted by the Langevin function, which in any case will require a quantum correction. Hence, under intense-field conditions, Booth's "bottom-up" approach to the dielectric constant would be best replaced by a "top-down" analysis.

For dipoles close to an ion, it may be assumed that the interaction between the permanent moment and the ion displacement may be given by rewriting Eq. (23) as follows for a single dipole:

$$\Delta g_{ul,A} = (-)(:_v.\mathbf{A}_A/2 - :_v.\mathbf{E}_A/2 - \mathbf{X}_A) \qquad (52)$$

where $\mathbf{X}_A$ is defined in Eq. (22). This assumes that the Lorentz and Onsager cavities have disappeared, so $q_A = 1$ and the permanent moment has reverted to its vacuum value. The angle between the moment and the displacement can be assumed to be 0. The induced dipole will be calculated separately. Since $\mathbf{E}_A = \mathbf{A}_A/\varepsilon_A = \mathbf{A}_A + \mathbf{E}_{p,A}$, we obtain from Eq. (22):

$$\Delta g_{ul,A} = (-)(:_v.\mathbf{A}_A + :_v.\mathbf{E}_{p,A}/2 - W_A) \qquad (53)$$

---

* Booth[124] suggests 5, but this seems unlikely. The tetrahedral group will be expected to take up an orientation with the base of the pyramid towards the ion. Two the base water molecules can rotate to align themselves in the direction of the ion, while the other must be bent through about 50°. The other two dipoles will be less affected by the field.

which is equivalent to the familiar expression used by Bernal and Fowler,[16] in which the negative $\mu_V.E_{p,A}/2$ term is the repulsive energy per dipole due to the presence of all other dipoles in the system, and W_A is the work to detach the selected dipole. This work may be calculated by integration:

$$X_{ul,A} = -(\mathbf{P}_A.\mathbf{E}_A + W_A) = -\int_{F_{A,l}}^{F_A} \mathbf{P}_A \, d\mathbf{F}_A = -\mu_{eff} \int_{F_{A,l}}^{F_A} \mathbf{L}(x_A)\, d\mathbf{F}_A$$
$$= -(AkT/B)\ln[x_{A,l}(\sinh x_A)/x_A(\sinh x_{A,l})] \qquad (54)$$

where $F_{A,l}$, $x_{A,l}$ are the values corresponding to the lower limit of structure-breaking, and F_A, x_A are the values close to the ion. However, in view of all the uncertainties given above, $X_{ul,A}$ may be equated to the work of breaking one hydrogen bond (although some degree of hydrogen bonding may be possible at the side of the dipole away from the ion).

We now note that in Eq. (35), the local dielectric constant ε_A is equal to $\mathbf{A}_A/(\mathbf{A}_A + \mathbf{E}_{p,A})$, so that it may be calculated in a "bottom-up" manner if the average geometries of successive shells of dipoles are known. The dipole field is proportional to $1/a^3$, but the number of dipoles per shell increases as a^2, so the summation should be carried out until sufficient accuracy is achieved. Section IV attempts to do this for the inner, second, and third shells.

9. The Ion-"Continuum" Interaction in Polar Liquids

From Eqs. (18), (23), and (24):

$$d\Delta G_A = (-)(\mathbf{P}_{ul,A}.\mathbf{A}_A/2 + \mathbf{P}_{e,A}.\mathbf{A}_A/2)dV \qquad (55)$$

From $\mathbf{P}_{ul,A} = \alpha_{ul} n_o \mathbf{E}_A = (\mathbf{A}_A/\varepsilon_A)(\varepsilon_A - n^2)/4\pi n_o$; $\mathbf{P}_{e,A} = \alpha_e n_o \mathbf{E}_A = (\mathbf{A}_A/\varepsilon_A)(n^2 - 1)/4\pi n_o$, we obtain:

$$d\Delta G_A = -(\mathbf{A}_A^2/8\pi)[(1 - 1/\varepsilon_A)]dV \qquad (56)$$

Using Eq. (49), which is valid to $\mathbf{L}(x_A) \approx 3$, Eq. (44) may put in the form:

$$d\Delta G_A = -(\mathbf{A}_A^2/8\pi)[1 - (\varepsilon_o^2 - 2b\mathbf{A}_A^2)^{-1/2}]dV \qquad (57)$$

After putting $dV = 4\pi a^2 da$, expanding, and integrating from a_o to ∞, the result is:

$$\Delta G_A = -(z^2e^2/2a_o)[(1 - (1/\varepsilon_o)(1 + t/5a_o^4 + t^2/6a_o^8 .....)] \quad (58)$$

where $1/\varepsilon_o \approx 0.013$, and $t = bz^2e^2/\varepsilon_o^2 \approx 11.7z^2$ (with a in Å). We are interested in a_o values for z = 3 of about 5.2 Å, where the terms corresponding to the advent of dielectric saturation make no more that about an additional 0.04% contribution to the total Gibbs energy of interaction of the ion with the continuum.

Buckingham[96] reached a similar conclusion using a Born "self energy" argument. Instead of using $(\varepsilon_o \mathbf{E}_A.\mathbf{E}_A/8\pi)dV$, with $dV = 4\pi a^2 da$, integrated from a_o to ∞, he used its equivalent differential for the electrostatic energy density in dV, $\mathbf{E}_A d\mathbf{A}_A/4\pi$[133], integrated from 0 to $\mathbf{A}_A$, multiplied by $dV = 4\pi a^2 da$ integrated from a_o to ∞. He expanded ε_A in an even power series,[121] concluding that the distances in second and higher water dipole shells made the higher terms negligible, thus dielectric saturation there could be ignored.

As in Eqs. (19) and (20), the integration here is to ∞, and so represents the infinite dilution case. In the relatively concentrated (0.1-1.0 M) solutions used in electrochemical kinetic experiments, the summation or integration should be taken over the appropriate number of shells to electroneutrality. Since the Debye-Hückel approximation* will not apply to such cases, this will not be identical with the Debye reciprocal length, but may be given by a pseudo-lattice approximation.[134]

It follows that an equation of Born type, but based on different physical principles (Eq. 56) is a good approximation for the continuum energy in dipolar liquids up to the onset of dielectric saturation at x = 3, provided it is integrated from an appropriate distance somewhat less than that of the superdipole center of the innermost solvation shell from the central ion. This corrected radius will differ from the distance from the ion to the dipole centers of the solvation shell under consideration by about 50% more than the radius of a water molecule.

---

* The Poisson equation should in any case not be applied where there is a gradient of E, e.g., in radial geometry[121], see footnote on p. 207.

10. Induction Effects

Moelwyn-Hughes[93] examined the ion-solvent interaction energy outside of the first coordination shell or Inner Sphere by a non-Born charging method using the same Inner Sphere induction term as Bernal and Fowler[16] and Eley and Evans,[92] i.e., $-\alpha_e(\mathbf{E}_A)^2/2 = -\alpha_e(\mathbf{A}_A)^2/2$ with $\varepsilon_A = 1$ (c.f., discussion under Eq. 18). He also used the Inner Sphere expression for the nuclear part of the polarization, i.e., $-ze\mu_v/a^2$ without no dielectric constant or orientational term $\cos\theta$. The use of this (incomplete)** expression (see Eq. 18) for the nuclear part of the polarization led him to believe that the interaction between an ion and permanent dipoles outside the first coordination shell could be disregarded, since it results in a physically meaningless integral for the Gibbs energy, i.e.,

$$-\int_{a_o}^{\infty} 4\pi n_o a^2 (ze\mu_v / a^2) da = (-\infty) \qquad (59)$$

The correct expression for this interaction to $\mathbf{L}(x<3)$, i.e., $[\alpha_{u,A}\varepsilon_A(\mathbf{E}_A)^2/2]dV$ (Eq. 19) has the same form as that for the induced dipole energy $[\alpha_e\varepsilon_A(\mathbf{E}_A)^2/2]dV$. The use of the combined expression with $\alpha_A = (\varepsilon_A - 1)/4\pi n_o$ (Eq. 19) ensures that it contains the induced electronic component, equal to about 2.3% of the total at 298 K.

11. Polarization of ut Type

The possible presence of polarization of ut type $(\mathbf{P}_{ut,A})$ induced in the non-uniform field rather close to an ion, but still within the validity of the assumptions of Eq.s (48)-(51), (57), and (58) is a possible source of error. Physically, ut polarization consists of dipole translation along field towards the ion, increasing the local value of $\mathbf{A}_A$, $\cos^{-1}\mathbf{L}(x)_A$, and $\mathbf{P}_{ul,A}$. To examine this requires knowledge of the binding forces and energies between water molecules. The potential energy Mie function for each pair is[137]

$$\Phi = Ad^{-12} - (1 + s_c)Cd^{-3} - (1 + s_b)Bd^{-6} \qquad (60)$$

** Marcus[43a], following Mandel and Mazur[135], and Brown[136] stated that many earlier expressions for the polar term for intermolecular energy were incomplete or wrong.

where A, B, and C are constants, d is the distance between the dipole centers of nearest neighbors, and s_c, s_b are structural factors covering interactions with next-nearest and subsequent neighbors. B is the sum of two terms, the first being the dispersion energy, $0.75Z^{1/2}h\nu_e\alpha_e^2$ (= 6.81×10^{-59} erg-cm^{-6}), where Z is the number of electrons, of frequency ν_e, the second being the electronic induction energy,[137] $2\alpha_e\mu^2$, where μ may be put equal to an effective liquid water dipole moment, e.g., 2.42 D,[123] giving 1.69×10^{-59} erg-cm^{-6}. Ref. 137 assumed no dielectric constant in the summation of s_b, s_c to infinity, which cannot be correct. No dielectric constant may be required between nearest neighbors (see later discussion), but an ε_A term is required for next-nearest and subsequent neighbors. Since this will be large, longer-range interactions and s_b, s_c may be neglected.

The minimum energy for two pairs of nearest neighbors, is 49.18 kJ-mole^{-1} in liquid water.[138] The hydrogen bond distance d is 2.76 Å at the melting point and 2.9 Å at 293 K.[103,138] C is $f\mu^2$, where f is a function of the nearest-neighbor angles, with a maximum value of 2.[137] Putting the differential of Eq. (60) equal to zero at d = 2.9 Å, and using Eq. (60) with Φ equal to 4.082×10^{-13} ergs per dipole pair gives A = 6.50×10^5 erg-Å^{12} and C = 1.095×10^{-11} erg-Å^3, i.e., C = $1.87\mu^2$. The number of nearest neighbors in liquid water[138] is actually about 4.4-4.6. With this correction, C falls to $1.57\mu^2$–$1.66\mu^2$, but Pople[103] indicated that using more than 4 nearest neighbors is unjustified, since the larger numbers result from the partial collapse of the second shell. The expression for the interaction of two dipoles[139] inclined at half of the H–O–H bond angle of 104.45°[140] gives f = 1.23. The simplest model for the charge distribution[95] is derived from Rowlinson,[141] but it places all of the negative charge on the oxygen, rather than located symmetrically out of the H-O-H plane.[142] Better models will include the lone pair geometry[143,144] or use the central force potential[145] using repulsive terms for H...H and O O, and an attractive-repulsive potential well for O H.

Duncan and Pople (DP)[143] placed the lone pairs at ±60.1° to the dipole axis. With one end of each molecule aligned at this angle, and the other aligned at half of the bond angle gives f = 1.30. These values assume that the field corresponds to that of a simple dipole of vanishingly small length. An accurate calculation using the DP charge distribution (Section V) shows much higher local fields than predicted by the assumption of simple dipoles at distances of 2.9 Å from the oxygen atom. The fields in line with the H–O axes are ca. 40% higher

than those for an oriented dipole with the Coulson-Eisenberg moment,[123] and those along the sp hybrid orbital–O axes are 10% higher. This explains why the calculated dielectric constant is somewhat low.[103]

The above results give us the possibility of calculating the distortion of the water structure in the shells surrounding the coordination shell or inner solvation sphere of an ion, and an estimate of magnitude of the electrostrictive or translational polarization energy in the continuum to the point of partial dielectric saturation near an ion. The inner shell for 2+ and 3+ ions is a puckered trikisoctahedron,[39,146,147] with dipoles in two overlapping layers at different distances. The dipoles in the (distorted) shell next to the eight outer trikisoctahedron dipoles for ions with z = 3 have centers averaging approximately 5.0-5.2 Å from the central ion. Looking at the system from a simple one-dimensional viewpoint (i.e., along the direction of the electric displacement), it is possible to set up a series of simultaneous equations involving the differentials of Eq. (60) and the differential of $-\mathbf{P}_{ul,A}.\mathbf{A}_A/2$ to give the forces between the various layers. These equations can be solved graphically after being all set equal to zero to allow the amount of electrostriction between the layers to be estimated. The results show that z = 3, the distance between a water dipole with its center initially situated at 5.2 Å from the ion before its charge is "switched on" will translate down the field. However, the one-dimensional translation will be hindered by lateral compression, so that the effective translation will be only about 0.025 Å. A dipole initially situated at 5.5 Å will correspondingly move by 0.02 Å. A dipole situated in the next shell, at about 9 Å from the central ion will move by ≈ 0.005 Å. The movement in subsequent shells will be negligible. The corresponding increases in interaction energy (proportional to r^{-4}) is about 2% at 5.2 Å for z = 3, and 1.8% at 5.5 Å. The cumulative motion in the shell at 8.0-8.3 Å (about 0.03 Å) results in increase of about 1.5%, a percentage which falls slowly in subsequent layers (e.g., 3% at 10.9 Å). Both the small displacement, and the small change in interaction energy are approximately proportional to z^2, so these figures must be multiplied by about 0.44 for z = 2, and by 0.11 for z = 1. A calculation to determine the energy in individual shells suggests that the predominant $(-\mathbf{P}_{ul,A}.\mathbf{A}_A/2).dV$ terms adds about 1.5% to the total electrostatic energy in the continuum measured from r = 5.2 - 5.5 Å for an ion with z = 3, about 0.7% for z = 2, and less than 0.2% for z = 1. The electronic polarization energy terms $(-\mathbf{P}_{e,A}.\mathbf{A}_A/2).dV$ will be similarly affected. For z = 3 and r = 5.2

Å, the estimated dielectric constant is 63.5 from Eq. (35), and $\mathbf{E}_A = 8.3 \times 10^3$ esu-cm^{-2}. The estimated electrostrictional molar volume change (0.144 x 18) is 0.26 cm^3-mole^{-1}. This is in good agreement with the estimates of Desnoyers, Verrall, and Conway[148] for this field strength. The effect of the term $(-\mathbf{P}_{ut,A}.\mathbf{A}_A/2).dV$ on the interaction energy of interaction up to dielectric saturation is small, but not negligible.

12. Quadrupole or Multipole Effects

A trigonometrical calculation[96] shows that an water quadrupole-ion displacement interaction energy at ionic (charge ze) distance a from the dipole center is:

$$d\Delta\Phi_A = -ze(\mu/l)[(l\cos\theta/a^2 \pm y^2(1 - 3\cos^2\sigma\sin^2\theta)/2a^3] \qquad (61)$$

where partial charges $\pm\mu/2l$ are on the protons and oxygen, 1, y are the dipole length and half of the distance between the partial positive charges, σ is the angle of y to the plane containing a and the dipole axis, and θ is the mean angle $\cos^{-1}\mathbf{L}(x)_A$ of the dipole axis to the field. The $\pm$ signs before the angle independent quadrupole terms refer to positive and negative ions respectively, i.e., if a is measured from the dipole center, the interaction energy to a positive ion is more negative than that of an equivalent simple dipole. In most texts, ion distance is measured from either the geometric center or center of gravity of the water molecule. The latter is situated about 0.066 Å from the oxygen atom, so a further term $\pm[(0.066)^2 - (l - 0.066)^2]/a^3$ must be added within the square brackets. The effect of the differently defined quadrupole moment may be to reverse the difference between the ions at constant a (see Appendix).

Equation (61) is $-\mathbf{P}_{ul,A}.\mathbf{A}_A$ for a simple molecular quadrupole. Assuming free rotation, the average value of $\cos^2\sigma \approx 1/3$, giving a ratio of the mean quadrupole to dipole interaction equal to $[1 \pm (y^2\cos\theta)/2al)$, or from Eq. (50) and the definition of $\mathbf{A}_A$, $[1 \pm (1 - n^2/\varepsilon_o)y^2ze/8\pi\mu_{eff}n_oa^3l]$. After inserting numerical values,* this is $(1 \pm 1.085z/a^3)$, with a in Å. Multiplying Eq. (57) by this amount and integration from a_o to ∞ gives:

---

* Dipole length l = 0.5871 Å, bond angle 104.45°, bond length 0.9584 Å[140], hence y = 0.7575 Å.

$$\Delta G_A = -(z^2e^2/2a_o)[(1 - 1/\varepsilon_o) \pm 1.085z(1 - 1/\varepsilon_o)/4a_o^3 - t/5\varepsilon_o a_o^4 \pm 1.085z(-1)t/8\varepsilon_o a_o^7 - t^2/6\varepsilon_o a_o^8 ..)] \quad (62)$$

where t is defined under Eq. (57). For z = 3 and a_o = 5.2Å, the first quadrupole term contributes only about 0.1% to ΔG_A, with negligible contributions for higher terms. The same argument should be applied to DP multipoles in Kirkwood tetrahedral groups, but there is no reason to believe that the result would be very different.

13. At Dielectric Saturation

The local dielectric constant $\varepsilon_A = \mathbf{A}_A/(\mathbf{A}_A + \mathbf{E}_{p,A})$ is $n^2 + 4\pi\mathbf{P}_A/\mathbf{E}_A$ only for a constant, parallel field. The factor 4 in $4\pi\mathbf{P}_A/\mathbf{E}_A$ will become smaller at small distances, when individual dipoles are no longer parts of quasi-continuous shells of charge (Appendix 1). Within the limits of his assumptions, Booth rather rigorously obtained an expression for ε_A containing the Langevin function, whose derivation uses the Boltzmann distribution and classical statistical mechanics. These may both become invalid for a small cohort of dipoles whose interaction with the field approach kT. In a parallel field, a large number of dipoles of all energies may be readily found, so that Stirling's formula for factorials of large numbers used in deriving the Boltzmann distribution depends should be satisfied.

In radial fields near an ion, the population of Langevin dipoles in a given interaction range becomes rapidly less with decreasing ion-dipole distance, e.g., in a shell of thickness 5.8 Å with a center at 6.3 Å there are about 20 superdipoles, with about 5 times as many in the next shell. A less approximate Stirling expression

$$\ln N! = 1/2\ln 2\pi N + N\ln N - N \quad (63)$$

gives an acceptable value for N! even for small N (–7.8%, – 4.0%, –2.7%, –1.4% for N = 1, 2, 3, 6 respectively). The modified Boltzmann distribution then is approximately:

$$N_i/N = (\exp - e_i/kT)(\exp - 1/2N_i)/\Sigma(\exp - e_i/kT)(\exp - 1/2N_i) \quad (64)$$

where N_i is the number of molecules in the ith state of energy e_i, in a total population of N molecules. The numerator and the partition function f in the denominator contain the weighting factor $\exp -1/2N_i$

for each N_i. As a minimum (see above), we are interested in N_i values corresponding to a fraction of the subpopulation of molecules in the first shell for 1+ ions, whose motions (see below) have transitioned from free rotations to large amplitude librations under the influence of the ion field. The distortion in the energy distribution function is to give smaller weighting factors for large e_i and small N_i. The smaller f values will result in smaller mean thermal energies than the classical Boltzmann values, which will generally result in smaller mean angles of the dipole to the field, i.e., somewhat smaller effective values of ε_A near the ion than Booth's theory predicts. This error will become progressively less so for successive shells.

The Boltzmann distribution assumes no interaction between molecules, i.e., an ideal system. When dipoles are oriented by a strong field, they interfere with each other. In relatively weak fields, free rotation of solvent dipole groups occurs, as the Kirkwood-Booth model of the low-field value of the dielectric constant requires. The Schrödinger equation for a rigid rotating dipole cluster of effective moment undergoing planar rotation in an internal electrostatic field $\mathbf{F}_A = ze\mathbf{q}_A/\varepsilon_A a_A^2$ is:

$$\partial^2\psi/\partial\phi^2 + (8\pi^2 I/h^2)(E - V\cos\theta_A)\psi = 0 \qquad (65)$$

where θ_A is the mean angle between the dipole and the field, ϕ is the angular displacement from θ_A, E is kinetic energy, and $V = ze\mathbf{q}\mu'/\varepsilon_A a_A^2$, with μ' as in Eq. (34) and a_A equal to the distance from an ion. The other symbols have their usual meanings. This equation has one total energy minimum at $\theta = 0$. Similar wave equations with two minima (at $\theta = 0$ and π, for hindered rotation in a crystal) and for three-dimensional rotation with n minima (at $q \approx 0, 2\pi/n, 2\pi/2n$, etc., for hindered internal rotation of, e.g., CH_3 groups within a molecule rotating in space) have been evaluated.[149,150] The eigensolutions for such equations transition from those for a non-degenerate free rotation (when $V << 0.25kT$) to approximately those for a harmonic vibration (when $V >> 0.25kT$). From Eqs. (35) and (36), this transition will occur at practically the bulk ε_o value at 7.3, 10.3, and 12.6 Å from ions with z = 1, 2, and 3 respectively. For z = 1, this is a little beyond the center of the first Continuum shell, while for z = 3, it is closer than the center of the second shell. At the center of the first Continuum shell at 6.3 Å for z = 1 ions (Sections III-2 and IV), Eqs. (49) and (35) show x = 0.34 and ε_A = 77.8. For z = 3 ions at 7.6 Å, the corresponding values are x = 0.72

and $\varepsilon_A = 75.8$. Under these circumstances, Booth's assumptions (including the use of the classical Boltzmann distribution may still approximately apply), and the superdipoles with maximum energy of kT per axis will be performing large-amplitude librations. The frequency of free rotation (ν_o) of superdipoles under energy equipartition conditions at 298 K is estimated as 1.25×10^{11} s^{-1} in Section VI-1. The libration frequency[151] will be slightly less at $\nu_o(1 + 1/16x)^{-1}$. Both are well within the classical range, so quantum corrections to the energy function are not required. Thus, we conclude that while physically, Booth's assumptions and the approximations considered here may still have value to x = 3, in reality, they can be abandoned at x = 0.3-0.75. At higher field strengths, the dipoles become fully oriented and dielectric saturation rather suddenly occurs.

We therefore arrive at Eq. (53), the classical expression used by Bernal and Fowler[16] for the inner sphere, with the addition of a small additional term, which may be regarded as a $+T\Delta S$ term for the break-up of the solvent structure, which can be replaced by an estimate of the energy to break the structure of water.

14. Summary of Ion-Solvent Interactions

The above discussion shows that the electrostatic free energy of solvation can be divided into an coordination shell or inner solvation sphere in which ε_A is close to 1, where the $\mathbf{P}_u$ interaction depends only on $-\mu\mathbf{A}_A$, and an outer solvation sphere where the $\mathbf{P}_A$ interaction depends to a good approximation on Eqs. (55)-(57), but in which the electrostatic Gibbs energy may be approximated by the integral in Eq. (58), which resembles the Born charging equation, but it is obtained in a different way with a more definite physical meaning.

An accurate estimate of the electrostatic Gibbs energy of interaction between an ion and the polar molecular "continuum" should be summed to the point of electroneutrality over all time-averaged solvent molecule charge positions and configurations, but a sufficiently accurate expression may be obtained by the above integration from a carefully chosen minimum distance. This distance is the weighted mean of the dipole center distances in the first shell of the continuum surrounding the solvated ion, minus a correction term equal to about 2.00 Å. Almost 60% of the continuum energy is typically in the first "outer" shell, which is characterized by a somewhat lower dielectric constant than the bulk value estimated by the Kirkwood-Booth

theory.[72,73,124,125] However, since the local value of the dielectric constant, ε_A enters into the final energy expression via a factor $[1 - 1/\varepsilon_A]$, the overall change in Gibbs energy due to the change in dielectric constant is small. Grahame[117] reached a similar conclusion using Born charging in conjunction with the differential dielectric constant, Eq. (42).

To a good approximation, the quadrupole or multipole model of the water molecule may be considered to be a dipole to estimate the electrostatic Gibbs energy of interaction with the continuum. Booth's expressions[73,124,125] for the dielectric constant break down more rapidly in large radial fields than in parallel fields. The dielectric constant to be used under these conditions can only be determined by evaluating the opposing local counterfields. The limit corresponds to $x \approx 3$, where Booth's model would begin to be increasingly inaccurate if it were still physically relevant. Because of the abruptness of the change from high values of the local dielectric constant to essentially vacuum values, Bernal and Fowler's division of the energy of interaction of an ion and a dipolar solvent into Inner and Outer Spheres[16] is justified.

IV. THE INNER SPHERE(S)

1. Multivalent Cations as Trikisoctahedra

A model is given here for multivalent cations with large Gibbs energies of hydration with "puckered" trikisoctahedral[39,146,147] primary or inner solvation shells. These dipoles are in direct line-of-sight of the ion and have an intense interaction with the displacement $\mathbf{A}_A$ in a given volume element dV. It has been suggested that they may be surrounded by monomeric water, depending on the ionic charge[152], but this improbable given the discussion in Sections III-12 and -13. Multivalent single-atom anions should behave like cations, but large multiatomic anions should have a single-shell structure.

It has been generally assumed[16,92,93] that the Langevin function $\mathbf{L}(x)_A$ for these dipoles will be close to unity. Because of the close line-of-sight interactions, the assumptions required for the presence of Onsager and Lorenz cavities fail under these conditions. Frölich's requirement[108] that the cavity must be a spherical volume large enough to have the dielectric properties of a macroscopic specimen, and contain a sufficient number of charges to be treated by classical statistical mechanics cannot be so next to an ion, where the internal to external

field ratio q_A will be close to unity, and the effective moment μ_{eff} should be close to the vacuum value (discussed under Eq. 37).

Booth's theory[73,124,125] predicts that ε_A will fall to n^2 in intense fields, however the space involved in ion to nearest-neighbor-dipole interactions is not bathed in an electronic medium. The ion itself is not polarized, since there is no net field in spherical symmetry. Thus, n^2 should be unity for the primary shell and other nearest-neighbor interactions, c.f., Bernal and Fowler,[16] Eley and Evans.[92] The dipole fields $\mathbf{E}_{p,A}$ opposing the ion dielectric displacement $\mathbf{A}_A$ may be calculated from the fields of nearest-neighbor and more distant dipoles to obtain the local dielectric constant $\varepsilon_A = \mathbf{A}_A/(\mathbf{A}_A + \mathbf{E}_{p,A})$. Components of $\mathbf{E}_{p,A}$ determine the repulsive energies between pairs of dipoles, and produce the net external field $\mathbf{A}_A/\varepsilon_A = \mathbf{A}_A+\mathbf{E}_{p,A}$, whose internal field creates induced dipoles. Previous work[10,92,93,152] has generally ignored the effect of the dipole fields on induction, which can lead to considerable error for high-z ions with up to 14 trikisoctahedral dipoles. At dielectric saturation, the Gibbs energy of ion-nearest-neighbor-dipole interaction is given by Eqs. (52) and (53), with q_A, n^2 and $\cos\theta$ close to unity, with μ_{eff} close to μ_v. With $\mathbf{E}_A = \mathbf{A}_A/\varepsilon_A = \mathbf{A}_A + \mathbf{E}_{p,A}$, we obtain the equivalent of the Bernal and Fowler expression[16] for the inner sphere ion-permanent dipole interaction:

$$\Delta g_{ul,A} = (-)(:_v.\mathbf{A}_A + :_v.\mathbf{E}_{p,A}/2 - W_A) \qquad (66)$$

in which $:_v.\mathbf{E}_{p,A}/2$ is the energy per dipole due to the presence of all other dipoles in the system, and W_A is the work to detach the dipole from its environment in the presence of $\mathbf{A}_A$. In principle, W_A may be calculated (Eq. 54). Work is first required to orient the axes of freely-rotating transient groups of superdipoles, then more is needed to detach water molecules from these. Per dipole, this may be equated to the work of breaking a maximum of one hydrogen bond, since some hydrogen bonding should always be possible in the direction away from the ion.

The inner sphere of relatively small ions is generally accepted to have 4 or 6 dipoles in symmetrical tetrahedral or octahedral coordination, depending on the ion size and charge. In principle, these might respectively accommodate 4 and 8 other oriented intercalated dipoles as a second shell. In the tetrahedral case, the second dipole group would be at $(180 - \phi)°$ from the first, where ϕ is the tetrahedral angle, i.e., at 70.53°. In the octahedral arrangement, the second set are

at $\phi/2$, i.e., at $\sin^{-1}(2/3)^{0.5} = 54.74°$ from the first. The octahedral arrangement is most frequent with high-z ions with octahedral d-orbitals, which make at least some contribution to their solvation energies.[153]

If the ion-dipole center distance is 2.75 Å and the overall packing corresponds to the closest approach distance for water (taken as 2.76 Å), then the second set of dipoles are 15% further away than the first, whereas if it is 2.5 Å, the second group are 31% further away. The concept of a tightly bound inner shell and a more loosely bound second shell offers a good explanation for the coordination number (c) and hydration number (n).[154,155]

Inner sphere equilibrium solvation energy calculations have generally used rather simple models, rather than attempting to determine the energy well parameters. Bernal and Fowler[16] included ion-permanent dipole and ion-induced dipole terms with Van der Waals attractions and Mie ion-water repulsions, with no exact calculations. Eley and Evans[92] replaced the permanent dipole term by point charges, and Moelwyn-Hughes[93,98] used Mie repulsive terms. Since the quadrupole concept was introduced,[96,141] a quadrupole term has generally been added to the permanent dipole term.[154] Often[154,156] no Mie repulsion term has been used, the ion-dipole distance being taken as the ion crystal- plus water molecule radii, where a reactive wall occurs. Such a model cannot give a correct description of the energy well and the force constant. The pair potentials[144,157] used in molecular dynamic simulations in recent years are also rather simple, and do not use the feedback of electrostatic fields.[145,158]

2. Inner and Second Sphere Energies

From Eq. (18), the potential energy of interaction Φ_{inner} of permanent $:_p$ and induced dipoles $:_i$ close to an ion may be written:

$$\Phi_{inner} = -:_p.\mathbf{A}_A - \tfrac{1}{2}:_p.\mathbf{E}_{p,2} + \mathbf{W}_{A,p} - :_i.\mathbf{A}_A - \tfrac{1}{2}:_i.\mathbf{E}_{p,1} + \mathbf{W}_{A,i} + \Sigma\phi_i \qquad (67)$$

where $\mathbf{W}_{A,p}$, $\mathbf{W}_{A,i}$ are the work to create the dipoles, $\mathbf{E}_{p,1}$, $\mathbf{E}_{p,2}$ are the dipole field vectors along the ion displacement and μ_p axes, and the ϕ_i terms are the Mie repulsions between the dipole, its closest neighbors, and the ion. The factor 1/2 in the $\mathbf{E}_p$ terms avoids double counting. Following Eq. (18), $\mathbf{W}_{A,i} = +:_i.\mathbf{F}_A/2 = +:_i.(\mathbf{A}_A + \mathbf{E}_{p,1})/2$, giving:

$$\Phi_{inner} = -:_p.\mathbf{A}_A - \tfrac{1}{2}:_p.\mathbf{E}_{p,2} + W_{A,p} - :_i.\mathbf{A}_A/2 + \Sigma\phi_i \qquad (68)$$

The work $W_{A,p}$ to break up the superdipole structure in associated polar liquids is small compared with $+:_p.\mathbf{A}_A$. We see that the repulsive interaction between the induced electronic dipole and the total dipole field along the displacement axis has disappeared, i.e., all repulsive energy terms for each $:_i.:_i$ and $:_i.:_i$ pair are included in their work of formation, and repulsive terms containing $:_p.\mathbf{E}_{p,2}$ only involve those between permanent dipoles, giving an important simplification. If required, the appropriate quadrupole corrections can be added to the $\mathbf{E}_{p,2}$ values along the axis of each $:_p$, but this greatly complicates the calculations. By definition:

$$:_i = \alpha_e(\mathbf{A}_A + \mathbf{E}_{p,1}) \qquad (69)$$

The dipole field creating $:_{i,1}$ along the ion displacement axis is a geometrical function of all permanent dipole $:_p$ and induced dipole $:_i$ terms for a system of n dipoles:

$$:_{i,1} = \alpha_e\mathbf{A}_{ion} + \Sigma g_{p,j}:_{p,j} + \Sigma g_{i,j}:_{i,j} \qquad (70)$$

where the $g_{p,j}$, $g_{i,j}$ terms are geometrical factors associated with the displacements for jth dipoles of each type. If appropriate, these may contain the optical refractive index n^2. A similar equation is written for each $\mu_{i,j}$ and the simultaneous equations are solved for each $:_{i,j}$ for the given system geometry. The net field $\mathbf{E}_A = \mathbf{A}_A + \mathbf{E}_{p,1}$ along the ion displacement axis is thus obtained from Eq. (68), giving the local dielectric constant $\varepsilon_A = \mathbf{A}_A/(\mathbf{A}_A+\mathbf{E}_{p,1}) = \alpha_e\mathbf{A}_A/:_i$. A simple illustration for two dipoles of induced moment μ_i with centers at distance x from an ion, both permanent moments μ_p inclined at θ to the ion displacement has $\mu_i = \alpha_e(A_{ion} - g\mu_p\cos\theta/x^3 - g\mu_i/x^3)$. Rearranging:

---

* The first water molecule model used here assumed for simplicity that the negative dipole charges are at 0.15 Å from the oxygen atom center, in the H-O-H plane[92, 159]. This was modified as necessary as the fitting proceeded. This model results in a dipole length of a 0.436 Å. At the distances considered (with x at about 5 times the dipole length), the repulsive terms for a dipole differ from those of an aligned water quadrupole by less than 1%. However, both the axial field term, and the potential energy of interaction estimated from the point charges are 12-13% higher than those for the corresponding x^3 and x^2 terms for the corresponding quadrupole approximation.

$$\mu_i = (zex - g\mu_p\cos\theta)/(x^3/\alpha_e + g) = \mu_p(2.377zx - g\cos\theta)/(0.693x^3 + g) \quad (71)$$

where g is the appropriate geometrical factor, the numerical factor 2.377zx (with x in Å) is the ratio zex/μ_p, with μ_p nominally equal to 2.02 D, and $0.693x^3$ is x^3/a_e ($a_e = 1.444 \times 10^{-24}$ cm^3). At typical values of x for z = 1, A_{ion} is such that μ_i is rather small (e.g., $0.3\mu_p$). It becomes much more important for z = 3. This is performed for all dipoles in the system until the necessary accuracy is obtained. Often it is only necessary to consider dipoles of one type in a single shell, as above. Some properties of such an assembly of permanent dipoles may be illustrated by considering a simple model of a line of permanent dipoles with an effective number of closest neighbors equal to n (a Madelung constant for the line[160]), at a closest neighbor distance x'. The dipole displacement at an angle α to a line intersecting the center of a dipole μ_p at an angle β at a distance x', and where γ, γ', are the angles subtended by the planes containing the angles α and β and a reference plane containing the line (Figure 4)* is given by[139]:

$$\mathbf{E}_p = -(\mu_p/x'^3)[2\cos\alpha\cos\beta - \sin\alpha\sin\beta\cos(\gamma - \gamma')] \quad (72)$$

For the dipole array in question, $\gamma = \gamma' = 90°$, and putting $\alpha = \beta = (1 - \theta)$, the dipole field $\mathbf{E}_{p,2}$ along the axis of each dipole will be $+n\mu_p(1 - 3\sin^2\theta)/x'^3$, so the interaction energy of one dipole with the others is $+\mu_p\mathbf{E}_{p,2}/2$, where the 1/2 avoids double counting. The dipole field $\mathbf{E}_{p,1}$ perpendicular to the line opposing the displacement $-\mathbf{A}_{ion}$ will be equal to $+n\mu_p\cos\theta/x'^3$. The field orienting the dipole array is $-\mathbf{A}_{ion} + (n\mu_p\cos\theta)/x'^3$, so $\varepsilon_A = A_{ion}/[A_{ion} - (n\mu_p\sin\theta)/x'^3] = \alpha_e\mathbf{A}_{ion}/:_i$, allowing $:_i$ to be calculated. For simplicity, $\alpha_e\mathbf{A}_{ion}/:_i$ is assumed independent of $\cos\theta$, but the electron distribution will be anisotropic due to the directional nature of the chemical bonds.[99,121] The electrical potential energy of each permanent dipole is:

* The description of the angles is unclear in Ref. 139.

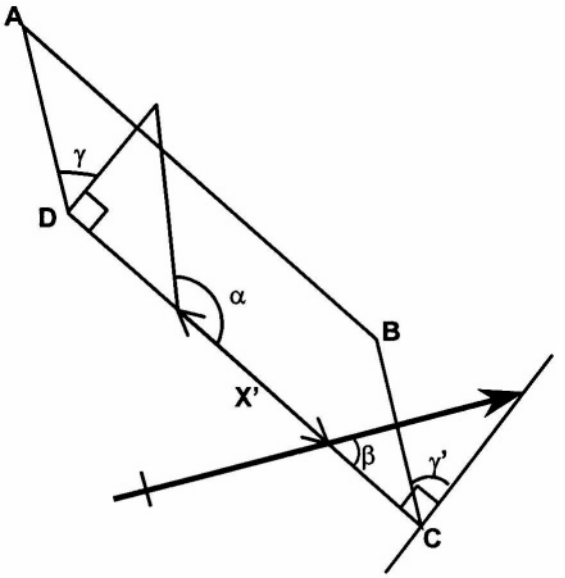

Figure 4. Dipole field angles. ABCD is a reference plane.

$$\Phi = -A\mu_p\cos\theta + n\mu_p^2(1 - 3\sin^2\theta)/2x'^3$$
$$= -A_{ion}\mu_p\cos\theta + 1.5n\mu_p^2\cos^2\theta/x'^3 - n\mu_p^2/x'^3 \quad (73)$$

where the $-n\mu_p^2/x'^3$ term is the potential energy of a dipole in the undisturbed dielectric fluid. Equation (73) minimizes at $\cos\theta = 1$ for $A_{ion} > 3n\mu_p^2/x'^3$, and at $\cos\theta = A_{ion}/(3n\mu_p/x'^3)$ at $A_{ion} < 3n\mu_p/x'^3$.

To illustrate the properties of a spherically symmetrical dipole assembly around an ion, we first consider only permanent dipoles to see the effects of counterfields and repulsion terms. If the examination of second and third shells shows little effective energy for permanent dipoles, there is no point in examining induced dipoles, since the induction fields will be negligible. In spherically symmetrical systems are more complex than the above examples, but show similar characteristics. The $\mathbf{E}_{p,1}$ axial field terms due to each neighbor type depend on the angles via a multiplier equal to $(2 - \cos\gamma)\cos^2\alpha_i\cos\theta_i + \cos\gamma_i\cos\theta_i - (2 - \cos\gamma_i)(\sin\alpha_i\cos\alpha_i)\sin\theta_i$, where α_i is the angle between

the displacement axis and the line joining the centers of neighboring dipoles of the ith type, and γ_i is the angle to the dipole to the plane of these neighbors. Molecular models shows that rotation away from the plane to a point mid-way between nearest neighbor sites reduces overall interactions to a minimum. The angular rotations, δ_i, are then ±60° for tetrahedral, and ±45° for octahedral symmetry.

The $\mathbf{E}_{p,2}$ repulsive fields between symmetrically arranged dipoles in the same shell along their axes are $+(\mu_p/x_i^3)(n_i/y_i^3)[2(\cos^2\theta_i - \sin^2\alpha_i) + (\cos^2\theta_i - \cos^2\alpha_i)(\cos 2\gamma_i)] = g_{p,i}(\mu_p/x_i^3)$, where $g_{p,i}$ is the geometrical factor (n_i/y_i^3) of the ith type. From geometrical considerations. $\sin\gamma_i = \sin\theta_i\sin\delta_i$, so $\cos 2\gamma_i = 1 - 2\sin^2\theta_i\sin^2\delta_i$, and $\cos\gamma_i = (1 - \sin^2\theta_i\sin^2\delta_i)^{0.5}$.

The potential energy of interaction of an ion with a single solvent permanent dipole in a spherical shell is given by:

$$\Phi_{inner} = -A\mu_p\cos\theta + \sum g_{p,i}\mu_p^2/2x^3 + \sum\phi_i \qquad (74)$$

If required, the attractive interaction can be represented by the quadrupole expressions (Eqs. 61 and 62), and the $\mathbf{E}_{p,A,1}$ field term can be estimated assuming point charges. This results in the appearance of additional terms in $\cos^3\theta$ and higher powers. These refinements will be ignored for the present.

Equation (74) minimizes for $\cos\theta$ for any given value of x, and for x at any given value of $\cos\theta$. We can find the distance at which $\cos\theta$ is equal to unity in simple systems (tetrahedral, octahedral) by differentiating Eq. (74) with respect to $\cos\theta$, and putting $\cos\theta$ equal to unity in the equilibrium condition. For tetrahedral groups $\cos\theta = 1$ for $x > 1.594$ Å for univalent ions, assuming an effective value of $\mu_p = \mu_v$ in water = 2.02 D, to be refined as required. However, the minimum energy with $\cos\theta = 1$ would be at 0.362 Å i.e., at $x = 3(n/y^3)(1 - \sin^2\alpha/2)\mu_p/2ze$, which is physically meaningless. In tetrahedral symmetry, the corresponding figures are $x > 2.676$ Å for $\cos\theta = 1$, with minimum potentials are $x = 1.394$ Å for $z = 1$, and 0.697 Å for $z = 2$. Graphical calculation* shows that the function is unstable, with no potential well, if x and θ are allowed to vary simultaneously where this is physically meaningful. A symmetrical group of dipoles will then move down the field towards the central ion, and $\cos\theta$ will go from

* Graphical simulations were performed using the graphing calculator function on an Apple Macintosh PowerPC personal computer.

unity to successively smaller values as the repulsive energy term increases, but the energy of attraction still continues to increase as x becomes less, until the Mie repulsive energy terms between the ion and the dipoles, and between the dipoles themselves, take effect.

Because of the instability of the functions, we are justified in making the simplifying assumption that the dipole axes are aligned along the displacement axis in the high fields close to the ion, when the basic assumptions for the theory of the Langevin function have broken down. It has been suggested that this may not occur, to allow for the possibility of more favorable hydrogen bonding to associated water molecules.[161] This is discussed in the Appendix, which shows that the *effective* dipole axis for multipoles may not coincide with the normal symmetrical dipole axis.

3. Dipole Nearest Neighbors

In tetrahedral symmetry, there is only one first shell interaction (nearest neighbor, n = 3), whereas in octahedral symmetry, there are both nearest-neighbors (n = 4) and second-nearest neighbors on the other side of the ion (n = 1). The interactions between the first shell and the second may be handled similarly. In this case, the geometry of the axes is not an isosceles triangle and the equations for calculating the angle expressions in the g_i terms are more complex, but the principles are the same. Since the problem is a many-bodied one, reasonable simplifying assumptions are needed to make it tractable. The first is that $\cos\theta = 1$ for the inner shell. Hence, the weak interactions of second-shell dipoles with the central ion, along with the various repulsions, may give a $\cos\theta$ term in the second shell. For the second shell of a trikisoctahedron, there are three nearest-neighbor interactions between a second shell dipole and first shell dipoles, and three second-nearest-neighbor interactions. There are three nearest-neighbor interactions between second shell dipoles, three second-nearest neighbor (diagonal) interactions, and one diagonal interaction with the dipole on opposite side of the ion.

So far, all interactions have assumed that μ_p can be considered to be a dipole. This is a good approximation for repulsions, but not for attractive interactions at shorter range, which require a multipole approach to improve accuracy. Since all calculations were numerical, it was easy to regard the water molecules as having point charges. For simplicity, in initial simulations the center of each positive charge was

at each proton, separated by 2 x 0.757 Å, and the center of negative charge was considered to be at the molecular center of water[16,159] or 0.15 Å from the oxygen nucleus, i.e., a dipole length of 0.436 Å with an effective charge of 2.317×10^{-10} esu for a moment of 2.02 D. Changes were made as needed to improve fitting. The interaction energy (in ergs) of a cation with a fully-aligned permanent quadrupole at an ion-dipole center distance a (in Å) will then be $-ze^2(0.964 \times 10^8)\{(a - 0.218)^{-1} - [(0.757)^2 + (a + 0.218)^2]^{-0.5}\}$.

A test was conducted on the eight identical dipoles of the second shell of a trikisoctahedron. The inner six dipoles in octahedral symmetry with $\cos\theta = 1$ were located nominally at 2.5 Å, to be adjusted to account for experimental energy values and force-constants. In setting up the preliminary equations, electrostatic repulsions were expected to predominate in the loosely-bound second shell, so Mie repulsions between nearest-neighbor water dipoles were first of all ignored, as were attractive London d^{-6} dispersion forces, i.e., crystal field effects, since these are overwhelmed by r^{-4} ion-induced dipole terms for 2+ and 3+ ions. This procedure is the same as eliminating the Mie repulsive terms by differentiating, setting to zero, and minimizing the energy expression.[98] For the two trikisoctahedron shells and the "Outer Sphere," three simultaneous equations were used, with water-water repulsions and dipole-dipole repulsions for all possible dipole pairs included between the first two shells, and the system was iterated until it was self-consistent.

The nearest neighbor distance between a first shell dipole and one in the second shell was initially assumed to be the diameter of a water molecule (2.76 Å). Under these conditions, the distance between the central ion and the center of a second shell dipole is 3.30 Å when the primary shell ion-dipole center distance 2.5 Å. After various iterations described below, the view that adjacent water molecules had their geometric centers at 2.76 Å was abandoned.

The first problem for trikisoctahedral symmetry was to find the minimum energy configuration for the second shell. One assumption made was that rotation of the dipole in the second shell was the same as that in octahedral symmetry, i.e., towards diagonal neighbors, or towards one nearest neighbor in the first shell. Molecular models show that there appear to be nine second-shell nearest-neighbor pairs in which one neighbor lies on the plane containing the dipole centers and the central ion. In these cases, the second nearest neighbor lies on a plane of rotation inclined at 54.74° to this plane. Of the remaining three pairs of nearest neighbors, one has both neighbors lying on the plane

joining their centers and the central ion, one has one neighbor at +54.74° to the plane with the other at +90°, and the other is at +54.74° and –90°. Similarly, of the twelve diagonal pairs, nine are at 60° and 0° to their plane, one has both dipoles on the plane, and two pairs are at +60° and ±54.74°. If ϕ, ϕ' are the angles between the planes of rotation and the plane which includes the dipole centers and the central ion, and θ is the (common) angle on each plane of rotation between the corresponding dipole and the displacement axis on the plane of rotation, the required functions in Eq. (72) may be calculated. We find that $\cos\alpha$, β are equal to $\cos\theta(1 - \sin)^2\theta\sin^2\phi, \phi')^{-0.5}$, $\sin\alpha$, β are $\sin\theta\cos\phi, \phi'(1 - \sin^2\theta\sin^2\phi, \phi')^{-0.5}$, $\cos\gamma$, γ' are $\cos\theta(1 - \sin^2\theta\sin^2\phi, \phi')^{-0.5}$, and $\sin\gamma$, γ' are $\sin\theta\cos\phi, \phi'(1 - \sin^2\theta\sin^2\phi, \phi')^{-0.5}$. When these are inserted into Eq. (74), complex expressions result, which contain sums of $\cos^2\theta$, $\sin\theta\cos\theta$, $\cos^2\theta$, $\sin\theta\cos\theta$, and $\sin\theta\cos^2\theta$ terms. The latter have alternate ± signs whose values depend on the method of counting. They certainly cancel for $\theta = 0$, and they appear to cancel (or nearly cancel) for all values of θ. They were therefore ignored. The repulsive terms between one second shell dipole and the seven other second shell dipoles were then calculated. The interaction between the three first shell nearest neighbors assumed a rotation towards one neighbor, and angles of 120° with the remaining pair, with opposite rotations in respect to the positions of the inner shell second neighbors. A simpler expression was obtained for the interactions between the first and second shell dipoles, since the first shell permanent dipoles were assumed to have $\theta = 0$. It is clear from Eqs. (67) and (68) that $:_p$ interacts repulsively with the $\mathbf{E}_p$ due to the permanent dipoles, whereas $:_i$ does not, so only the effects of the permanent dipoles in the first shell on those of the second need be considered. Having determined the orientations and fields of the permanent dipoles, the values of the induced dipoles can then be determined by calculating the relative field multipliers in Eq. (70), and solving the simultaneous equations for each shell.

The potential energy of each of the eight second shell permanent dipoles is given by $[-245.8(2.377z(\cos\theta)/a_2^2 + f(\theta,\phi,\phi')/a_2^3]$ kJ-mole^{-1}, where a_2 is the second shell ion-dipole center distance (3.30 Å in this example), and the factor 245.8 is $N\mu_p^2$ in $(\text{Å}^{-3}\text{-erg-mole}^{-1}) \times 10)^{-10}$. The potential thus obtained corresponds to the potential energy change in solvating a gas-phase ion with a gas-phase dipole. To obtain the approximate Gibbs energy of solvation of a gaseous ion by liquid water in the second shell, a quantity equal to the energy of the number of

hydrogen bonds broken per water molecule surrounding the ion should be removed. This average number is uncertain. However, at least one hydrogen-bonding position (i.e., two half-bonds) is blocked by the ion. In tetrahedral symmetry, it is possible to argue, from geometrical considerations, that the effective value is one hydrogen bond per water molecule[95], but in octahedral symmetry the geometry makes this less certain. However, the equivalent of one hydrogen bond per solvating water molecule, or about $20.9\ \text{kJ-mole}^{-1}$, is plausible and was adopted. In addition, there is the work of forming a cavity in the liquid large enough to contain the ion and its oriented solvation shell(s). The radius of the cavity may be put equal to the distance b to the centers (strictly, the dipole centers) of the first shell of bulk water molecules (i.e., of "continuum" water). The energy to form such a cavity can be estimated electrostatically, or more simply from the surface energy, γ, of water. The energy of formation of the cavity is $+4\pi b^2\gamma$, but it will include other terms such as those for the formation of straight or bent[103] hydrogen bonds, which are accounted for separately. The compressive forces in the cavity are opposed by an unknown repulsive Mie term acting over part of b, which is ultimately borne by a repulsive terms between the ion and the first shell of water molecules. However, we can estimate the value of this term by putting the differential of the electrostatic and Mie energy terms equal to zero to determine the equilibrium condition when the opposine forces are equal.[93,98] If the Mie energy term depends on $(qb)^{-12}$, where q is a fraction, it can be put equal to $+A'b^{-12}$, where A' can be eliminated from the equilibrium condition at b_o, which is $+12A'b_o^{-13} = 8\pi b_o\gamma$. Thus, $A'b^{-12}$ is $+4\pi b_o^2\gamma/6$, and the total energy of cavity formation is $+4.67\pi b_o^2\gamma$. We will see below that for an ion of z = 3, b_o is about 6.2 Å. Thus, the energy of cavity formation is about 4.5×10^{-12} ergs for a trikisoctahedron of 14 water molecules, or 280 kJ/14 per mole of water molecules. This corresponds almost exactly to the energy of one hydrogen bond.

4. Initial Simulation Results for First and Second Trikisoctahedron Shells

Some EXAFS data on metal ion-oxygen distances are available for hexaaquo transition metal ions.[94] These are generally about 2.1 Å for 2+, and 2.0 Å for 3+ ions, and correspond to those determined by X-ray diffraction in crystals.[94] Some symmetrical breathing mode vibrational frequencies are also available, allowing force constants for a reduced

mass equal to that of one water molecule to be calculated.[71,162] They are about 390 and $490\ cm^{-1}$ for 2+ and 3+ states.

The ion-dipole interaction may be approximately expressed as $f = +Aa^{-n} - \Sigma Ba^{-m}$, where the first term is for Mie repulsions and the second is the effective sum of the ion-permanent dipole $(ze\mu a^{-2})$ and ion-induced dipole $(z^2e^2\alpha_i a^{-4}/2\varepsilon_A)$ interactions and electrostatic repulsions. The latter are dominated by the repulsions in the first and second shells (see later discussion), which are generally proportional to a^{-3}. From the equilibrium condition, $nAa_o^{-n} = \Sigma mBa_o^{-m}$, where a_o is the equilibrium ion-dipole center distance at ϕ_O, the bottom of the energy well. Writing $a = a_o(1 + x/a_o)$ and expanding the powers of $(1 + x/a_o)$ to the quadratic terms, the first binomial terms vanish and we obtain:

$$f = 2(\phi - \phi_o)/x^2 = \Sigma m(n - m)Ba_o^{-(m+2)} \qquad (75)$$

where f is the force constant. Both the ion-permanent dipole and ion-induced dipole terms are significant. The force constants vary between approximately $1.5r^{-4}$ and $2.25r^{-6}$ for 2+ and 3+ ions where r is the ratio of the bond lengths in the 3+ and 2+ states, depending on the relative importance of the two terms. The relative frequencies $(\propto \sqrt{f})$ will therefore vary by factors of between 1.65 and 2.6, the most likely value being about 2, which is much more than the experimental result.

Initial simulation results showed that second shell water molecules regarded as dipoles aligned along the axis of the displacement, i.e., $\theta = 0$ for all z values, thus simplifying the problem. The equilibrium position of the second shell could not be determined by assuming that nearest-neighbor water molecules were located at between 2.76 and 2.9 Å apart. Repulsive Mie energy terms between water molecules were added to the electrostatic attractive and repulsive forces added to reproduce experimental solvation energies, the best fit being n = 12. Other powers in the range 9-14 and exponential expressions[163] were examined, but these were less satisfactory for bond-length reasons. The value of the dipole moment was chosen to give the best fit, starting with 2.02 D (Eq. 36).

Bernal and Fowler[16] and Eley and Evans[92] suggested that positive ions should align along the dipole axis since they considered the negative charges to be on the centerline, on or close to the oxygen, negative ions aligning more or less along one O–H bond axis. Verwey[161a] went further in considering that positive ions should also be off axis, following his earlier suggestion[161b] that the negative charges

and bonds are arranged tetrahedrally. These "Verwey Positions" would be stabilized by allowing three hydrogen bonds towards the bulk solvent, rather than only two[161a].*

Early calculations in the present work for higher-valency ions assumed water dipoles of Rowlinson type in axial positions, using both dipole and point-charge calculations. Any refinement with DP multipoles in the Verwey and axial positions (see Appendix for z = 1) requires considerable time and effort, and is unlikely to give radical changes, since it results in only slightly different bond-lengths. For positive ions, the Verwey positions may be favored because the dipole-dipole interactions appear to be more attractive in the most favorable rotational orientations for four tetrahedral or six octahedral dipoles (average about +1.7kT per dipole at 298 K for the octahedral case at a dipole center-positive charge distance of 2.1 Å, compared with +10.8kT per dipole for aligned dipoles. For tetrahedral solvating dipoles, see Appendix). Whether this is enough to offset the lower positive ion attraction in the Verwey position compared with that for oriented dipoles and to swing the balance for 2+ ions and particularly, 3+ ions, for which a much larger part of the interaction is via induced dipoles, remains to be seen. Since the electronic polarizability is not isotropic,[121,129] it may maximize along the dipole axis, giving a further reason for steering the water molecules in this direction (see Appendix 2).

The Mie term used for second-shell water molecules was the same as that used following Eq. (60) (6.50×10^{-8} erg–Å^{12} per pair). However, there is no net potential energy in the combined first and second shells due to water molecule repulsions. The second shell molecules press the first shell inwards, and are repelled by the ion Mie terms, so the repulsive energies cancel.

The two simultaneous equations for the first and second shell energies were solved to obtain the induced dipoles in the second shell, which gave $0.624\mu_p$, $0.408\mu_p$, and $0.213\mu_p$ for z = 4+, 3+, and 2+ respectively. For z = 1, a large value of 9 was obtained, giving counterfields of opposite sign, with $\mu_i = 0.338\mu_p$, giving -9.1 kJ-mole^{-1} (3.6kT) for the induced dipole interaction. This effect is an artifact, which would disappear if a third shell is considered. The corresponding ε_A values for the second shell, ignoring the effects of

* From Pople's work[103], these would be bent, since a solvated ion has a moment of inertia at least as great as that of a water superdipole.

counterfields due to the third or subsequent shells (see below), were 2.02, 2.32, 2.96, and 0.93 for z = 4+, 3+, 2+ respectively. Thus, the overall interactions for the eight members of the second shell of the trikisoctahedron situated at a distance $a_{o,2}$ = 3.30 Å from a central ion with a primary shell ion-dipole center distance $a_{o,1}$ of 2.50 Å with the above assumptions represent about 20%, 18%, and 18% of the total solvation energies of about –8,300, –4,600, and **–1,890 kJ-mole^{-1}** for z = 4+, 3+, and 2+ ions.

Similar functions were examined for $a_{o,1}$ = 2.3 Å and 2.8 Å. Somewhat less negative values of the interaction were found at both distances. At 2.8 Å, the packing of the first shell is more open and x is slightly shorter than at 2.5 Å (3.164 Å vs. 3.30Å), giving higher repulsions. At 2.3 Å, the first shell is more densely packed, squeezing the second shell dipole out to 3.35 Å, reducing the net interaction somewhat. Further examination showed that at x = 2.5 Å, a marginally higher net interaction was possible if the nearest-neighbor distance was increased to give $a_{o,2}$ = 3.4 Å, slightly reducing the repulsive terms.

5. The Third and Fourth Shells

Assuming for the moment complete water molecule separation from superdipoles, the third trikisoctahedron shell can have 24 or 12 dipoles, occupying the space between one in the first shell and two in the second. A reasonable range of first shell ion to water molecule center distance $a_{o,1}$ for high-z and low-z ions is from 1.9 Å to 2.6 Å. The oriented second shell dipoles then have ion-to-center distances $a_{o,2}$ of 3.428, 3.429, 3.426, and 3.327 Å for $a_{o,1}$ values of 1.9, 2.0, 2.1, and 2.6 Å respectively, illustrating the squeezing effect on the second shell as $a_{o,1}$ becomes shorter. The 24 third shell dipoles lie at $a_{o.3}$ distances of 4.454, 4.504, 4.571, and 4.882 Å at the same respective $a_{o,1}$ distances. The z = 4 case at a bond-length of 1.9 Å slightly squeezes the first shell water molecules to a distance of 1.344 Å, less than the normal radius of 1.38 Å. The second shell water molecules do not interfere with those in the third shell for z = 1, 2 and 3, but do for z = 4, giving a center-to-center distance of 3.01Å, rather than 2.9 Å.

The alternative second shell of 12 dipoles lie adjacent to two second shell dipoles, equidistant from, and touching, two first shell dipoles. However, due to interference from second shell dipoles, their closest approach is the same as that for the 24 dipoles shell discussed above. The third or fourth shells are more complex to model than the

Calculated Third-Shell Interactions (24 Dipoles)

z	ε_A	$L(x_A)$	$-\phi_{ul,3}$ kT units	$-\phi_e$ kT units
1	15.01	0.212	1.11	0.05
2	13.37	0.475	5.71	0.28
3	10.39	0.702	13.29	0.85
4	6.83	0.855	23.07	2.45

second sphere, so approximations were made as required. The most important terms were the symmetrical repulsions between the second and third shell dipoles, rather than the more neutral terms resulting from repulsions in the first and third shells. The latter orient added dipoles to a greater θ value, reducing repulsive interactions. We may rewrite Eq. (35) as

$$\varepsilon_A = n^2 + 4\pi n_0 \mu_v (\varepsilon_A/A_A) L(x_A) \tag{76}$$

for intense fields, where $L(x_A)$ is assumed to equal $A_A\mu_v/\varepsilon_A kT$. Approximate interactions were obtained by solving Eq. (76) graphically for ε_A at the appropriate distances for 24 dipoles, assuming the above $a_{o,1}$ values for z = 4+, 3+, 2+, and 1+, respectively, and nominally putting μ_v equal to 2.0 D. The results are shown Table 1 for overall interactions $-\phi_{ul,3}$ per permanent dipole for third shells of 24 dipoles in kT units at 298 K. The final column contains the corresponding electronic induced dipole interaction $-\phi_e$ from Eq. (55) with $q_A = 1$, i.e., using $-P_{ul,A_\bullet}A_A(1 + q_A/\varepsilon_A)/2 = -\mu_v L(x_A)A_A(1 + 1/\varepsilon_A)/2$, and $-P_{e,A_\bullet}A_A/2 = -\alpha_e A_A^2/2\varepsilon_A$.

The dielectric constants have reasonable values, considering that the packing of 24 dipoles around the trikisoctahedron preserves the four-nearest-neighbor water structure. Induced electronic dipole effects at this distance are small for z < 4. Whether a 24 or 12 dipole model is reasonable is obtained by estimating the volume of the shell extending from the inner to the outer edge of the 24 dipole distance (i.e., $a_{o,3} \pm r_w$, where r_w is the water molecule radius of 1.38 Å) for z = 4. This volume is 7.04×10^{-22} cm^3, which would contain 23.5 (i.e., 24) water molecules at the bulk water density. For z = 4, the total interaction per dipole is about 3 times the hydrogen bond energy, so the water structure will be significantly broken. After subtracting the hydrogen bond energy, the

total interaction will be about 12% of the total solvation energy. For z = 3, the total interaction energy will be about 1.7 times the hydrogen bond energy, i.e., about –335 kJ/mole, slightly more than 7% of a typical –4,600 kJ/mole total solvation energy. For z = 2, no water breakdown will occur, and the energy of the shell will be about 19% of a typical –1,900 kJ/mole solvation energy. The effect for z = 1 is similar.

The fourth shell was also examined assuming single dipoles with moments approaching the vacuum value, and no Onsager or Lorentz cavities to give an upper interaction limit. Fourth cell packing was irregular, with distances varying from about 6.0 6.7 Å, 6.1 6.8 Å, 6.2 6.9 Å, and 6.7 7.4 Å for the greatest interactions for z = 4 to z =1 respectively. The calculated ε_A, and permanent dipole interaction $-\phi_{ul,4}$ were 12.63, 13.97, 14.81, and 15.28, and 7.65kT, 4.06kT, 1.70kT and 0.31kt respectively. For z = 4, the induced dipole interaction was 0.40kT, so the total interaction is almost equal to the hydrogen bond energy and a dipole in the fourth shell should still just be attached to a more distant nearest neighbor. However, the x_A value (about 2.1) would suggest no free rotation. Multiplication of the dipole moments by the Lorentz cavity terms $(n^2 + 2)/3$ for the critical z = 4 case gave a dielectric constant of 20.29, $x_A = 1.617$ $[L(x_A) = 0.461]$, increasing the interaction energy value $-\phi_{ul}$ to 7.89kT by increasing the apparent dipole moment. The addition of an Onsager cavity term $q_A = 3\varepsilon_A/(2\varepsilon_A + 1) \approx 1.5$ in the Langevin function increased ε_A to 29.27 with $x_A = 1.671$ $[L(x_A) = 0.475]$ and gave a slightly higher $-\phi_{ul,4}$ value of 8.14 kT. However, $-\phi_{e,4}$ is decreased by the higher dielectric constant to 0.17kT, partly offsetting this effect. Finally, the use of Booth's second set of assumptions for the superdipole moment (A = 1, B = 7/3, Eq. 37) gives a local dielectric constant of 64.67 with $L(x_A) = 0.494$, $-\phi_{ul,4} = 8.22kT$ and $-\phi_4 = -\phi_{ul,4} - \phi_{e,4}$ of 8.30kT, just less than the hydrogen bond strength.

The above shows the lack of sensitivity of $-\phi_4$ to the value of ε_A or the underlying assumptions, which is clear from the form of the expression $-P_{ul,A}.A_A/2$, which mainly depends on the value of $L(x_A)$, which is almost exactly proportional to A_A to $x_A \approx 3$ (Eq. 50). The water structure may be just broken in the fourth shell for z = 4+, but not for z = 1+, 2+ ,3+. Calculation shows that the corresponding dielectric constants for the fourth shell using Booth's assumptions are close to the bulk values for z = 1+, 2+, 3+ (76.20, 74.19, 70.59 respectively), with x_A values of 0.300, 0.720, and 1.173, $L(x_A)$ values of 0.099, 0.232, and

0.359, and $-\phi_4$ values of 0.32kT, 1.80kT, and 4.32kT at 298 K. These all correspond to the Dielectric Continuum range. The fifth shell for z = 4 (at about 8.4 Å) gives a dielectric constant of 73.72, $x_A = 0.790$, $L(x_A) = 0.253$, and $-\phi_4 = 2.15kT$. Again, this is in the Continuum range.

6. "Bottom-Up" Modeling of the Third Shell

Since the effects of the third shell are not negligible for high-z ions, it was approximately modeled using the same simultaneous equations as those for the second shell, i.e., to take a "bottom-up" calculation of the dielectric constants rather than using Booth's "top-down" method.[73,124,125] As expected, adding the third shell slightly reduced the net interactions in the second shell. Again, the principal conclusion was that the third shell for z = 2 would not show sufficient interaction to break the structure of water. Thus for z = 1, the second shell may considered the start of the Continuum Bora-like term, where Booth's Langevin function should still apply. For z = 2 and the above dimensional assumptions, it is the third shell, and for z = 3 and 4, the fourth shell.

The effect of the first sphere fields on the interactions in the third shell was small. A spherical shell of charge should be equivalent to that of an equivalent single charge at its center. However, shells consist of dipoles with discrete lengths and thicknesses with equal and opposite charges on each side. The central charges should therefore cancel, giving no net external or external field. However, the shells considered here are neither continuous, and they interpenetrate geometrically. For more remote molecules within the continuum electrolyte, the tendency to see no dipole field from either successive shells towards the ion, or from shells farther away from the ion, will become more apparent (see Appendix). The local dipole field will then largely result from nearest neighbor dipoles within the same shell. We note that the Kirkwood-Booth theory of the dielectric constant[72,73] only involves nearest neighbors, and ignores longer-range interactions.

7. Simplified Modeling

If the innermost sphere can be treated independently of the second, it would simplify calculation. This can be tested by considering induced dipoles in the first shell independently of the second using Eq. (73), or via those in the second shell using two simultaneous equations based on

Eq. (72). The simultaneous calculation using the previous dimensions shows μ_i for the inner shell to be 1.469, 1.018, 0.570, and $0.268\mu_p$ for z = 4+, 3+, 2+, and 1+ respectively. Disregarding the fields of the second trikisoctahedron shell gives 1.622, 1.172, 0.721, and $0.271\mu_p$ respectively. Thus, the second shell may be disregarded for z = 1+, but not for z = 2+, 3+, 4+. Accurate modeling for z = 4+ requires all three shells.

The attractive interaction per dipole is $-ze(\mu_p + \mu_i/2)/a^2$ and the total equilibrium interaction, including the repulsive permanent dipole-dipole and Mie repulsion terms, was typically about 85% of this value, assuming that the Mie repulsion term varies as $1/a^{12}$. This may be demonstrated by determining the equilibrium point by setting the derivative equal to zero.[93,98] Moelwyn-Hughes[93,98] used a simple analysis with a $1/x^9$ Mie term, but he overstated the μ_i terms by not considering the effects of the inner shell repulsive fields on their creation. If these are not included, the corresponding μ_i values at $a_o = 2.5$ Å are 2.196, 1.648, 1.098, $0.549\mu_p$ for z = 4+, 3+, 2+, and 1+ respectively. The error in the equilibrium energy is small (ca. 1%) for z = 1, where the minor interactions with the second shell have little effect. Ignoring the second shell overstates the interaction energy by about 6% for z = 2, falling to 4.5% for z = 4. In view of the uncertainties introduced by minor order terms (e.g., crystal field interactions and induced electronic dipole-dipole dispersion) these may be ignored, or the μ_i terms for z = 2+, 3+, 4+ may be reduced by a nominal multiplier, e.g., 0.95. Finally, if $\varepsilon_A = \mathbf{A}_A/(\mathbf{A}_A + \mathbf{E}_{p,A})$ can be estimated from the vector sum of the dipole fields, it is clear from Eqs. (68)-(70) that the overall interaction of each dipole in a given shell, with all dipoles assumed to be oriented along the ion displacement, dropping vector notation, and neglecting $+W_{A,p}$, is:

$$\Phi_{inner} = -\mu_p A_A(1 + 1/\varepsilon_A)/2 - \alpha_e A_A^2/2\varepsilon_A + \sum\phi_i \qquad (77)$$

The first term in this useful and easily-handled expression combines the ion-permanent dipole energy $-\mu_p A_A$ and its repulsive interaction with all permanent dipoles $+\mu_p E_{p,A}/2 = +\mu_p.A_A(1 - 1/\varepsilon_A)/2$ (compare Ref. 16).

8. The "Continuum" Energy

The Born-like Continuum energy term may be reasonably accurately replaced by an integration (Eq. 19), the lower limit being a point between the inner edge and the center of the first shell of superdipoles. The upper limit has usually been considered to be the Debye length determined from the linearized Poisson-Boltzmann distribution,[44] but this cannot apply in the electrolyte concentrations used in kinetic experiments. For these, the distance a_n at which the sum of the surrounding positive and negative charges around an ion, plus is own charge, becomes zero is relevant. Milner[164] attempted to determine the virial of such systems, taking into account the interactions between all charges present. If n_v is the molecular salt concentration whose complete dissociation produces z_n cations and z_p anions of valences $+z_p$ and $-z_n$, the anionic and cationic charge concentration at distance 'a' from a selected cation are $-n_v z_p z_n \exp + q/a$ and $+n_v z_n z_p \exp - z'q/a$, where $q = z_n z_p e^2/\varepsilon_o kT$ and $z' = z_p/z_n$. For electroneutrality, the charge on the reference cation must equal the total surrounding charge, i.e.,

$$4\pi n_v z_n \int_{a_c}^{a_n} a^2 \left[\left(\exp - \frac{z'q}{a} \right) - \left(\exp + \frac{q}{a} \right) \right] \cdot da = 1 \qquad (78)$$

where a_c is the closest approach distance for cations and anions. For a selected anion, we have $z' = z_n/z_p$.* At high dilution the integral is $\sqrt{2}/\kappa$, where κ is the Debye reciprocal length, so Eq. (78) should be divided by $\sqrt{2}$ to give the correct result. Since it uses a non-linearized Boltzmann distribution and does not involve the Poisson equation, it should be applicable at higher concentrations than the Debye-Hückel theory. Activity coefficient calculations using this method[165] show a cube-root dependence of activity coefficient on concentration to about 0.1 M,[166,167] after which the Robinson-Stokes solvent activity corrections[168] become controlling.

For a 1:1 electrolyte at a randomly-chosen closest approach distance of 7.16 Å, Eq. (78) divided by $\sqrt{2}$ predicts an electroneutrality length of 10.4 Å at 0.1 M, where κ is 9.6 Å, and $(\kappa + a_c)$ would be 17.0 Å. If salt-like effective lattice spacings[134,166,167]

* This should be a summation, but numerical integration is sufficiently accurate.

occur in higher concentrations, then by analogy with the mean energy of an ion in a lattice, the electroneutrality distance will be given by a/α, where 'a' is the mean cation-anion distance and α is a Madelung constant.[160] Assuming a rock-salt-like lattice, 'a' would be 28.6 Å and 13.3 Å at 0.1 M and 1.0 M, and α is 1.748. The effective electroneutrality distances may then become very short in electrolytes used in practical experiments or devices, e.g., 16.3, 7.6, and 4.2 Å in 0.1, 1.0 and 6.0 M 1.1 electrolytes.*

As indicated in Section III-2, the Continuum may be modeled as spherical shells of five-molecule water superdipoles with an effective radius of 2.9 Å. Their real radius is the distance between nearest neighbors (2.9 Å), plus the radius of a water molecule (1.38 Å). They therefore interpenetrate or interlock as in gears in free rotation, accounting for the effective number of nearest neighbors at 298 K of about 4.4, rather than 4.[95,103,138] Similar interpenetration with the solvation shell of ions is likely, with an average 2.9 Å nearest-neighbor distance between outer superdipole molecules and ion solvation shell molecules. We note that the moments of inertia, therefore equipartition energy rotation rates, for 1+ ions and water superdipoles are similar, permitting coupling of rotations. However higher valency trikisoctahedral ions have considerably higher moments of inertia, give rotation rates about a factor of two less than superdipoles. This will encourage energy exchange, and also push the superdipoles somewhat farther out on average. Molecular models suggest that the superdipole centers lie at 4.9-5.0 Å beyond the Inner Sphere dipole centers for 2+ and 3+ ions, and at 3.8-3.9 Å for 1+ ions. These distances must be corrected to give the correct a_o value in the integral in Eq. (19) to approximate the Continuum interaction energy. With the effective electroneutrality distances given above, the first two Continuum shells, containing about 75% of the total energy summed to infinity, are the only ones of importance in 0.1 M 1:1 electrolytes. In 1.0 M 1:1 electrolytes, only the first shell, with 55-60% of the energy to infinity, is important. In 6.0 M 1.1 electrolytes, the Continuum energy effectively disappears.

As noted in Section IV-5, 4+ cations will have a layer of single somewhat oriented water dipoles of moderate ε_A around the

---

* Energy calculations for ionic lattices show $\varepsilon_A = 1$[160]. Molten salts can form transient dipoles and multipoles as ion pairs and clusters, but it is unlikely that these contribute to a dielectric constant. For charge transfer in molten salts, the equivalent of an FC process is the change in electroneutrality length as valence changes.

trikisoctahedron. This should be separately modeled, but a good approximation may be had by adding 5.0 Å to the inner shell center distance, correcting to give a_o, and integrating, since $(1 - 1/\varepsilon_A)$ for $\varepsilon_A \approx 10$ is close to unity.

9. Solvation Energy Estimates

Calculations for higher-valency ions were performed early in the study. In the Rowlinson molecular model,[141] the vacuum dipole center lies at 0.293 Å from the oxygen center, whereas in the DP model,[143] it lies at 0.1225 Å. The water molecule structure used initially placed partial positive charges on each proton as in the Rowlinson model, but placed the negative charges at the molecule center,[16,159] which gives reasonable values for the solvation energy difference between positive and negative ions at constant oxygen distance and for the ion-oxygen distance for multivalent ions.[95,170] Both point charge and simple dipole models were used. The force constants and frequencies[71] calculated from the energy wells were satisfactory for the symmetrical breathing three-dimensional oscillator for 2+ ions, but those for 3+ ions give higher frequencies (see discussion, Section IV-4). The experimental values for 3+ ions must refer to cooperative modes between the first and second trikisoctahedron shells. In later work, the exact DP multipole model was used instead of a simple dipole model. Recomputing with DP multipoles in both the Verwey and dipole axial positions is desirable (see Appendix), but it is unlikely to radically change the model, because calculations were made to fit experimental values, and changes in dipole orientation would only result in slightly different bond-lengths for each assumed dipole moment value.

Some early computations for cations are given below. In all cases, the loss of two hydrogen bonding positions per water molecule was assumed (i.e., 20.9 kJ/mole of water), and the dipole is in the axial position. In the Verwey positions, only one hydrogen bonding position may be assumed to be lost. Solvation energies are the "quasi-absolute" values from Ref. 95. p. 106. Distances are ion to dipole center.

Monovalent cations, tetrahedral results:

- Li^+, –542.7 kJ/mole, first shell at 2.500 Å (Continuum –181.3 kJ/mole; 33.4%).
- Na^+, –428.0 kJ/mole, 2.782 Å (Continuum –168.7 kJ/mole; 39.4%)

- K^+, –344.3 kJ/mole, 3.068 Å (Continuum –156.7 kJ/mole; 45.5%)
- Rb^+, –323.0 kJ/mole, 3.157 Å (Continuum –154.5 kJ/mole; 47.7%)
- Cs^+, –298.7 kJ/mole, 3.269 Å (Continuum –151.0 kJ/mole; 50.6%)

Monovalent cations, octahedral results:

- Li^+, –542.7 kJ/mole, 2.680 Å (Continuum. –173.1 kJ/mole; 31.9%)
- Na^+, –428.0 kJ/mole, 2.978 Å (Continuum –161.0 kcal; 37.6%)
- K^+, –344.3 kJ/mole, 3.267 Å (Born –150.7 kcal; 43.8%)
- Rb^+, –323.0 kJ/mole, 3.356 Å (Born –147.9 kJ/mole; 45.8%)
- Cs^+, –298.7 kJ/mole, 3.466 Å (Born –144.4 kJ/mole; 48.3%)

Typical early results for multivalent ions:

- z = 2: Total solvation energy taken as –1852.3 kJ/mole. Inner octahedral shell at 2.641 Å, outer trikisoctahedral shell (8 water molecules) at 4.185 Å. Inner shell to outer shell dipole-dipole center distance 3.243 Å. Inner shell, 56.34%, Outer shell, 14.51%, Continuum, 29.15% of net solvation energy. Inner shell induced dipole 1.036 D, outer shell induced dipole, 0.200 D. Inner shell dielectric constant, 1.862. Outer shell dielectric constant. 3.960.
- z = 3: Total solvation energy taken as –4495.5 kJ/mole. Inner octahedral shell at 2.499 Å, outer trikisoctahedral shell at 3.951 Å. Dipole-dipole center distance 3.050 Å. Inner shell, 50.24%, Outer shell, 15.04%, Continuum, 34.75% of net solvation energy. Inner shell induced dipole 1.986 D, outer shell induced dipole, 0.372 D. Inner shell dielectric constant, 1.677. Outer shell dielectric constant. 3.587.
- z = 4: Total solvation energy taken as –8082.9 kJ/mole. Inner octahedral shell at 2.409 Å, outer trikisoctahedral shell (8 water molecules) at 3.800 Å. Dipole-dipole center distance 2.927 Å. Inner shell, 56.65%, Outer shell, 14.47%, Third shell (24 dipoles) and Continuum, 28.88% of net solvation energy. Inner shell induced dipole 2.990 D, outer shell induced dipole, 0.566

D. Inner shell dielectric constant, 1.599. Outer shell dielectric constant. 3.396.

Comparison of the above ion-dipole center distances with experimental EXAFS 2+ and 3+ ion-oxygen distances (e.g., 2.1 Å, 2,0 Å respectively)[94] show them to be too long. Taking 50% of the total net solvation energy to be in the innermost shell and using the DP multipole dimensions with ion dipole center distances of 2.205 Å and 2.095 Å for 2+ and 3+ respectively to correspond to the experimental ion-oxygen distances, after a careful correction of the dipole center distance to allow for electron displacement in forming the induced dipoles gave a result later used in estimating redox activation energies. Fitting this time used the vacuum value of the permanent dipole moment (1.86 D), and was based on Eq. (77). The counterfield values were split into two parts after a series of iterative processes. One part (29.4% of the total for 3+ ions, 34.6% for 2+) was associated with inner shell permanent dipole repulsions, proportional to $1/x^3$, and the second was associated with dipoles and superdipoles external to the inner sphere. The latter counterfield may be put equal to $A_A(1 - 1/\varepsilon_A)$, i.e., for most purposes, it may be assumed to be proportional to A_A. For 3+ ions with an assumed net solvation energy of 4468.4 kJ/mole, the inner sphere dielectric constant was 1.988, and for 2+ ions with an assumed net solvation energy of 1879.4 kJ/mole it was 2.515. Since energies were fitted to enthalpies, the values obtained for each solvating water molecule may be considered as enthalpies. These energies were –158.95kT and –72.09kT (T = 298.16 K) before correction for the ground state of the three-dimensional oscillator. The calculated force constants were 475,460 and 166,880 dynes/cm* for 3+ and 2+, giving frequencies of 668.8 cm^{-1} and 396.2 cm^{-1}, the latter in excellent agreement with experiment.[71] The corresponding $h\nu$ values were 3.23kT and 1.91kT, i.e., the zero-point energies for the three-dimensional six-member oscillator are 4.85kT and 2.87kT.

This work suggested that the distances obtained for monovalent cations were also too long. For K^+, the inner and second shell were examined on this basis, and a fit could be made at a first shell ion-dipole center distance of 2.253 Å, with an induced dipole of 0.461 D (ε_A = 3.094), with a second shell just apparent at 4.560 Å, where the induced dipole was 0.050 D (ε_A = 6.650). This distance is certainly too

* 1 dyne/cm = 1 mN-m^{-1}.

short, and about 2.7 Å appears more probable, when the second shell largely disappears.

A modified Bernal-Fowler model appears to be a reasonably good approximation for monovalent ions, in which the first layer of water is fully oriented, the second layer has some orientation, and following layers may be treated as Continuum, with good accuracy. The Continuum energy term derived as described varies from about 46% for large ions to 35% for small ones.[170] It may be approximately fitted by log-log plots, e.g., if the total water quadrupole or dipole energy in the first shell is $(\Sigma\varepsilon)$, the total solvation energy in the same units is $12.99(\Sigma\varepsilon)^{0.64}$ with $(\Sigma\varepsilon)$ in kJ/mole $[7.758(\Sigma\varepsilon)^{0.64}$ in kcal/mole, $9.367(\Sigma\varepsilon)^{0.64}$ in kT] for univalent ions, before correction to account for lost hydrogen bonds. The same model is also a good approximation for trikisoctahedral 2+ – 4+ ions, provided second (and for 4+ ions third) oriented shells are considered. About 50% of the energy is then in the first shell, 14% in the second, and the rest in the Continuum. Whether the Verwey positions should be used requires further consideration.

V. THE STRUCTURE AND ENERGIES OF LIQUID WATER AND SOLVATED H_3O^+

1. Preliminary Approaches

The calculations described above for multivalent ions, or univalent ions with a single positive charge center (e.g. K^+) were relatively straightforword. However, in any solvated ion system without a definite single charge center, computational problems are more complex. For solvated protons, calculation must be matched to experimental information. The O O in H_3O^+–H_2O has been placed in the range 2.45 Å (based on the radii of O, H, and OH under strong-bond conditions, i.e., for H_2O, H_2 and O_2) to 2.5 Å (for the short hydrogen bonds in acid salts such as KH_2PO_4). These are discussed on p. 98 of Ref. 170, but 2.55 Å is also given on p. 118, with a possible preferred value of 2.49 Å in $HNO_3.3H_2O$. The length is determined by the requirement for a sufficiently high proton tunneling rate to permit conduction via "hopping".[171] Preliminary modeling used a flat configuration for the three dipoles solvating H_3O^+ with a single + charge close to the O, with three dipoles in the plane of the three H_3O^+

Figure 5. (Left): $H_9O_4^+.H_2O$ structure as finally determined (H_3O^+ bond angles 115°, bond length 1.02 Å). "Bottom" H_2O O…O distance 2.599 Å, "Top" O…O distance 3.213 Å. (Right): Corresponding $5H_2O$ structure showing rotation of "Top" H_2O.

protons. This results in the lowest repulsions, including those with the "top" H_2O (Figure 5). The H_3O^+ structure was taken as a flat pyramid with bond angles of 115°, bond lengths of 1.02 Å, and an estimated dipole moment of 1.49 D (p. 55-56 of Ref. 170). The latter was used to estimate the bonding electron positions[143b], with a lone-pair–oxygen distance as in water.

To estimate the H_3O^+–H_2O interactions, the Halliwell and Nyburg[170,172] values for the overall enthalpy of H_3O^+ solvation (1090.8 ± 10.5 kJ/mole, 262.7 ± 2.5 kcal/mole), an acceptable estimate for the proton affinity of water (711 ± 8 kJ/mole, 170 ± 2 kcal/mole, Ref. 168, p. 58), and the Continuum energy determined by the fitting procedure (Section IV-9) were used as a starting point. This resulted in a distance between O in H_3O^+ and the water dipole center of ca. 2.45 Å, i.e., an O O distance of only 2.18 Å. If the proton charge is equally shared by the three H atoms, each of the three identical solvating H_2O molecules (called here "bottom" molecules) may be considered to lie next to 1/3 of a proton charge. First attempts to iterate using 2.49 to 2.45 Å O O distances for the "bottom" H_2O molecules gave values ranging from –27.5kT to –38.0kT respectively. For the "top" H_2O, the values varied between –13.3 and –16.2kT, assuming O O distances between H_3O^+ and the "bottom" H_2Os of 2.24 Å and 2.46 Å. The latter distances were chosen to represent a minimum of two O radii (2.24 Å) and the O O distance corresponding to two water radii with the oxygens facing each other [2 x (1.38 – 0.15) Å]. At 2.46 Å, the induced dipole for each of the "bottom" H_2Os was about –4.1kT, assuming an effective dielectric constant determined separately from the dipole counterfields for K^+ ion of about 2.96. The "bottom" dipole-dipole repulsive energies (one half of two pairs each) were about +0.7kT, while the "top"–"bottom" repulsions (one half of one pair) were +1.4kT. The "top" water molecule lay at an equilibrium O O distance of 2.67 Å from the O in H_3O^+. Its induced dipole energy was estimated as –1.2kT, and its repulsive energy (one half of three pairs of dipoles) was about +4.2kT. After correction for the equilibrium values of the inverse 12-power repulsions, obtained by differentiation, it was estimated that the "bottom" equilibrium energies should be adjusted by –0.5kT, and the "top" by +2.6kT.

These results may be of the correct order with a reasonable estimate of the magnitude of the continuum term using the scaling expression for monovalent ions. They are therefore in the range 430-520 kJ/mole (102-125 kcal/mole) before conventional correction of about 84 kJ/mole (20 kcal/mole) to account for broken hydrogen bonds,

and before zero-point energy corrections. These are somewhat larger values than those derived by Halliwell and Nyburg[172] by extrapolation, including Outer Sphere contributions. The small induced electronic dipoles were ignored.

This *Version A* geometry placed the "bottom" dipoles in the plane of the three protons of the solvated H_3O^+ in an apparently preferred position minimizing dipole-dipole repulsions. Further calculation showed that the minimum energy position lay with the dipole axes below and at 46.8° to the perpendicular to the plane of the three protons in H_3O^+. The motions of the bottom H_2Os were rather loose, with a kT energy difference for 55.9° – 46.8° and 46.8° – 35.0°. The corresponding O O distances were 2.62 Å and 2.48 Å, with 2.54 Å at the minimum, within the requirements of Ref. 170. The interaction energies for the "bottom" and "top" dipoles were –22.6RT and –33.9kT, corresponding to a total (including Continuum) interaction of –510 kJ/mole (–121 kcal/mole) before hydrogen bond and zero-point energy correction. This time, the "top" water molecule lay at an O O distance of 2.93 Å due to the higher repulsions of the three "bottom" dipoles to the "top" dipole in the 46.8° rather than the planar 180° positions. In this *Version B* case, the effective dipole moment was taken as 2.138 D (see Appendix), with a DP dipole center at 0.1225 Å from the oxygen center.[143]

A problem with the *Version A and B* geometries was the inconsistency of the x^{-12} repulsive terms, which varied in a purely arbitrary manner by more than a factor of 3 for the "bottom" water molecules, and by a factor of 23 for the "top" water. Using experimental data for water to allow a common repulsive term to be calculated based on the average water O–O bond distance provided a different approach. The time-averaged three-dimensional energies (in kT units at 298 K) of water superdipoles may be:

$$u = (1 + 0.0574)Ar^{-12} - 1889.92r^{-6} - (0.4495)1889.92r^{-6} - 156.00/r^{-3} \quad (80)$$

where r (Å) is the average O O bond distance in water, A is the repulsive term for neighboring molecules in an inverse 12 power field, and 0.0574 is the correction term for 4-fold coordination summed over all molecules.[173] The corresponding term for inverse 6-power induced dipole-induced dipole and electron dispersion force attractions is 0.4495.[173] The average permanent dipole-dipole interaction is

discussed below. Setting the derivative equal to zero gives the mean energy u_o, in terms of the mean distance r_o:

$$u_o = -[(12-6)/12](1.4495)1889.92r_o^{-6} - [(12-3)/12]156.00r_o^{-3} \quad (81)$$

u_o (including the zero-point energy of the three-dimensional oscillating dipole) is known to be –9.92kT from the latent heat of evaporation, and the r^{-6} multiplier may be readily calculated.[173] The mean three-dimensional dipole-dipole (r^{-3}) and repulsion (r^{-12}) terms may be obtained if r_o is assumed to be 2.707 Å, the mean O O distance in liquid water estimated from its density. From the gas-phase moment, the dipole-dipole term is $-\{2\cos\theta_a\cos\theta_b - \sin\theta_a\sin\theta_o\, b[\cos(\psi_a - \psi_b)]\}84.04kTr^{-3}$, where θ_a, θ_b are the angles measured in the same sense between the axes of the dipoles and the line joining their centers in a plane containing their centers, and ψ_a, ψ_b are the angles subtended by the axes and perpendiculars passing through their centers. The maximum value of the angle term is 2, and a comparison of the experimental value at $r_o = 2.707$ Å suggests that the vacuum moment applies, giving A = +823,986. However, this approach assumes that water molecules are distributed in a diamond lattice, so improvement was required.

A simple model for associated water was needed in which oxygen-oxygen repulsions in water could be equated to those in $H_2O\text{-}H_3O^+$, which required examination of the energy and associated structural changes on the addition of an unsolvated proton to a liquid water superdipole. Pople's modification[103] of Kirkwood's[72] static water dielectric constant model assumes restricted rotation with bent hydrogen bonding between tetrahedra. The dipole to central dipole $\cos\theta$ value, including second-and later-shell bending is given by the Langevin function of a rather large number, so $L(x_A) \approx 1$. The dipole moment of each nearest neighbor along the axis of the central dipole is $\mu_m\cos\theta$, where μ_m is the mean liquid water moment. Using Eqs. (31-(35), the total moment induced by the four first shell dipoles along the length of each central dipole is $4 \times 2\alpha_e\mu_m\cos\theta/a^3$, where a is the mean dipole-dipole center distance. The total dipole $A\mu_v$ (Eq. 35) along this axis is $\mu_m = \mu_v + (2\alpha_e\mu_m)\Sigma n_i\cos\theta_i/a_i^3$, where n is the number of nearest neighbors, and i refers to the ith shell. Hence,

$A = 1/(1 - 2\alpha_e\Sigma n_i\cos\theta_i/a_i^3) \approx 1/(1 - 8\alpha_e\cos\theta/\varepsilon_A a^3)$.* The superdipole moment $B\mu_v = \mu_m(1 + 4\cos\theta)$, so $B = A(1 + 4\cos\theta)$. Putting the experimental 298 K ε_o, n^2 values in Eq. (36), X = AB = 2.765. Thus, with $\alpha_e = 1.444 \times 10^{-24}$ cm^{-3} and a = 2.90 Å, $\cos\theta = 0.2737$.

Pople[103] assumed that the lone pairs and the –OH bonds were both at 105°. The DP angle[143] for the lone pairs is 122.2°, which gives a lone pair O–H bond angle of $\cos^{-1}[-\cos(105/2)\cos(122.2/2)]$. However, the bond is not quite aligned in the lowest energy *trans* and *cis* states (see below), being at +63.05° and –49.8° to the line of centers respectively. Hence, cos (122.2/2) should be replaced by an averaged cosine, e.g., 0.55. Thus, using a modification of Pople's expression, $\cos\theta = 0.55\cos 52.5(Lg/kT)^2$, where g is the bending force constant of the hydrogen bond. This gives Lg/kT = 0.904, and g = 10.4, in excellent agreement with Pople's value obtained from the radial distribution function of water.[103] The contribution of the second and higher shells will reduce the effective value of $\cos\theta$ in the expression for A, giving a smaller g value. The g energy term is $F_{(\theta=0)} + g\cos\theta$, where θ is the deviation from the minimum value of $F_{(\theta=0)} + g$. For small θ, this corresponds to $+g\theta^2/2$ above the minimum, so g has the form, if not the dimensions, of a force constant. For small θ, the curvature of the calculated energy well for hydrogen bonds (see below) corresponds to g = 13.7kT, which becomes less at larger values of θ due to anharmonicity. Energies of ±kT were calculated at an average of 26° on either side of the most probable *trans* energy well, i.e., Lg/kT = cos26 = 0.899, i.e., g/kT = 11.25, in good agreement with Pople's estimate from the radial distribution function.

From $\mu_m = \mu_v/(1 - 8\alpha_e\cos\theta/a^3)$ with μ_v = 1.86 D, we obtain μ_m = 2.138 D for the effective dipole moment in liquid water from the 298 K bulk dielectric constant. When this is used to estimate the cohesive energy between water molecules in approximately tetrahedral superdipoles at dipole-dipole or O O distances of 2.9 Å, the results are about a factor of three too small. The simple dipole-dipole model for water was therefore replaced by a DP multipole-multipole point charge model for hydrogen bonding (c.f., Lih[173]), and the interactions

* Since ε_A is determined by the counterfields from the second and further shells, increasing incoherence with rising number of shells will tend to compensate for the increasing value of the summation as the number increases, so its effective value will be close to unity. An experimental value of $\cos\theta$ derived from the bulk dielectric constant is used here, which will give an effective value.

between two DP multipoles at a 2.900 Å O O distance were calculated using the same approach for the interaction between positive and negative charges and DP multipoles (Appendix 2). A non-coulombic inverse 12-power repulsion based on the O O distance was assumed.

The most consistent values showed energy minima with the nearest neighbor H–O–H plane lying at angles of +63.05° and –49.8° to the line joining the oxygens of neighboring water molecules. The nearest neighbor has one lone pair almost facing one O–H bond in the first molecule. In the first case, this energy minimum corresponds to the nearest neighbor H–O–H plane in the *trans* position relative to the non-bonding O–H bond in the first molecule. The combination of attractive and repulsive coulombic terms, combined with the assumption that the inverse 12-power repulsive potential operates between the O O atom centers results in the bonding lone pair of the neighbor not being exactly in line with the line passing through O–H...O. It lies 1.95° below this line of centers, pointing in the direction of the non-bonding O–H bond in the first molecule. With the H–O–H plane in the neighbor in the *cis* position relative to this O-H bond, the bonding lone pair in the neighboring molecule lies at 11.30° below the O–H...O line. These are indicative of bending or kinking of the hydrogen bond.[103,158b] Before correction for second-nearest-neighbor dipole-dipole interactions (see below), the minima lie at –10.48kT in the *trans* position, and –8.73kT in the *cis* position. Removal of the mechanical constraint of a linear O–H...O coordinate will require considerable computing, but it will result in very little difference to the calculations, since libration of the H–O–H plane between +93° and +41° and –23° and –75° in the *trans* and *cis* cases respectively results in energy increases above the minimum of +kT. The maximum between the *trans* and *cis* states occurs with the H–O–H plane at 10.7° below the O–H...O line, pointing towards the non-bonding O–H in the first molecule. This maximum lies at only +3.04kT. The maximum with the H–O–H plane in the other direction lies at –1.8° below the 0–H...O line, and is equal to –7.19kT. Thus, transitions from the *trans* to *cis* positions via libration will be easy. They will also be easy by free rotation around the O–H...O bond. As before, calculations showed that induced dipole terms could be neglected.

The distances between the dipole centers of the four outer water molecules (4.6 – 4.85 Å) were probably sufficient for the dipole

approximation of their electrostatic interactions to be reasonable.* After some somewhat tedious calculations, these energies proved to vary from +1.90kT (outer H_2Os of *Type A,* bonding with their O–H bond, both in the *trans-trans* configuration) to –1.09kT (one *Type A* outer H_2O and one *Type B* bonding via a lone pair, both *cis-cis*). This permitted the most probable configurations and values of the average hydrogen bond to be determined, after differentiation and using the usual equilibrium assumption. All *trans* gave –9.65kT, all *cis* –9.25kT, and *cis-trans-cis-trans* –9.48kT, while the others were A *cis,trans,* B *trans,trans* –8.81kT; A *trans,trans,* B *cis, trans,* –9.16kT; A *cis,cis,* B *trans,trans,* –8.12kT; A *trans,trans,* B, *cis,cis,* –8.19kT. Thus, this study showed the mean H-bond energy to be –9.65kT, i.e. 23.9 kJ/mole (5.72 kcal/mole). However, a further term to be estimated is the induced dipole-induced dipole term, although it is debatable whether this should be counted in the hydrogen bond calculation (the same is true of dispersion forces). The induced dipole-induced dipole term is $2\alpha_e\mu^2/a^6$, where μ is an effective dipole moment along that axis.

For two water molecules linked in the hydrogen bond positions, the total coulombic attraction in the trans position at x = 3.061 Å (O O distance 2.9 Å) before correction for the inverse twelve-power repulsion is –14.29kT (5.883×10^{-13} erg), which may be put equal to $Q\mu^2/a^3$, where Q is a geometrical factor. This gives an effective $Q^{1/2}\mu$ value of 4.108 D, which can now be used to calculate $Q\alpha_e\mu^2/a^6$. With α_e (assumed isotropic) equal to 1.444×10^{-24} cm^{-3}, $Q\alpha_e\mu^2/a^6$ is –0.72kT. The inverse twelve-power repulsions corresponding to this term are $+(12 - 6)bQ\alpha_e\mu^2/12a^7$, where a is the twelve-power repulsion distance (assumed to be 2.9 Å). Hence the net change in overall hydrogen bond energy due to the induced dipole-induced dipole term is only –0.34kT. For a hydrogen bond between two water molecules, the value of the displacement vector **A** is about three times less than that for the corresponding vector at a water molecule solvating K^+. From the discussion following Eq. (48), this is precisely the range of **A** in which a rapid transition from the bulk value of the static dielectric constant to dielectric saturation takes place, so that effective local dielectric

* Calculations for two water molecules with their dipole axes and one lone pair each parallel (i.e., in parallel Verwey positions for positive ions, as would be possible in a Helmholtz double layer) in which an accurate DP point charge model was compared with a simple dipole model showed the latter to be 11.6% high at 2.0 Å separation, and 4.6%, 1.5%, 0% high at 2.25, 2.5, and 2.75 Å, and 1.4%, 2.6%, and 3.3% low at 3.0. 3.5. and 4.0 Å.

constant will be quite large. Hence induced dipole-induced dipole effects may be neglected.

As is shown in Appendix 2, the DP multipole model[143] for water accounts very well for the differences in solvation energies of positive and negative ions. It also gives an excellent value of the hydrogen bond energy. This suggests that Stilinger and Raman's ST2 potential[144,157] frequently used in molecular dynamic calculations, is too over-simplified to give a good account of detailed interactions between water molecules. The same conclusion is also likely to be true of the central force potential (CFP).[145,158] A major concern is that these analyses permit "stacking" of water molecules around an ion, (e.g., in 9 or 10 random coordination in one geometric shell), which is counter-intuitive to what would be expected geometrically if all of the appropriate coulombic forces are considered. The same argument applies to improved quantum simulations using quantum path integral and Born-Oppenheimer (BO) potential energy surface in the combined local-density-functional method (BO-LDA-MD) for H_3O^+ and H_2O–H_3O^+.[175]

2. H_3O^+ Solvation

The inverse twelve-power O O repulsion constant (in units of $kT\text{-}Å^{-12}$ at 298 K) derived from the last hydrogen-bond calculation was 1.7599×10^6. This permitted a calculation of H_3O^+ solvation, regarding each component (H_3O^+ with bond lengths and angles 1.02 Å and 115°; H_2O in the Verwey position) as DP multipoles. For simplicity, the H_3O^+ lone pair–O distance was assumed to be at the same as in H_2O, and the bonding electrons are at the same proportionate distance along the bond. The preliminary result showed an exact alignment along the line of the O–H bond in H_3O^+ and the H_2O lone pairs, with a "bottom" H_2O coulombic attraction (corrected for the inverse twelve-power repulsions) equal to –33.72kT (at 2.653 Å O O distance, with the H–O–H plane pointing towards the "top" position), and –29.55kT (at 2.671 Å, with the plane pointing in the opposite direction).

Before refining these values, and adding dipole-dipole repulsions and induced dipoles, the "top" H_2O was examined to see if it would influence the most probable "bottom" position. Because DP multipole point-charge calculations are tedious, some simplifying assumptions were made. The H_3O^+ lone pair points directly at the O in the "top" H_2O, whose lone pairs point downwards in either a symmetrical or Verwey position. However, the repulsions between the 6 H_3O^+ bond electrons and the 4 "top" H_2O lone pair electrons appear to steer the

latter to a dipole axial position. The dipole approximation gives a good account of the interaction energies between multipoles in in-line dipole axial positions at distances beyond 3.00 Å, so the H_3O^+ ion may be regarded as a dipole with a superimposed charge. Its dipole moment was calculated to be 1.383 D, rather than 1.49 D (p. 55-56 of Ref. 170), with a dipole center at 0.040 Å from the O. The positive charge was regarded as being shared by each proton. With the "bottom" H–O–H plane pointing upwards, the net attractive energy was –12.71kT at an O O distance of 3.213 Å, whereas pointing downwards, the energy was –10.65kT at 3.220Å. Respective energies were (multipole attractions) –17.50kT and –17.41kT, (H_2O–H_3O^+ dipole-dipole repulsions) +3.75kT and +3.73kT, (induced dipole attractions, effective local $\varepsilon_A = 2.96$), –0.70kT and –0.69kT, and "top"–"bottom" dipole-dipole repulsions, +0.29kT, and +0.32kT, and (inverse twelve-power repulsions) +1.45kT and +1.42kT. Thus, all energies indicate that the "bottom" H–O–H plane facing upwards is favored. Induced dipole-induced dipole effects are only about –0.05kT, which requires an increase in twelve-power repulsions by +0.02kT. The net "top" energy is therefore –12.74kT.

A detailed model of the "bottom" H_2Os gave a net energy of –38.62kT at 2.599 Å. The energies were (multipole attractions) –53.82kT, ("bottom" H_2O H_2O dipole-dipole repulsions) +1.47kT, ("top" to "bottom" H_2O H_2O dipole-dipole repulsions), +0.10kT, (induced dipole attractions, effective local $\varepsilon_A = 2.96$), –4.84kT, (H_3O^+–H_2O induced dipole-induced dipole attractions, effective local $\varepsilon_A = 2.96$), –0.12kT and (inverse twelve-power repulsions) +18.60kT.* No further iterations in the energy of the "top" H_2O to account for minor changes in the "top" to "bottom" repulsive energies due to the change in "bottom" O O distance from 2.653 Å to 2.601 Å were considered necessary given the limits of accuracy of the calculation. Thus, the net solvation energy of the Inner Sphere is –128.6kT (–318.8 kJ/mole, –76.2 kcal/mole) before zero-point energy correction. The bonding of each of the three "bottom" H_2Os lies in a rather broad potential energy well. Their calculated stretching frequency force constant was 91,500 dynes/cm. The $h\nu$ values for the non-degenerate joint three-dimensional symmetrical vibration of the "bottom" H_2Os

* The "bottom" H_2Os librate in a very shallow energy well with an amplitude of over 100°. This is because the dipole-dipole interactions go from positive to slightly negative on rotation through 90°. At the same time, the attractive interactions become less negative.

estimated from the properties of an almost flat regular pyramidal molecule were 1.42kT, with a ground state lying at 2.12kT. The well energy for the "bottom" H_2Os lay at the ground state of +2.12kT between 2.481 Å and 2.766 Å. The additional thermal energy required to attain a minimum distance of 2.45 Å for effective proton tunneling for conduction [Ref. 170, p. 98] was +1.58kT (3.90 kJ/mole, 0.93 kcal/mole). The stretching force constant for the "top" H_2O was 7,990 dyne/cm, with a ground state of 0.23kT ($h\nu$ = 0.46kT). Corrected for the ground state energies, the Inner Sphere energy was –126.5kT (–313.5 kJ/mole, –74.9 kcal/mole). The correlation function gives a total energy including the Continuum of –207.4kT (514.0 kJ/mole, 122.9 kcal/mole). A Continuum integration with a lower limit of 3.9 Å gives –175.7 kJ/mole (–42.0 kcal/mole) for the Continuum energy, giving –489.2 kJ/mole (–116.9 kcal/mole) total. Both are before correction for lost hydrogen bonds. The latter is probably the most reliable value.

On "switching on" a proton in a five-molecule tetrahedral water cluster, two hydrogen bonds of *Type B* are converted into "bottom" H_3O^+–H_2O hydrogen bonds, their only major motion being a shortening of the bond, accompanied by minor sideways translations and rotations to account for changes in bond angle. One *Type A* water molecule detaches, rotates through about 107° and translates to allow for the change in angle as one lone pair on the central water molecule becomes a pair of bonding electrons. The "top" *Type A* water molecule detaches, rotates through about 120° and translates sideways (Figure 5). Taking bulk water as the ground state, the solvated H_3O^+ ion must have minus four hydrogen bonds (–95.7 kJ/mole, –22.9 kcal/mole) added to its Inner Sphere solvation energy. The net energy for the "top" H_2O is only –3.09kT, so it will be highly labile. Taking the outer Continuum energy into account using the best result given above gives a solvation energy of –393.5 kJ/mole (–94.0 kcal/mol). Assuming –711 kJ/mole (–170 kcal/mole) for the proton affinity of water, the result is in good agreement with Halliwell and Nyburg's value of –262.7 ± 2.5 kcal/mole.[170,172]

VI. SOLVATION AND CHARGE-TRANSFER

1. FC Redox Processes

Although hetero- and homogeneous electron transfer has normally been held to occur under FC conditions, especially for nonadiabatic or weakly coupled processes, there are suggestions in the literature[90] that "for adiabatic reactions with strong coupling between the redox couple and the metal surface, electron transfer occurs gradually as the system moves along the reaction coordinate." As we have seen in Section II-5, this appears to have been the intent of the original Hush theory,[50] which he recently reviewed in the context of later work.[176] If the flow of charge q during the reaction is rather slow ($\approx h/kT$, 1.6×10^{-13} s at 298 K, as in normal transition state bond-breaking/making), the Continuum dipoles should be able to keep up their motion with the change of field, so that there will be no Continuum outer-sphere activation energy term. The transient superdipoles[72] in water have a $q_A\mu'$ value (Eq. 34) of ≈ 8.9 D and a moment of inertia $\approx 6.7 \times 10^{-38}$ g-cm^2. Remote from an ion, their rotational period is 8×10^{-12} s (frequency 1.25×10^{11} s^{-1}) at the equipartition energy value. Their lifetimes will be a few periods, perhaps 5×10^{-11} s. For superdipoles centered at 8-9 Å from z = 3 and z = 2 ions (corresponding approximately to the first superdipole shell, containing about 50% of the total Continuum energy), the Langevin energy interactions with the central dipole are 0.94-0.75kT and 0.63-0.5kT respectively, corresponding to Langevin angles of 72.8-74.3° and 78.3-80.6°. The time to rotate from the equilibrium 3+ to 2+ position and vice versa will be $(1.2\text{-}1.4) \times 10^{-13}$ s, approximately h/kT. FC conditions apply to complete electron transfers proceeding much more rapidly than this.

The 2+/3+ transition in the Marcus model or its successors involves only small Inner Sphere changes in solvation molecule coordinates in the radial direction to and from the ion. Electron transfer under FC or Born-Oppenheimer conditions demands that an activation energy in the outer Continuum should resist one-electron transfer via a continuum inertial term $\lambda = (e^2/2r')(1/n^2 - 1/\varepsilon_o)$* where r' is an effective intermediate reactant-product radius. To avoid error, λ can be

* Marcus (Appendix to Ref. 44) suggested substituting a mean *differential* dielectric constant $\partial\varepsilon_A/\partial A_A$ for ε_o (or ε_A) as dielectric saturation is approached.

estimated from the Continuum solvation energy $(z^2e^2/2r)(1 - 1/\varepsilon_o)$, which is about 35% of the total interaction energy for typical 2+/3+ ions (Section IV-9). This gives an average of about 170 kJ/mole for $(e^2/2r')(1 - 1/\varepsilon_o)$, and 96 kJ/mole for $\lambda = (e^2/2r')(1/n^2 - 1/\varepsilon_o)$. Hence, neglecting work-of assembly terms, the Marcus equilibrium inertial energy $\lambda/4$ is about 24 kJ/mole (0.25 eV, 9.7kT). In a 1.0M solution usually used for kinetic experiments, $\lambda/4$ will be about 50% of this (Section IV-8), far less than experimental equilibrium activation energies.[90,177]

We are therefore forced to search for an Inner Sphere activation energy term. A model of the reaction coordinate for the Inner Shells of 2+ and 3+ ions based on the latest Section IV-9 model is given in Figure 6. It shows a stretch of 0.11 Å in equilibrium ion-dipole center distance on going from the 3+ ion at 2.095 Å to the 2+ ion at 2.205 Å. These are equivalent to ion-oxygen distances of about 2.0 and 2.1 Å. The intersection of the terms is at 1.043kT per oscillator, at 2.140 Å. Before correction for the ground states of the three-dimensional oscillators, the equilibrium energies of each inner sphere water molecule were –159.70kT and –72.21kT at 298 K. The inner sphere dielectric constants for 3+ and 2+ were 1.988 and 2.515, the inner sphere repulsive counterfields being respectively 29.4% and 34.6% of the total counterfields. The corresponding force constants were 475,000 and 167,000 dyne/cm, giving frequencies of 2.07×10^{13} ($669\ cm^{-1}$, $h\nu = 3.23kT$) and 1.19×10^{13} ($396\ cm^{-1}$, $h\nu = 1.91kT$). Corrected for the $3h\nu/2$ ground states, the inner sphere energies are 953.3kT (2363 kJ/mole, 564.9 kcal/mole) and 430.4kT (1068 kJ/mole, 255.2 kcal/mole).

The 6 x 1.043kT barrier height must be reduced by about $(\sum 3h\nu/2)/2$ to give an overall height of only about +2.41kT. The barrier height in the second shell is small enough to be neglected. Including the maximum value (9.7kT) of the Continuum term, and before any reductions for coupling of reactant-product energies, the total Inner plus Outer λ value is +12.1kT per ion (0.31 eV, 30.0 kJ/mole, 7.2 kcal/mole). It should also be noted that even after correction for the oscillator ground states, the reactant and product energy wells are at equal enthalpy, not equal free energy. The $T\Delta S$ correction to place the curves at electrochemical equilibrium, will further reduce the barrier height.

Because of the small activation energy, the Tafel plots will show considerable curvature. An obvious problem is that the anharmonicity

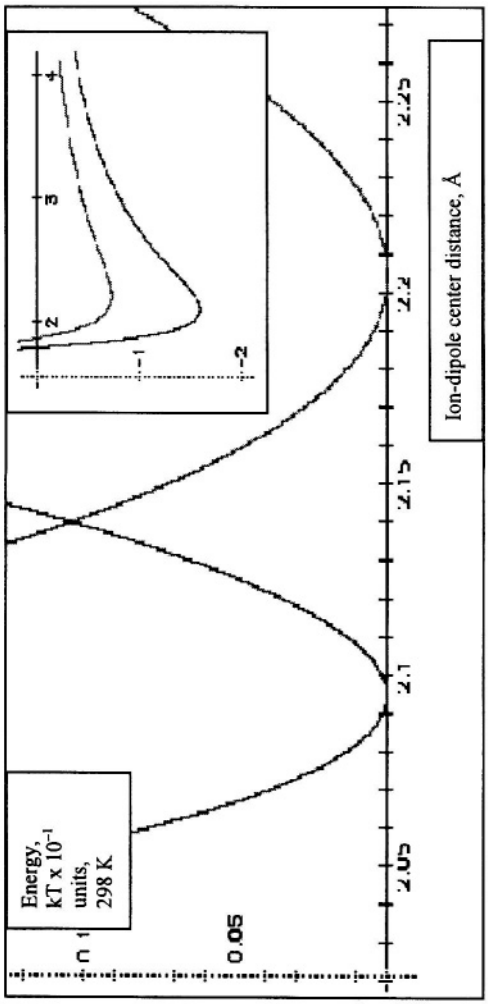

.Figure 6. Calculated two-dimensional energy surface for heterogeneous Franck-Condon transition of each member of the three-dimensional 6-oscillator trikisoctahedral Inner Shells of 3+ and 2+ ions at equal potential energies (before ground state energy correction). Crossing point at +6.26kT at 298 K at 2.140 Å for the three-dimensional oscillator (+15.52 kJ/mole). Corrected for ground state energies (+4.84kT and +2.87kT), the crossing point is at +2.41kT (equilibrium potential energy of activation 5.97 kJ/mole). The Inset (x-axis kT x 10^{-2} units) shows absolute energies of 3+ (minimum −159.697kT at 2.095 Å) and 2+ (minimum −72.21kT at 2.205 Å), corresponding to ion-oxygen distances of about 2.0 and 2.1 Å.

argument for the inner sphere energy terms[71] cannot be used to straighten out the Tafel slope, since the form of the wells near the energy minimum is nearly parabolic, even though they are distorted upwards in the direction of the ion, and downwards away from it. We must seek an explanation elsewhere for the straight experimental Tafel lines in the careful work of Curtiss et al.[177]

2. FC Proton Transfer

Proton transfer is a more demanding case than simple electrochemical electron transfer (ECET)[90] redox processes. It involves coupled ion-electron transfer or electrochemical ion transfer (ECU), recently described[90] as a process in which partial loss of the solvation sphere occurs, adsorption is involved, with "for univalent ions.....the occupation number* changes gradually (adiabatically) as the ion approaches the surface," which is reminiscent of Hush.[50,176] Schmickler et al.[90,91,178] and others[179] have generally used the extended Anderson-Newns adsorption model[180,181] for such processes, using Kramers modifications[182] of transition state theory.

The period of a single water molecule rotating around the oxygen-protons axis is about 5×10^{-13} s. Hence the time for an incomplete rotation to assemble, e.g., the $H_9O_4^+$ ion or the solvation shell of a simple ion will be about 2×10^{-13} s, $\approx h/kT$. As Section VI-1 shows, the time for equilibrium Langevin angle change during or following a one-electron transfer is $1.2\text{-}1.4 \times 10^{-13}$ s, so the Continuum can keep up with this process under non-FC electron transfer conditions controlled by the motions of water disassembly and solvation shell assembly. The rate of the step $H_{ads} + H_2O \rightarrow H_3O^+$ is high under conditions where the Gibbs energy for the step is close to zero, i.e., the electrocatalyst (e.g., platinum) is at or near the top of the electrocatalytic volcano.[183] The corresponding activation energy must be low, which is in line with the requirements and activation energy for proton conduction[171] via rotation of solvated H_3O^+ and water supermolecules and proton "hopping" (Ref. 170, p. 96).

As in the redox case (Section VI-1), we will first discuss the reaction under FC conditions, corresponding in part to the Dogonadze-Levich model,[82] and somewhat analogous to Fawcett's EITC

---

* Sic, i.e., the electronic charge of the intermediate or transition state.

models.[184,185] It is helpful to consider the reaction in the anodic direction. From the model for proton solvation in Section V-2, the Continuum activation energy term $\lambda/4$ under FC conditions would be 98.8/4 = 24.7 kJ/mole (0.26 eV, 10.0kT). The crossing point between H_2O–H_2O + H_{ads} → H_3O^+–H_2O where the two water molecules on the left side are respectively of *Type A* and *B* (i.e., no rotation is required for assembly) was calculated in the same way as Figure 6. It occurs at a bond length of 2.710 Å, and is at 1.1kT above the minimum at $\Delta G = 0$. For water, the stretching force constant is about 16,800 dyne–cm^{-1} and hν for the three-dimensional oscillator is 0.61kT (126 cm^{-1}), so the ground state for each *Type A–B* molecule is at 0.31kT. The correction for the ground states of the stretching frequencies [(l/3)(3/2)(l.58+0.61)72 per water molecule, i.e., –0.55kT] gives a total of +1.1kT activation energy for the two *Type A–B* molecules. The other two water molecules required to form $H_9O_4^+$ must either detach from their H-bonded state (requiring about +9.7kT each), or rotate to some compromise position between initial and final states. Calculation shows that 90° rotation from the minimum energy position to the approximate half-way point requires an energy equal to +8.23kT above the minimum. This option will be energetically preferred. Again, this must be corrected for the ground state energies. The bending frequency, as calculated here (c.f., Pople[103]) is $(1/2\pi)(g/I)^{1/2}$ or 282 cm^{-1} (hν = 1.36kT). The value for solvated H_3O^+ is probably about 50% higher, so the correction is –0.85kT per water molecule. Thus, the total energy to assemble the Inner Sphere in a compromise configuration between that of the reactants and the products is +15.9kT. With the Continuum term, we have a total activation energy under equilibrium conditions of +25.9kT (0.67 eV, 64.2 kJ/mole, 15.3 kcal/mole). If assembly of the solvation shell of the adsorbed proton under equilibrium conditions occurs from the solvation shell of the electrode, i.e., the Helmholtz double layer, the net energy of assembly will be the same, since the Helmholtz layer must be reconstituted after proton discharge. The value +25.9kT for proton discharge is much too large, as the results of Marković and Ross[186] (discussed below) indicate. Platinum is at the top of the $-H_{ads}$ Volcano, so the reaction takes place under equilibrium conditions close to zero overpotential.[183]

3. The Inertial Term

Libby[30] and Weiss[32] both stressed the inertial energy present in the Continuum as the energy barrier to FC electron transfer, which we have seen in Section VI-1 requires a relaxation time of about $(1.2\text{-}1.4) \times 10^{-13}$ s to accommodate itself to the change in charge. Weiss considered that the inertial energy was always the inertial energy difference between the solvent surrounding the reactants and products in their ground states, i.e., for a change of z to z + 1, $[(z+1)^2 - z^2]e^2(1/n^2 - 1/\varepsilon_o)/2r'$. In contrast, Marcus[41-43] considered that the barrier could accommodate itself to a compromise position between reactants and products prior to electron transfer, so that his $\lambda = e^2(1/n^2 - 1/\varepsilon_o)/2r'$, corresponding to Weiss's barrier expression for a one-electron transfer, is reduced at equilibrium to $\lambda/4$ by intersection of similar parabolic energy terms for reactants and products. This arises from his use of $-(2m-1)(\mathbf{E}^* - \mathbf{E})^2\alpha_u dV/2$ (Sections II-3 and III-2) integrated over the electrolyte volume outside the reactants, where the field term is the difference between the excited and final states in the same configuration, and m is the Lagrangian undetermined multiplier used in minimizing. How the system can rearrange itself to a compromise $\mathbf{E}^*$ value (not a thermal energy value) *prior to and in anticipation of* electron transfer requires discussion. If the solvent model is imagined to have coordinated harmonic thermal electron oscillations for reactants and products (ions of different valency for homogeneous redox processes, and a typical ion and one of infinite radius for electrode reactants) then such a model may be envisioned.

However, the Continuum model developed Section III-2 is molecular and has no place for such coupled oscillators. The remote rotating superdipoles can influence the free energy of a reacting ion if the average value of the cosine of the Langevin angle θ is permitted to change because of changes in the energy distribution in the solvent. Bockris and Sen examined this problem[4,187] using an equivalent to the expression $V = x_A \cos\theta$ for the potential energy V of remote dipole-ion charge interactions in the classical maximized entropy Maxwell-Boltzmann calculation for the mean energy [V] in the averaging expression:

$$\frac{d(V_i N_i)}{N} = \frac{V_i (\exp - V_i / kT) d\cos\theta}{\sum (\exp - V_i / kT)} \qquad (82)$$

where V_iN_i/N is the fraction of the number of molecules with a potential energy V_i in the angular interval $\cos\theta_i$ and $\cos\theta_i + d\cos\theta$. This was evaluated for classical small energy intervals by integrating the numerator and denominator as usual. The mean square energy $[V^2]$ was then evaluated by substituting V_i^2 for V_i in the left numerator. The standard deviation $\sigma^2 = [V^2] - [V]^2$ gave the fluctuation of the system from thermodynamic equilibrium about the mean value. The probability of a large number (N) dipoles having a cumulative random fluctuation from the mean is equal to the very small Gaussian distribution value $N \exp - \frac{\{V - [V]\}^2}{2\sigma^2}$, so the probability of providing sufficient energy to overcome any Born-Bjerrum inertial or Marcus activation energy barrier would be very small. This work has not received much attention.[188] The probability may also be determined via the relationship between the Langevin angle and the total dipole energy from the Boltzmann distribution[103]:

$$\langle \cos\theta \rangle = \int \cos\theta \sin\theta (\exp - V/kT) d\theta / \int \sin\theta (\exp - V/kT) d\theta \qquad (83)$$

We replace the energy in the numerator and denominator by $\exp -\varepsilon_i/kT \exp + u/kT$, where ε_i is the kinetic energy of the population of dipoles dN_i, which itself has a subset of energies depending on the value of $\cos\theta$ in the potential energy term u. The second and more distant shells contain a sufficient number of superdipoles to make the Stirling approximation and the Boltzmann distribution reasonably accurate. The $\exp -\varepsilon_i/kT$ terms cancel, so $\langle \cos\theta \rangle = L(x_A)$ is independent of the kinetic energy. This again implies that activating the ion via electrostatic coupling in the electrolyte is improbable.

The Soviet school model considered that Outer Sphere or dielectric continuum dipoles perform small harmonic vibrations at a relatively low frequency.[58,59] The implication of vibrations is that the minimum of the potential energy of interaction $V = -B\cos\theta$, i.e., $B = -(A_A/\varepsilon_o)\mu'$ must be greater than $\varepsilon/2$, where ε is the relevent kinetic energy of the superdipole.[151] This may be taken as the equipartition energy for rotation in the two dimensions at right angles to the field vector. If we assume that the first layer of superdipoles is centered at 8.6 Å from a trivalent ion, with their structures intact, and the bulk dielectric constant still applicable, their maximum interaction with z = 3 will be –0.6kT, so they will be librating. In principle, such a model

may be described by the electrostatic equivalent of the ferromagnetic effect, in which residual polarization is present because of order-disorder phenomena,[189] but such an explanation cannot be used for liquids. In any case, the next layer of superdipoles centered at a distance of 13.9 Å from the ion, will be rotating with a maximum interaction energy of – 0.2kT for z = 3. These interactions are at an effective temperature greater than that of the electrostatic equivalent of the Curie point in ferromagnetism, so built-in polarization cannot occur. We should note that the period of rotation $\pi(2I/\varepsilon)^{1/2}[1 + B/2\varepsilon + (9/16)(B/\varepsilon)^2]$, where ε is the total energy, will decrease from shell to shell as 'a' increases and B becomes less. However, at the same time, the maximum interaction between superdipole groups in adjacent shells remains constant at about –0.4kT, providing a coupling mechanism overriding the fall in B. It would be expected that nearest neighbor superdipole groups will rotate in opposite directions, so that they line up in the linear nose-to-tail position perpendicular to the field vector, and are in the parallel nose to tail position parallel to the field vector. Again, it is difficult to see how these motions influence the electronic energy of an ion.

In conclusion, the barrier height to FC change transfer, as envisioned by Weiss,[32] may be correct. In a 1.0M electrolyte, it would be about 50 kJ/mole (0.5 eV, 20kT, 12 kcal/mole). This appears to be of the correct order.[90,177] However, an alternative view is discussed below.

VII. NON-FC CHARGE TRANSFER

1. Water Molecule Rearrangement in Solvation Shell Assembly

The driving force for rearrangement of water molecules before instantaneous FC proton-electron charge transfer presents a problem. A five-molecule water superdipole assembly might acquire +25.9kT of thermal energy, but there will be a low probability that its subsequent rearrangement will direct it towards that for an intermediate state for FC electron transfer and proton discharge. This is not necessarily true for

the simple linear rearrangement required for redox valence change, but the "half-way" rearrangement of water molecules from their normal aqueous state to that for a solvation shell in a 0 to ±1 transition and vice

versa must require some "steering" activity. The present discussion applies to such transitions.

For these, a different process is suggested, which may be related to Schmickler's concepts.[90,91,178] The activation energy for such a process may be less than that for FC electron transfer. If this so, the lower activation energy process with more probable rearrangement possibilities will be kinetically favored. In the suggested process, electron transfer occurs slowly over 10^{-12}-10^{-13} s so that the moving molecules during the assembly of the Inner Sphere solvation sheath are "steered" by the slow acquisition of charge, i.e., by the change in $\Psi\Psi^*$, where Ψ is the wave function of the transferring electron and Ψ^* is its complex conjugate. Such processes must be adiabatic since the transfer probability as a function of time must be high. The Outer Sphere or Continuum energy term will then disappear, since the inertial energy of its dipoles can keep up with the relatively slow change of field. A simple model for such a mechanism seems to be that of Hush.[50,176] He considered a "flow of charge" from state "ze" to "ze±e" during an apparently slow charge transfer process in which a sequence of ground states of intermediate charge occur. He only considered changes in ion-dipole interactions during the process (Section II-5), which resulted in activation energies much less than experimental values. After Marcus' early publications,[41] he therefore added an outer Continuum inertial term.[67] This effectively canceled his concept of slow flow of charge.

2. Non-FC Redox Electron Transfer

If an induced dipole term is added to Hush's[50] permanent dipole term, the resulting activation energies are illustrated by the following simple argument. The permanent- and induced-dipole terms along the reaction coordinate may be approximated by $-(Bz)^{m/2}r^{-m}$, where m lies between 2 and 4, with B constant. Combining with an inner sphere repulsion $+Ar^{-n}$, and minimizing using the derivative, the equilibrium energy well at $r_{o,z}$ is $-[(n - m)/n]Bz^{m/2}(r_{O,z}^{-m})$. A is approximately constant and equal to $(m/n)Bz^{m/2}(r_{o,z})^{n-m}$, so $r_{o,z-1}/r_{o,z} = (z/z - 1)^{m/2(n-m)}$, where z, z – 1 are the initial and final valence states. Eliminating the r_o terms gives $\phi_{z-1} = \phi_z(z - 1/z)^{mn/2(n-m)}$, where the ϕ values are equilibrium potential energies. This energy expression is formally similar to Johnston's bond-energy-bond-order (BEBO) transition state model.[68] The energy in excess of ϕ_z along the reaction coordinate is $\phi' = -(\phi_z - \phi_{z-q} - y) + q(\phi_z - \phi_{z-1} - y)$, where z – q is an intermediate charge, and y

contains the overpotential. ϕ_{z-q}, ϕ_{z-1} are $\phi_z(1 - q/z)^{mn/2(n-m)}$ and $\phi_z(1 - 1/z)^{mn/2(n-m)}$ respectively, with ϕ_z negative. Expansion as far as the quadratic binomial terms gives $\phi' = (\phi_z/z^2)p[q(1 - q)] + y(1 - q)$, where $p = mn(2m + mn - 2n)/8(n - m)^2$. The derivative is zero when $q = q^* = 1/2 - y/2(\phi_z/z^2)p$ The activation energy ϕ^* is therefore $(\phi_z/z^2)p/4 + y/2 + y^2/4(\phi_z/z^2)p$, which is identical in form to the Marcus expression,[41,42,44,50,67,176] and will therefore show the same type of Tafel curvature and change of symmetry factor with overpotential as that identified in Section II-8.

In early simulations of non-FC ECET, separate ion-permanent dipole and ion-induced dipole terms were used, along with Hush's assumption that A could be considered to be constant on going from reactants to products. This imposed restrictions introducing inaccuracy, so a model was used based on that in Section VI-1 for 2+ and 3+ ions. Reasonable assumptions made were (a) the ion-dipole center distance was proportional to the change in fractional charge on going from 2+ (2.205 Å) to 3+ (2.095 Å) which is reasonable since the z/x^2 and $(z/x^2)^2$ terms in the permanent and induced dipole energies can be expanded to linear expressions with good accuracy, and (b) any changes in the outer counter-field terms were also linear functions of the change in fractional charge.

The calculated non-FC barrier between the 2+ and 3+ states is shown in Figures 7A and 7B. The initial and final states are corrected this time for the ground states of the oscillators (Figure 7A). Motions along the reaction coordinate consist of the three-dimensional symmetrical stretching frequency and any independent stretching frequencies of the inner sphere oscillators, and those perpendicular to it. If ε_r, ε_i, and ε_p are the reactant, intermediate, and product ground state energies, it is reasonable to suppose $\varepsilon_i \approx (\varepsilon_r + \varepsilon_p)/2$ for motions perpendicular to the reaction coordinate. Along the reaction coordinate, it is assumed that motion is governed by the time constant of the Continuum superdipoles. The vibrational partition function in the transition state may therefore be replaced by $kT/h\nu_i$ in the usual way, where $1/\nu_i$ is the transition time for reactants to products, giving the preexponential frequency factor kT/h. If the barrier height with the two minima at equal energy is A, the minima may be adjusted so that the ground state energies are equal, then using the Brønsted rule, the

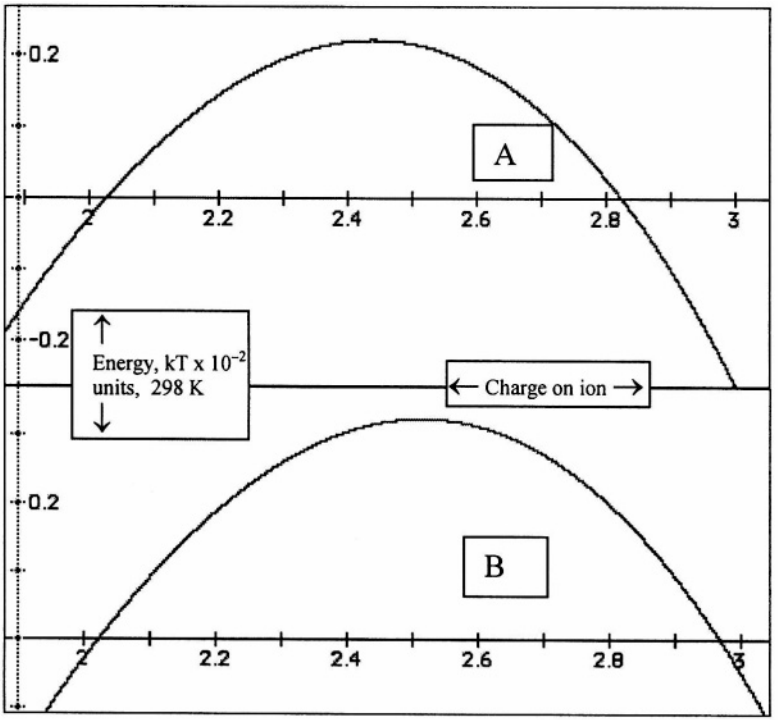

Figure 7. Calculated two-dimensional energy surfaces for heterogeneous non-Franck-Condon transition of the three-dimensional 6-oscillator trikisoctahedral Inner Shells of 3+ and 2+ ions at (A) equal potential energies after ground state energy correction; (B) at equal ground state free energies. Barrier height in B +22.9kT at 298 K (+56.9 kJ/mole, +0.59 eV, experimentally +0.59 eV[177]).

height of the barrier to the energy minimum for the intermediate becomes $(A - \varepsilon_r) + (\varepsilon_r - \varepsilon_p)/2 = A - (\varepsilon_r + \varepsilon_p)/2$. Alternatively, as in Figure 7, it may be done graphically. The barrier height is then 32.26kT. If kT/h appears in the preexponential, a further kT should be added to give the Arrenhius energy, E_{Arr}.

Since we are concerned with the Arrenhius activation energy under equilibrium conditions, a further correction should be made for the $T\Delta S$ change with the system in equilibrium under standard conditions, i.e., considering the relative standard entropies for for Fe^{2+}, Fe^{3+} equal to –137.7 and –315.9 J/mole-K,[190] a difference of –178.2 J/mole-K. The

Continuum entropies[98] relative to vacuum values are about –40.2 and –90.4 J/mole-K (Section III-1), a difference of –50.2 J/mole-K. We should point out that the assimilation of the oscillator potential energy to a portion of the 298 K experimental ion enthalpy may be somewhat in error (c.f., discussion for protons[191]), and the difference between the 2+ and 3+ entropies in Ref. 190 is 21% higher than for Latimer's original values.[192] In consequence, there is some uncertainty that the calculations truly represent equilibrium. However, the barrier height in Figure 7B is 56.9 kJ/mole (0.589 eV, 22.9kT, 13.6 kcal/mole), in very good agreement with the experimental value of 0.59 eV.[177] Other calculations showed that the activation energy is closely proportional to the oscillator energy in the transition state or to the mean solvation energy, in agreement with other work.[185] It is also roughly proportional to the mean charge on the transition state and to the change in bond-length at constant mean charge.

We should bear in mind that chemical processes in liquid media[193] (which should include at least some electrochemical processes) may follow the classical Berthoud-Hinshelwood expression for the reaction rate, in which internal classical vibrational modes reduce the potential energy of activation U_o by a term involving some effective number 's' of classical oscillators per molecule to give E_{Arr}, i.e., $E_{Arr} = U_o - skT$.[194,195] This will show an temperature-dependent E_{Arr}, which requires further study.

Assuming trikisoctahedral ions with average effective radii of 4.0 Å, that of the inner shell (Section IV-9) in collisions with single active water molecules (radius 1.4 Å), a collision frequency (Section II-8) of 1.8×10^{13} s^{-1} is obtained. Assuming an effective reaction layer thickness of twice the mean second trikisoctahedron shell radius, i.e., 10.8 Å, with an activation energy of 22.9kT at 298 K would yield an apparent rate constant of 2.2×10^{-4} $cm\text{-}s^{-1}$ at this temperature. The use of kT/h as the frequency factor (6.2×10^{12} s^{-1} at ambient temperature) or the frequency ($\propto T^{1/2}$) of superdipole transition between redox states (7.7×10^{12} s^{-1}, c.f., the period $\approx 1.3\ 10^{-13}$ s in Section VI-1) gives 7.6×10^{-5} $cm\text{-}s^{-1}$ and 9.4×10^{-5} $cm\text{-}s^{-1}$ respectively. The experimental value[177] is 5×10^{-5} $cm\text{-}s^{-1}$. Considering the assumptions made, the agreement may be considered good. As has been pointed out[91] the interpretation of kinetic data is often distorted by double layer effects.[196]

3. Proton Transfer and Other ECIT Processes

Before correction for ground states, the *Version C* model for proton solvation, giving importance only to ion-dipole averages (which may introduce some error) gave a total barrier height of only 6.81kT for all four water molecules (Figure 8). The ground states of the initial states were 2.35kT (one three-dimensional and one linear oscillator), and the estimated value for the hydrogen-bonded products was 1.45kT, giving a correction of 1.9kT. The same procedure as that for the redox case was used to estimate the ground state energies of the transition state as an increase in barrier height of 1.24kT, so the barrier height falls from 6.81kT to 6.15kT. The next question is the activation energy associated with the discharge process $H_{ads} + H_2O \rightarrow H_3O^+$, where H_{ads} has $\Delta G^o = 0$

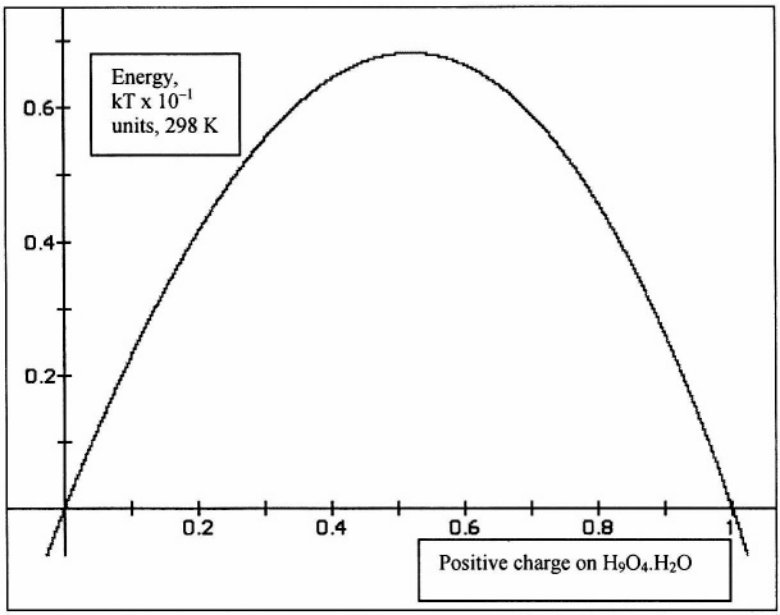

Figure 8. Calculated two-dimensional energy surfaces for heterogeneous non-Franck-Condon transition between $H_9O_4^+.H_2O + e^-$ and $5H_2O$ at equal potential energies, before correction for ground states. Barrier height +6.15kT (+15.2 kJ/mole, +0.16 eV) after correction for ground state energies.

at equilibrium. An attempt to examine this (along with the other hydrogen electrode steps) was made by Bockris and Srinivasan[197] using the semiempirical Eyring-Polanyi approximation[198] of the Heitler-London method to calculate the potential energy surface. This method is simple to use for normal chemical processes involving atom exchange, but it is not so clear how it should be used for electrochemical processes, i.e., how the terms for different species, particularly the electron, are to be accommodated at equilibrium. Attempts to apply it appear to show low barriers at equilibrium, although the assumption that the metal water interaction (the third interaction in a pseudo three-atom process M–H–H_2O process) can be ignored leads to incorrect results, as simulations carried out in the present work have shown. The reaction between the emerging H^+ and H_2O, a pseudo-two-atom process, is so strongly exothermic that a barrier would not be expected, as in, for example, $H + H \rightarrow H_2$.[199] Thus, the total activation energy of proton discharge under equilibrium conditions appears to be very low, even less than that for water dipole rotation (16.3 kJ/mole in liquid water, about four times less than in ice),[200,201] which partially contributes to it. Any contribution corresponding to the formation of $H_3O^+ + e^-$ from H and H_2O is similar mechanistically to the tunneling transfer of H^+ between water molecules.[171] The crossing of the FC potential energy surfaces for this process is shown on p. 99 of Ref. 170. The barrier is low enough and thin enough to be transparent to protons.

At overall H_2 and H^+_{aq} electrochemical equilibrium and under equilibrium conditions for the intermediate $-H_{ads}$ at the Volcano maximum, the barrier must be further corrected for the absolute entropy of H^+_{aq}, which from thermal cell studies[202] is about –20.9 J/mole-K.[203,204] Thus using the Brønsted rule, barrier should be lowered by $-0.5T\Delta S$ or 1.26kT at 298 K, giving a final value of 12.1 kJ/mole (0.126 eV, 4.89kT, 2.90 kcal/mole), which may or may not represent the potential energy of activation (U_o) rather than the experimental Arrhenius energy, i.e., $U_o + kT$ for a transition-state process with a preexponential kT/h.

Marković and Ross[186] have studied the hydrogen oxidation reaction (HOR) on well-characterized Pt(110)(1x2), (100) and (111) surfaces in 0.05 M H_2SO_4 as a function of temperature. The basic Pt(110)(1x1) surface consists of parallel lines of atoms separated by the unit cell length 'l' (3.924 Å), with each atom in the line separated by nearest-neighbor distance $l/\sqrt{2}$. Each rectangle of four atoms has a further atom at its center, situated $l/2\sqrt{2}$ below the plane of the others, giving a ridge

and furrow surface structure. The surface atoms have 6 missing nearest neighbors, whereas the furrow atoms have 2. This is an unstable configuration, and surface restructuring readily occurs, e.g., on annealing. The resulting (1x2) configuration has every other surface row missing, giving furrows twice as wide, with hexagonally close-packed (111) sides (4 missing nearest neighbors) at an angle of 54.74° to the perpendicular to the surface. To maintain numerical continuity, the surface has hexagonal steps to higher surface layers, giving terraces with missing row configurations. Unlike atoms on the (111) surface, which have 3 missing nearest neighbors, the surface atoms and furrow atoms are different in properties according to their number of closest neighbors. Pt(100)(1x1) is also known to reconstruct to a hexagonal form known as (5x20) from its LEED pattern under certain conditions, but the (1x1) surface was stable at the potentials examined.[186] Per l^2, the Pt(110)(1x2) surface ideally has 0.707 surface atoms, 1.414 atoms in the furrow sides, and 0.707 at the bottom, i.e., 2.818 in all. Ideally the surface packing density is 2.309 and 2.000 atoms per l^2 for the (111) and (100) planes.

The Tafel slopes for hydrogen oxidation obtained by Marković and Ross[186] at 274 K were A. (110)(1x2), RT/1.94F; B. (100) RT/0.49F (high current density), RT/1.47F (low current density); and C. RT/0.73F. The corresponding exchange currents and equilibrium activation energies were 0.98, 0.60, and 0.45 mA/cm^2 at 303 K and 9.5, 12, and 18 kJ/mole, respectively.[186] The authors considered that the corresponding mechanisms were A. dissociation (reverse combination) rds, rapid discharge (Tafel-Volmer, Process 1), B. electrochemical dissociation rds, rapid discharge (Heyrovsky-Volmer, Process 2), and C. either Process 1 or 2, respectively. A. is in good agreement with the expected value for the Tafel rds under high intermediate coverage conditions, with no other possible fit (low coverage results in a chemical limiting current). There are three possibilities for B: a switch from a second electron transfer step (Volmer) rate-determining under low coverage conditions to a first step (Heyrovsky) as overpotential increases, or the opposite at high coverage. Finally, it may represent a first electron transfer rds at high coverage, with a sudden switch to low coverage at an overpotential of +40 mV. C is considered later.

When filled with H_{upd}, the lines of atoms at the furrow tops of Pt(110)(1x2) are still unoccupied.[186] Even so, the weak structure shows a lattice expansion of 10% compared with 2% for the other low-index surfaces.[186] Unlike Pt(100), adjacent sites are available for Tafel

dissociation, which is favored under high coverage conditions in the limited overpotential range (0.05 V) examined.

Following the reduction of a partial coverage (to about 0.33)[204] of adsorbed anions (bisulfate),[186,204] the well-prepared (100) surface is fully covered (to one H_{ads} per Pt atom) by under-potential-deposited hydrogen (H_{upd}) in the potential range of interest, which follows a Frumkin isotherm, i.e., its free energy of adsorption falls linearly with coverage as sites are occupied and sideways forces and lattice expansion progressively occur.[186] Alternatively, the isotherm may be regarded as a succession of overlapping fractional Langmuir isotherms, whose average free energy for each segment reduces with coverage. The last segment, completing the total coverage, represents a small fraction of the total area whose free energy at this differential coverage is zero or rather negative. This fractional part of H_{upd} should be the major contributor to the overall anodic reaction intermediate, i.e. only a small part of the overall surface area should be active. The marginal H_{upd} species, i.e., that with the weakest adsorption, may be the reaction intermediate at small anodic overpotentials at high local coverage, and the Heyrovsky rate-determining step switches to the Volmer step under high coverage conditions on the (100) surface as overpotential increases.

In the potential range of interest, the hexagonal (111) surface is filled by H_{upd} whose Frumkin peak is broad, indicating a large $+r\theta$ value, where r is the change in free energy of adsorption with the coverage θ. Over the 0.15V examined, the electrode is in the medium coverage range. Examination of the complete kinetic equation for Heyrovsky rate-determining, Volmer in pseudoequilibrium under these conditions, including the preexponential θ, $(1 - \theta)$ terms and the exponential $\beta' r\theta$, $-(1+\beta' r\theta)$ terms, where β' is the Brønsted slope,[183] shows that a RT/0.73F Tafel slope may be readily fitted to this process over two decades. This provides an explanation for Case C, the (111) surface. Thus, on the (111) and (100) surfaces, the extrapolated Heyrovsky reaction appears to have activation energies of 18 and 12 kJ/mole respectively[186] under equilibrium conditions at high H_{upd} coverage, whereas the Tafel process has an activation energy of 9.5 kJ/mole under the same conditions on the Pt(110)(1x2) surface.

High coverages imply small experimental Arrhenius preexponential terms, which were (110) 0.043 $A\text{-}cm^{-2}$; (100) 0.070

$A\text{-}cm^{-2}$; (111) 0.570 $A\text{-}cm^{-2}$,* assuming E_{Arr} to be temperature-independent. If one assumes a dihydrogen solubility $\approx 10^{-3}$ moles/liter, with kT/h at 303 K = 6.31×10^{12} and a reaction zone thickness of 2.8 Å corresponding to one water molecule diameter, we obtain a theoretical preexponential factor of 0.177 $moles\text{-}cm^{-2}\text{-}s^{-1}$, i.e., 3.41×10^{4} $A\text{-}cm^{-2}$. Taking into account the surface packing densities, this indicates that on average only 1 surface atom pair in 7.9×10^{5} surface atoms is active on the (110)(1x2) plane for Tafel dissociation; and 1 in 3.5×10^{5} on the (100); and 1 in 4.5×10^{4} on the (111) for the Heyrovsky reaction.

Under cathodic conditions, the low activation energies require correction for the corresponding overpotential deposited hydrogen (H_{opd}) cathodic reaction intermediate under high coverage conditions. These have been examined by Conway and coworkers[204,205] as part of a somewhat controversial study of hydrogen evolution in sulfuric acid on platinum single crystals, which apparently shows much higher cathodic rates compared with the Marković and Ross[186] micropolarization data,. The $d\eta/d\theta$ slope[204,205] at $\theta = 0.5$ is equal to $(RT/F)[(r\theta/RT) + 4]$, giving r values of 5.7kT, 3.8kT, and 0.2kT for the (110), (100), and (111) faces. With $\beta' \approx 0.5$, the cathodic process (Heyrovsky rds at high coverage, Tafel slope RT/2F) extrapolated from moderate to high overpotentials should have activation energies at equilibrium of about 18 and 17 kJ/mole on the (111) and (100) faces, that on the (110) being unknown. At cathodic overpotentials, assuming a temperature-independent β, a barrier of this height ($\approx$7.3kT) will only allow a change in rate of 3.2 decades from the exchange current value before the process becomes activationless.[206] This presents a difficulty, because data for platinum (which appear acceptable, because of the techniques used) show a linear Tafel behavior up to 10^{2} A/cm^{2}.[207-209] The only apparent explanation is a basic difference between the exponential and preexponential terms on single crystal and polycrystalline platinum. Bowden's early work, dating before careful elimination of adsorbable impurities, reported an activation energy of 29-38 kJ/mole[15] on polycrystalline platinum, the higher value being on old electrode surfaces. At the lower activation energy value, this would allow 5.25 decades of rate change before the activationless condition occurs, making the results of Kabanow[207] and Bockris and Azzam[209]

---

* Bowden's early work, dating before careful elimination of adsorbable impurities, reported an activation energy of 29-38 kJ/mole[15] on polycrystalline platinum, the higher value being on old electrode surfaces. This suggests a preexponential value of about 0.5 A/cm^{2}.

plausible, though not mutually in agreement, since the latter showed hysteresis at very high current densities.

The hydrogen evolution reaction on mercury has an exchange current of about $10^{-12.3}$ A/cm^2,[210] an equilibrium activation energy of ca. 80 kJ/mole,[204] and therefore an Arrhenius prexponential factor of 50 A/cm^2, about 100 times greater than that on Pt(111). A convincingly straight composite Tafel plot[210] (potential independent $\beta = 0.60$) using results of Bowden and Grew[211] at low current density, of Bockris and Azzam,[209] and finally the apparently unpublished results of Nürnberg[212] extends from 10^{-9} A/cm^2 to $10^{+4.4}$ A/cm^2. The plot may be simulated without using the pseudoequilibrium assumption for H_{ads} coverage, since the back reactions are negligible at high cathodic overpotentials, where the forward rates for the electrochemical Volmer and Heyrovsky steps are high. Taking platinum to be at the top of the Volcano, the effective Heyrovsky rate constant on mercury will be increased by $\exp(1 - \beta')\Delta\Delta G_{ads}/RT$ compared with that on platinum, where β' is again the Bronsted slope, and $\Delta\Delta G_{ads}$ is the positive difference in the free energy of adsorption of H_{ads} between platinum and mercury. The rate constant of the Volmer reaction is correspondingly reduced by $-\beta'\Delta\Delta G_{ads}/RT$, and that of the Tafel reaction is increased by $2\beta'\Delta\Delta G_{ads}/RT$. A general expression for the rate of the overall Heyrovsky-Volmer process is $(k_1k_2 - k_1'k_2')/(k_1 + k_2 + k_1' + k_2')$, where the back reactions have primes and the k values contain the $\Delta\Delta G_{ads}/RT$ and electrochemical rate terms, but not the θ and $(1 - \theta)$ terms, which are reflected in the denominator. A similar more complex (quadratic) expression may be written for the Tafel-Volmer mechanism.

Assuming that β' (for H_{ads}) is $(1 - \beta)$, where β is the symmetry factor for changes in $H^+ + e^-$ on the opposite side of the energy barrier, the best fit for $\Delta\Delta G_{ads}$ for mercury for the Tafel plot is +68kT or about 168 kJ/mole more positive than the value for platinum, i.e., –83 kJ/mole, putting it very close to the low adsorption energy leg of Trassati's Volcano plot[213] shown by Conway.[204] The Volmer reaction should always rate-determining, with a potential-independent Tafel process to overpotentials of about –0.9 V, when it is overtaken by the Heyrovsky process as the fast step. The Brønsted slope of this leg, referring to the Volmer rds, is 0.32. On platinum, this rds has a rate of about 10^{-1} A/cm^2. Using this value results in a slightly steeper slope of 0.37, close to the 0.4 used in the simulation. It is also in good agreement with the presumed difference between the equilibrium activation energies on mercury and platinum (about 60 kJ/mole, or 0.36

x 168). An activationless process will occur a sufficiently high current density. Again assuming a potential-independent β, this would occur at $+10^{1.7}$ A/cm^2, or at higher values if some change of β at very high overpotentials take place. This may be occurring at the highest current densities shown in Ref. 210.

4. Tafel Plots for Redox ECET and ECIT Processes

The mechanisms discussed above for redox processes gives pseudo-parabolic V-i dependencies after binomial expansion of the energy terms, leading to Tafel curvature. The interesting result is the value of α, the transfer coefficient, which (in intervals of 4kT from equilibrium, or 0.1028 eV) is 0.432, 0.418, 0.403, 0.388, 0.373, and 0.359 (anodic); and 0.554, 0.539, 0.525, 0.511, 0.502, and 0.483 (cathodic). In these ranges, the effective charge on the transition state varies from +2.439 to +2.366, and from +2.432 to +2.524. The anodic and cathodic transfer coefficients at equilibrium correspond exactly to the fractional charge between the reactant and product at equilibrium, but deviate from it at higher overpotentials. This deviation is small in the anodic direction, but progressively much greater in the cathodic direction. Similarly, the sum of the anodic and cathodic transfer coefficients at constant rising current density deviates progressively from unity. An experimental anodic α for Fe^{2+} to Fe^{3+} at about 1 decade from equilibrium is 0.425.[90,177] The above results seem to be in good agreement with this, and Tafel behavior within experimental error occurs over about 5 orders of magnitude.

However, this model of kinetic behavior requires further discussion. The usual argument used to claim an experimental "straight" Tafel slope for the case of high overvoltage metals for hydrogen evolution at low coverage has assumed intersection of reactant and product energy curves, for example, those of Despic and Bockris[214] for metal deposition, extended later to the proton transfer case (Ref. 5a, p. 345, c.f., Bockris and Matthews[215]). The latter calculation is not very different from the intersection of Marcus continuum parabolic terms for reactants and products occurring high up one of the "legs" of the reactant parabola to give a rather constant Tafel slope of somewhat less than 2RT/F, c.f., Fischer.[216] However, such an intersection (after subtraction of the electron energy term on an absolute scale between reactants and products) implies that the reaction occurs under FC conditions, cf. Gurney, Ref. 8, and Figure 9A.

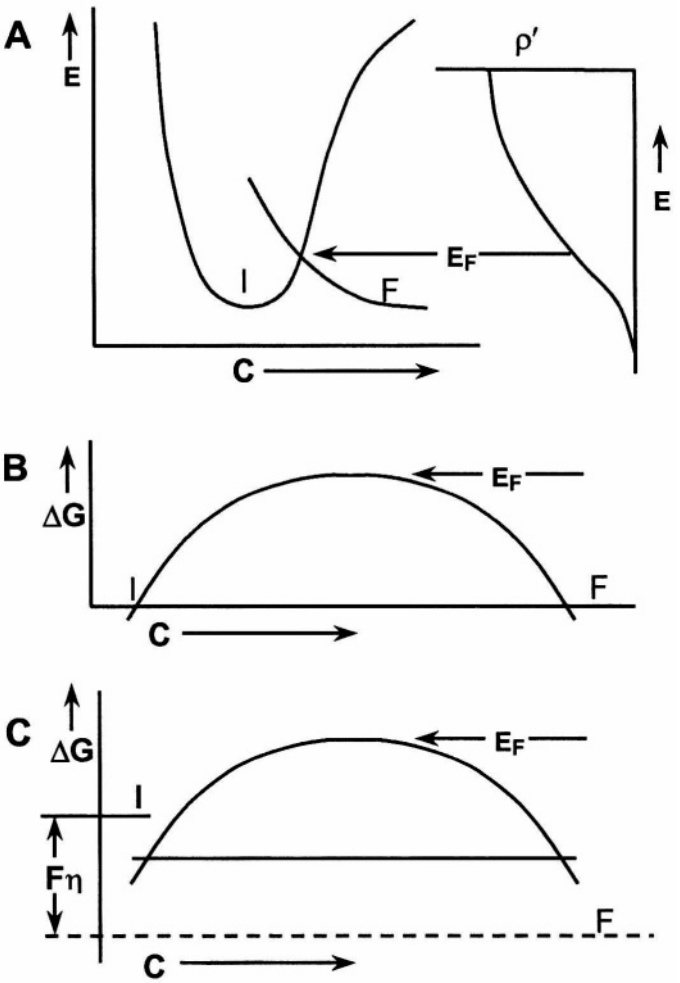

Figure 9. Illustration of how change in Fermi energy (E_F) acts on the energy barrier. E = potential energy; C = Nuclear configuration; ρ' = density of filled metallic states in metal electrode. (A). Gurney's model[8] with initial (I) and final (F) states at the same potential. (B). Non-Franck-Condon transfer in equilibrium. (C). Non-Franck-Condon transfer out of equilibrium.

Differing models for the transfer coefficient and symmetry factor, including a history of the terminology, were instructively reviewed by Bauer in 1968.[217] Parsons (1951),[218] c.f., Plonski (1969),[218] regarded it as equal to the fractional charge on the transition state, whose charge is mid-way between that of the initial and final states in a given step, and whose electrochemical potential is thereby governed by the solution potential. Vetter[219] regarded it (the *Durchtrittsfaktor*) as being the result of a *Durchtrittsreaktion,* in the sense of an unspecified stepping through from one state to another (c.f., Ref. 208, p. 151). Audubert[220] considered it to concern the transfer of kinetic energy to potential energy of an ion to overcome the barrier. However, it has also been associated with the way in which charge (electronic or ionic) is exchanged between the electrode and the solution, considered illustratively in Ref. 221 along with other interpretations, i.e., intersections of energy slopes.[214] Another view made it the work required in transferring charge through the double layer.[222] In some cases, it is the value of a parameter measured along the reaction coordinate, in others it is an energy at right angles to it. In equilibrium, the anodic and cathodic symmetry factors must equal unity, so that the Nernst equation emerges under reversible conditions.[217] However, away from equilibrium, this may not be so.

In a first approximation under non-FC conditions, the Tafel slope may be attributed to the action of the change in the free energy of electrons (i.e., the change in Fermi level of the electrode with respect to the electrostatic energy of the ions in the solution) on the fractional electronic change on the transition state. However, a persuasive case can be made that the experimental Volcano relations and Tafel slopes represent the same phenomenon.

The former must influence the barrier height following the Brønsted rule by acting on the ground state of adsorbates. Thus it would seem that the Tafel slope represents the same effect. The Brønsted rule should probably be examined using the Eyring-Polanyi-Heitler-London model of the potential energy surface (Section VII-3),[197,198] which yields cumbersome expressions in which the roles of the electron and overpotential are not clear. An approximation of the cross-section of the surface by using the BEBO model[68,210] with fitting of parameters to an assumed (experimental) activation energy under equilibrium conditions shows similar results to the model given above, i.e., translation of the barrier maximum towards the products as adsorption energy increases, with a corresponding change in $\beta' = (1 - n^*)^p$, where n^* is the bond order (for the reactants) at the

maximum, and p is close to unity. Again, the sums of the transfer coefficients at the same cathodic and anodic current densities progressively recede from unity as current density increases. A better physical formulation of the system which attempts to explain the experimental linear Tafel slopes is required.

5. Linear Tafel and Brønsted Slopes

In equilibrium, the electrochemical potentials of the reactants and products are equal. When an overpotential is applied, the reaction becomes irreversible. The Gurney FC model of an electrochemical process involving neutralization of an ion under radiationless transfer conditions may be used to illustrate some general observations. Radiationless transfer under non-FC conditions only changes the length of the abcissa, since it allows nuclear movement during the completion time for electron transfer. Integration of the Gurney expression for the rate of, e.g., proton discharge[8] in the anodic and cathodic directions[223] results in two expressions which may be equated at equilibrium. In previous work, this was used to derive an exchange current[223] under these conditions, which contains (as expected from other less precise quasi-thermodynamic considerations[224]) no major electronic parameter of the electrode material (e.g., Fermi level or work function) apart from an (integrated) small preexponential electronic density-of-states term. However, it does show that the condition of radiationless electron transfer does involve the fact that the Fermi level of the electrode has an energy *identical with the barrier maximum.* Thus under equilibrium conditions, the free energy (very close, if not precisely equal to, the potential energy[225]) of the electrons is in equilibrium with the top of the thermal energy barrier, not with the ions in solution. When an overpotential is applied, the reaction becomes irreversible, and part of the free energy corresponding to the overpotential of the half-cell reactions becomes generated enthaply, i.e., $-T\Delta S_{irrev}$. The radiationless transfer condition still of course applies, and the Fermi level in the electrode must still be at the same energy level as the top of the thermal barrier (Figure 9). In effect, application of an overpotential or the driving of the overall reaction in either the anodic or cathodic directions must drive the thermal barrier up or down according to its average charge at the peak. Taking a simple case, neutral species on one side of the barrier will not be affected by the change in potential, whereas singly-charged species on the other side will have their electrochemical potential changed by $\pm eF$. The transition state will have its

electrochemical potential changed by $\pm\beta eF$. This is illustrated in Figure 9, which gives some logic to the potential energy surface sections given without explanation by Gardiner and Lyons,[226] and Glasstone, Eyring, and Laidler.[227]

For redox processes, there is some evidence of Tafel slope curvature for certain processes under certain circumstances.[228,229] These may be a partial result of double layer effects.[196] In other cases experimental Tafel plots which are close to linear appear.[177,230] The controversial question of β possibly varying with temperature[231,232] will not be discussed here, although double layer effects[196] may often be responsible.

Because the observed Volcano relationships in combined ion-electron ECIT processes show similar linearity characteristics to the Tafel slopes, a similar explanation for this behavior appears probable. As discussed in the previous section, the BEBO approximation may be used to estimate the potential energy surface for normal bond-forming and bond-breaking processes. However, the Brønsted slope for these neutral molecule processes is only close to 0.5 when the enthalpy of reaction is zero. It deviates considerably from 0.5 at positive and negative enthalpy values, and at equal positive and negative enthalpy values the Brønsted slopes do not add up to unity. The argument is made above that under conditions of constant potential energy of adsorption of a neutral adsorbed intermediate (e.g., H_{ads}) under equilibrium conditions, the overpotential, i.e., the change in Fermi level of the electrode, only acts on the charge of the transition state, and may not influence it. Similarly, the change in potential energy of adsorption of a neutral reactant on the electrode surface at constant overpotential may also not change the charge on the transition state in a reaction of ECIT type. This is because this charge is governed only by the configuration of the forming or dissolving solvation shell, partly within, and partly without, the Helmholtz double layer. The physical model for this was sketched out by Conway and Bockris for metal deposition processes.[233] This configuration may be determined entirely by effective (in the Duncan-Pople sense) permanent dipole energies along the water molecule configurational vector, together with those resulting from the induced dipole. Setting the derivative of the simple electrostatic expressions for these energies equal to zero under equilibrium conditions determines the barrier maximum and the charge. This rather simple concept provides a consistent picture for ECIT processes involving adsorption.

VIII. CONCLUSIONS

It was at first apparent that one of the major problems in the understanding of the rates of different types of charge-transfer processes (those involving direct electron transfer, ECET, and ion plus electron transfer processes ECIT), was the failure to have a good model for solvation energy, both for the Inner and Outer Sphere. The former had a simple model,[16,92] but the latter had no molecular basis at all, only a conceptual electrostatic charging process[31] whose physics breaks down for electronic charges. Initial work looked at both of these concerns. The first was brought reasonably up to date, and the second was given a molecular basis. In addition, the whole problem of dielectric saturation was examined. After examining a number of alternative charge transfer processes, it appeared that activation energy effects concerning the Outer Sphere may in many cases be discounted, since many adiabatic reactions appear to proceed via non-FC processes in which the Outer Sphere dipoles or superdipoles have enough time to accommodate the changing charge on an ion as a function of time. The problems of the Outer Sphere and the approach to dielectric saturation may therefore be neglected in many cases. While an Outer Sphere explanation to certain charge transfer rate phenomena (particularly those which may be anadiabatic) is not discounted, non-Born-Oppenheimer or non-Franck-Condon phenomena may better fit the facts, as was suggested for proton transfer in earlier reviews.[234] Under adiabatic conditions, the process with the lowest free energy of activation will be the preferred one. If the activation energy contains an Outer Sphere term, it would be expected to change rapidly with ionic strength, reaching about 50% of the infinite dilution value at 1.0 M, and disappearing in very concentrated solutions, e.g., 6.0 M. This may be used as an experimental test.

A relatively constant Tafel slope for reactions not involving adsorption, and those involving adsorption with complete charge transfer across the double layer, distorted by second order effects, may also be explained in terms of a non-Franck-Condon process. Since adsorbed intermediates in charge transfer processes also show adsorption energies depending on potential in the same way as the potential energy barrier maxima, these should also follow the same phenomena.

APPENDIX

1. Applicability of $\varepsilon_A = 1 + 4n_o\alpha_{T,A}$

The inverse square law determines that the electric field inside closed shells of uniform charge distribution is zero. Hence, only the induced charge adjacent to a spherical condenser of radius 'a' with total charge q (equivalent to the charge on the central ion) need be considered as the opposing charge which reduces the field. If this charge is q', then the field $\mathbf{E}_A$ at the surface is $(q - q')/a^2 = \mathbf{A}_A - q'/a^2$. While the total induced polarization vector in any spherical shell with uniform dielectric properties surrounding a fixed molecule or charge necessarily vanishes,[72] the total scalar polarization in a shell of thickness 2s is $2sq' = P_A dV = P_A 4\pi[(a + 2s)^3 - a^3])/3 \approx 8\pi sa^2 P_A = 8\pi sa^2 n_o \alpha_{T,A} E_A$. Hence, $q'/a^2 = 4\pi n_o \alpha_{T,A} E_A$; $E_A = A_A/(1 + 4\pi n_o \alpha_{T,A})$; and $\varepsilon_A = 1 + 4\pi n_o \alpha_{T,A}$. When a approaches 2s, the exact expression for $dV = 4\pi[(a + 2s)^3 - a^3]/3$ should be used, so that ε_A becomes $1 + 4\pi(1 + 2s/a + 4s^2/3a^2) n_o \alpha_{T,A}$. This may be only approximate when the shells contain only small numbers of discrete charges, e.g., in molecular dipoles around an ion.

If we consider a uniform spherical shell of thickness 2s (the width of the volume of space containing a single molecular dipole), in which the moments are oriented by a central charge giving an electric displacement $\mathbf{A}_A$, it is clear from the inverse square law that the effective layers of equal positive and negative charge each produce equal and opposite fields at all points outside the shell. Thus, the only field outside the shell is that of the polarizing change at its center. If we consider an internal or external point located at a distance b (point b) from the center of such a shell of polarization of radius a, then the total moment in a ring of the shell located symmetrically around a line joining the center and point b is equal to $2\pi a \sin\theta \mathbf{P}_A(2s)ad\theta$, where θ is the angle subtended at the center of the sphere by the center and circumference of the ring. The electric field due to the polarization in the ring at point b from the center of the sphere is given by

$$\phi = 2\pi a \sin\theta(\mathbf{P}_A)(2sad\theta)f(\theta)/d^3 \qquad (84)$$

where d is the distance between point b and a point on the circumference of the selected ring, and $f(\theta)$ is a function of the angles between the polarization in the ring and that of an imaginary dipole

lying at point b along the line joining point b and the center of the sphere. $f(\theta)$ is equal to $-(2\cos\theta - 3\sin\theta\sin\beta\cos\beta - 3\cos\theta\sin^2\beta)$[137] from the system geometry, where β is the angle subtended at the ring by point b and the center of the sphere. Since $\sin\beta = (b/d)\sin\theta$ and $\cos\beta = (r - b\cos\theta)/d$, $f(\theta)$ is $-(2\cos\theta - 3ab\sin^2\theta/d^2)$, where $d^2 = a^2 + b^2 - 2ab\cos\theta$. Hence:

$$\phi = -2p\mathbf{P}_A(2s)a^2\int_0^{2\pi}\left(\frac{2\cos\theta\sin\theta}{d^3} - \frac{3ab\sin^3\theta}{d^5}\right)d\theta \qquad (85)$$

The field is zero for the special case where b = 0 and a = r. The general result is:

$$\phi = \left(\frac{\pi\mathbf{P}_A s}{b^2}\right)\left[d - \frac{2(a^2+b^2)}{d} + \frac{(a^2-b^2)}{d^3}\right]_{d=a-b}^{d=a+b} \qquad (86)$$

which is zero for all values of b except when b = a, when the lower limit is d = 0 and the expression is infinite, i.e., closed inner and outer shells of polarization do not contribute to the polarization field of the selected shell for which b = a. To determine the polarization field at the dipole center of a selected dipole in this shell, we integrate the value of d from a lower limit equal to the distance between the center of the selected dipole and the start of the next shell, i.e., the distance s. Thus the field due to the shell at b = r without the field of the selected dipole is:

$$\phi = \mathbf{E}_{p,A} = -(p\mathbf{P}_A s/a^2)[(4a^2/s) - s] \approx -4\pi\mathbf{P}_A \qquad (87)$$

Thus, the polarization field at the selected dipole is $\mathbf{E}_{p,A} = -4\pi\mathbf{P}_A$, and the external field $\mathbf{E}_A$ at the dipole is $\mathbf{A}_A - 4\pi\mathbf{P}_A$. However, $\mathbf{P}_A = \alpha_{T,A}n_o\mathbf{E}_A$, so $\mathbf{E}_A = \mathbf{A}_A/(1 + 4\pi n_o\alpha_{T,A})$, and ε_A equals $(1 + 4\pi n_o\alpha_{T,A})$ in radial geometry, provided that the number of dipoles in the shell considered is enough to make an integration (instead of a summation) sufficiently accurate. The same should be true for the polarization field at a selected solvated ion of e.g., diameter 2d, which may be several times 2s, but for which the shell thickness is 2d rather than 2s.

Equation (86) shows that $4a^2/s$ must be large compared with s, but this will be true even for the first shell of continuum dipoles. However, the treatment no longer applies at short distances, when $\mathbf{A}_A$ overwhelms

$4\pi\mathbf{P}_A$. The dipole field equation used in the derivation is reasonably accurate at distances of a few Å. The use of $2\pi a^2(2s)\sin\theta d\theta$ for the volume of each ring instead of $(2/3)\pi[(r+s)^3-(r-s)^3](\cos\theta_1-\cos\theta_2)$ will understate the volume, but the largest error occurs because of the non-continuous nature of the polarization distribution in the shell. The polarization in a shell of dipoles of radius a (measured to the dipole centers) was accurately estimated numerically for $s = a\sin(\pi/10)$, i.e., with a hydrogen-bond distance of 2.9 Å, a = 4.62 Å. This distance represents an approximate lower limit for the first continuum shell for univalent ions. The result obtained for the value of $\mathbf{E}_{p,A}$ was $-3.16\pi\mathbf{P}_A$, 79% of the value for $a = \infty$. As expected, small residual fields were found outside and inside the shell. The summation improves as 'a' increases to higher values. The effect of this summation of polarization fields will be significant at short distances, and it means that Eq. (87) will therefore overstate the value of ε_A, and understate the values of $\mathbf{E}_A$ and the interaction energy between the central ion and the surrounding continuum dipoles.

2. An Appropriate Model for Water Molecule Orientation

An introduction to the problem of inner sphere orientation is given in Section IV-4. Solvated monovalent negative ions apparently have more negative solvation energies than positive ones when both have the same ion-water distance.[95,98,170,172] This has been explained by dipole[98] and simple quadrupole models.[95] Consider an ST2 potential quadrupole[142] often used in molecular dynamic calculations[142,144,145,157] with charges +2e', –2e' with polar coordinates y, θ, and z, γ respectively from the molecule center and a line along the dipole axis joining it and an ion (charge e) at distance 'a'. Assuming a "hard wall" interaction, the potential interactions between the quadrupole and the ions in the dipole axial position are:

$$\phi = -2ee'\{[(a-y\cos\theta)^2+y^2\sin^2\theta]^{-1/2}-[(a-z\cos\gamma)^2+z^2\sin^2\gamma]^{-1/2} \quad (-\text{ ions}) \quad (88)$$

$$\phi = -2ee'\{[(a+z\cos\gamma)^2+z^2\sin^2\gamma]^{-1/2}-[(a+y\cos\theta)^2+y^2\sin^2\theta]^{-1/2} \quad (+\text{ ions}) \quad (89)$$

Expanding to the third binomial term and ignoring all terms higher than a^2 gives:

$$\phi = -\left(\frac{2ee'}{a^2}\right)\left[y\cos\theta - z\cos\gamma) \pm \frac{3(y^2\cos^2\theta - z^2\cos^2\gamma)}{2a}\mu\frac{(y^2 - z^2)}{2a}\right] \quad (90)$$

for negative (+,–) and positive (–,+) ions. At constant distance, differences must be in these terms, since induced dipoles, Outer Sphere interactions, and repulsive terms should cancel.[170] Thus:

$$\phi^- - \phi^+ = -(2ee'/a^3)[y^2(3\cos^2\theta - 1) - z^2(3\cos^2\gamma - 1)] \quad (91)$$

A convenient monovalent ion-water center distance in Halliwell and Nyburg's correlations[170,172] is 2.924 Å i.e, $(a + 1.38)^{-3} = 0.04$ Å^{-3}, when the solvation energy difference between negative and positive ions is –41.8 kJ/mole, i.e., 16.86kT/c per water molecule at 298 K, where c is the coordination number. The modified[95] Rowlinson quadrupole[141] has a partial charge e' = +0.33e on each proton with –2 x 0.33e on the oxygen (vacuum moment 1.86 D, bond length and angle 0.964 Å and 105°). With the origin at the molecule center (0.15 Å from oxygen), y = 0.880 Å, $\cos\theta = 0.4956$, z = 0.15 Å and $\cos\gamma = -1$, positive ions (–27.18kT) in the axial position[16,92,95] have enthalpies of solvation 3.67kT *more negative* than axial[95] negative ions (–23.51kT) at a = 2.924 Å. A more accurate point charge analysis gives –4.20kT difference (–26.03kT and –21.83kT for positive and negative ions). The only way to obtain a more negative solvation energy for negative ions compared with positive ions aligned along the dipole axis is by changing the off-axis charge. If θ is less than 53.57° at the same y value, the result is reversed, but this is unrealistic.

If we now consider the Verwey positions,[161] if the negative charges are considered to be on the oxygen,[95] a point charge calculation shows that for negative ions, the maximum interaction at 2.924 Å is –23.38kT with the ion-oxygen axis ±21.8° above and below the O–H bond direction, compared with –20.77kT when it is exactly aligned in the Verwey position (and –21.83kT on the dipole axis, above). For negative ions, the Verwey positions are stable, i.e, do indeed lie at marginal minima, but for positive ions, the only stable position is on the dipole axis at –26.03kT, and the Verwey positions (at 60.1° to the dipole axis) are unstable, and are significantly less negative. Considering the similar situation with the negative charges at the molecule center, for negative ions, the minima lie at –25.12kT and at

±14.2° above and below the O–H bond direction, with –21.03RT along the dipole axis. Again, for positive ions, the only stable position is the axial one, at –25.79kT.

Thus, using these simple quadrupole approaches, we may be led to believe that the electrostatic stabilization energy for positive ions will be more negative than that for negative ions due to the effects of the off-axis charges. A pre-quadrupole approach, ignoring off-axis charge,[98] gives –23.06kT and –28.05kT for positive and negative ions at a = 2.924 Å, i.e., the difference of –4.99ckT is approximately correct if c = 4. The real charges are indeed off-axis, and the DP multipole[143] should be a much more realistic molecular model. In it, the protons (+e, +e) are at +0.586 Å from the oxygen atom center (+6e) along the dipole axis, offset at ±0.764 Å (bond angle 105°). The lone pairs (–2e each) on the oxygen are located at right angles to and at ±0.275 Å above and below the proton-oxygen plane, at –0.158 Å along the dipole axis. The bond electrons (–2e each) may be located along the proton-oxygen bonds at +0.334 Å from the oxygen atom center along the dipole axis, offset at ±0.443 Å gives a dipole moment of 2.138 D (See Section V-1) to account for induction. The 8+, 8 charge separation means that the DP dipole length is very short (0.0557 Å for 2.138 D) compared with the 0.586 Å Rowlinson length, and its dipole center is at +0.1187 Å (at 2.138 D) from the oxygen compared with the Rowlinson value of +0.243. Thus, the dipole center for each lies on different sides of the water molecule center at +0.15 Å.

Appropriate coulombic potentials were used to obtain ion-DP multipole interactions at a = 2.924 Å. Instead of the "hard wall" model used above, a repulsive $+A/(a + q)^{12}$ interaction was assumed, where q is the ion-oxygen distance. The complete expression was differentiated to obtain the minimum potential at a = 2.924 Å. First the ions were assumed to lie along the dipole axis, giving a net interaction of –23.11kT for positive ions, and –19.99kT for negative ions, where the repulsive potentials were 16% and 17% of the total coulombic interaction respectively. Thus, the gross coulombic interactions for the DP model were –0.8kT (3.1%) and –1.6kT (7.3%) greater in this configuration than those for the corresponding point-charge Rowlinson model, which assumed a smaller dipole moment (1.86 D). Thus, in both point-charge calculations, positive ions situated at the same distance from the water molecules show greater interaction than negative ions. However, if the Rowlinson and DP models are regarded as simple dipoles, the first yields a greater interaction for negative ions, whereas the opposite is true for the second, due to the differing position

of the dipole centers with regard to the molecule center. The Rowlinson dipole model gives an approximately correct answer, but it is too artificial to be useful.

Point-charge interactions for the ion-DP multipole were then examined as a function of a, and as a function of the angle of the molecule. At typical distances, the orientation giving the most negative gross electrostatic potential for negative ions was in line with each of the H–O bonds, i.e., the Verwey[161] position. However, this was not true for positive ions in the O-lone pair direction, unless 'a' is very short. In the Verwey positions at a = 2.924 Å, the net interaction energies were –18.16kT for positive ions, and –23.54kT for negative ions, with inverse 12-power repulsions calculated from the minima equal to 18.6% and 22.8% of the gross coulombic potentials respectively.

Positive ions in the dipole axis position have more negative potentials than those in the Verwey position. The most negative position should be favored, which would result in the Verwey position for negative ions, and the dipole axis position for positive ions. This would result in *similar* potentials for both negative and positive ions at a = 2.924 Å. One of the reasons why the Verwey position is preferred is the greater opportunity for retained hydrogen bonding, whether complete or "bent".[103] The hydrogen bond is about –10kT (–5.95 kcal/mole, 24.9 kJ/mole[103]). It is usually assumed[95] that two half hydrogen bonds are broken per water molecule of solvation, so that on the dipole axis positive and negative ions under the above conditions will have effective partial solvation potentials of only about –13.11kT and –9.99kT, before induction effects are taken into account. In the Verwey positions, one half-bond is broken, giving –13.16kT and –18.54kT. With a = 2.924 Å, the DP dipole centers in neighboring Verwey positions of least repulsion at c = 4 (one *cis* and one *trans* pair) are about 4.8 Å apart, which makes the dipole-dipole interaction a reasonable approximation. These orientations give dipole-dipole interactions of +0.88kT per dipole for positive ions compared with +1.52kT when aligned along the dipole axis. The effect of this is likely to be marginal.

REFERENCES

1. J. Franck, *Trans. Faraday Soc.* **21** (1926) 536; Z. *Phys. Chem.* **120** (1926) 144; E. U. Condon, *Phys. Rev.* **28** (1926) 1182; **32** (1928) 858.
2. M. Born and R. Oppenheimer, *Annal. Physik* **84** (1927) 457.
3. A. J. Appleby, J. O'M. Bockris, R. K. Sen, and B. E. Conway, in *MTP Int. Rev. Sci., Phys. Chem. Ser. 1,* Ed. by A. D. Buckingham and J. O'M. Bockris, Butterworth, London, 1972, Vol. 6, p. 1.
4. (a) J. O'M. Bockris and R. K. Sen, *J. Res. Inst. Catalysis, Hokkaido Univ.* **21** (1973) 55; (b). *Molec. Phys.* **29** (1975) 357.
5. (a) J. O'M. Bockris and S. U. M. Khan, *Quantum Electrochemistry,* Plenum, New York, 1979; (b). S. U. M. Khan and J. O'M. Bockris, in *Comprehensive Treatise of Electrochemistry,* Ed. by B. E. Conway, J. O'M. Bockris , E. Yeager, S. U. M. Khan, and R. E. White, Plenum, New York, 1983, Vol 7, p. 41; (c). J. O'M. Bockris and S. U. M. Khan, *Surface Electrochemistry, A Molecular Level Approach,* Plenum, New York, 1993.
6. R. A. Marcus, *Naval Res. Rev.* **45-46** (1993-94) 9.
7. J. Franck and F. Haber, *S. B. Preuss. Akad. Wiss.* **56** (1931-32) 869.
8. R. W. Gurney, *Proc. Roy. Soc. London* **A134** (1931) 137.
9. L. Landau, *Phys. Z. Sowietunion* **1** (1932) 88; **2** (1932) 46.
10. F. Hund, *Z. Physik.* **32** (1925) 1.
11. W. A. Caspari, *Z. Phys. Chem.* **30** (1899) 89.
12. J. Tafel, *Z. Phys. Chem.* **50** (1905) 641.
13. J. A. V. Butler, *Trans. Faraday Soc.,* **19** (1924) 729.
14. T. Erdy-Grúsz and M. Volmer, *Z. Phys. Chem.* **150** (1930) 203.
15. F. P. Bowden, *Proc. Roy. Soc. London* **A125** (1929) 446; **A126** (1929) 107.
16. J. D. Bernal and R. H. Fowler, *J. Chem. Phys.* **1** (1933) 515.
17. (a). J. Sherman, *Chem. Rev.* **11** (1932) 98; (b). E. A. Moelwyn-Hughes, *Physical Chemistry,* 2nd Revised Edition, Perganon Press, Oxford, 1965, p. 890.
18. G. Gamow, *Z. Physik.* **51** (1928) 204.
19. R. W. Gurney and E. U. Condon, *Phys. Rev.* **33** (1929) 127.
20. R. W. Gurney, *Trans. Faraday Soc.* **28** (1932) 447.
21. R. W. Gurney, *Proc. Roy. Soc. London* **A136** (1932) 378.
22. H. Eyring and M. Polanyi, *Z. Phys. Chem.* **B12** (1931) 279.

23. H. Eyring, *J. Chem. Phys.* **3** (1935) 107.
24. K. F. Herzfeld, *Ann. Physik.* **59** (1919) 635.
25. J. Horiuti and M. Polanyi, *Acta Physicochem. URSS* **2** (1935) 505.
26. J. A. V. Butler, *Proc. Roy. Soc. London,* **A157** (1936) 423.
27. D. R. Bates and H. S. W. Massey, *Phil. Trans. Roy. Soc. London* **A239** (1943) 269.
28. R. Platzmann and J. Franck, *L. Farkas Memorial Volume,* Research Council of Israel, Jerusalem, 1952, p. 21; *Z. Physik* **138** (1954) 411.
29. J. E. B. Randles, *Trans. Farad. Soc.* **48** (1952) 828.
30. W. F. Libby, *J. Phys. Chem.* **56** (1952) 863.
31. M. Born, *Z. Physik* **1** (1920) 45.
32. J. Weiss, *Proc. Roy. Soc. London* **A222** (1954) 128.
33. P. Debye, *Polar Molecules,* Chemical Catalog Company, New York, 1929.
34. L. Landau, Phys. *Z. Sowietunion* **3** (1933) 664.
35. N. F. Mott and R. W. Gurney, *Electronic Processes in Ionic Crystals,* Clarendon Press, Oxford, 1940.
36. R. J. Marcus, B. J. Zwolinski, and H. Eyring, *J. Phys. Chem.* **58** (1954) 432; B. J. Zwolinski, R. J. Marcus, and H. Eyring, *Chem. Rev.* **55** (1955) 157.
37. K. J. Laidler, *Can. J. Chem.* **37** (1959) 138.
38. E. Sacher and K. J. Laidler, *Trans. Farad. Soc.* **59** (1963) 396.
39. K. J. Laidler and E. Sacher, in *Modern Aspects of Electrochemistry,* Ed. by J. O'M. Bockris, Butterworth, London, 1964, Vol. 3, p. 1.
40. H. Taube, *Adv. Inorg. Chem. Radiochem.* **1** (1959) 1.
41. R. A. Marcus, *J. Chem. Phys.* **24** (1956) 966.
42. R. A. Marcus, *J. Chem. Phys.* **24** (1956) 979.
43. R. A. Marcus, (a) *J. Chem. Phys.* **38** (1963) 1335; (b) **38** (1963) 1734.
44. R. A. Marcus, *J. Chem. Phys.* **43** (1965) 679.
45. R. A. Marcus, *Rept. 12, Project NR 051-331,* Office of Naval Research, Washington, DC, 1957; *Can. J. Chem.* **37** (1959) 155.
46. R. A. Marcus, *Disc. Farad. Soc.* **29** (1960) 21.
47. R. A. Marcus, *Ann. Rev. Phys. Chem.* **15** (1964) 155.
48. R. A. Marcus, *J. Phys. Chem.* **67** (1963) 853.
49. R. A. Marcus, *J. Chem. Phys.* **41** (1964) 2624.
50. N. S. Hush, *Z. Elektrochem.* **61** (1957) 734; *J. Chem. Phys.* **28** (1958) 962.

51. Ref. 17b, p. 394.
52. C. Zener, *Proc. Roy. Soc. London* **A137** (1932) 696.
53. C. A. Coulson and K. Zalewski, *Proc. Roy. Soc. London* **A268** (1962) 437.
54. H. Gerischer, *Z. Phys. Chem.* **26** (1960) 223.
55. V. G. Levich and R. R. Dogonadze, *Dokl. Akad. Nauk. SSSR* **124** (1959) 123; **133** (1960) 158.
56. R. R. Dogonadze, *Dokl. Akad. Nauk SSSR,* **133** (1960) 1368; **142** (1962) 1108.
57. V. G. Levich, in *Advances in Electrochemistry and Electrochemical Engineering,* Ed. by P. Delahay and C. W. Tobias, Interscience, New York, 1966, Vol. 4, p. 249.
58. V. G. Levich, in *Advanced Treatise of Physical Chemistry,* Ed. by H. Eyring, D. Henderson, and Y. Jost, Academic Press, New York, 1971, Vol. IXB, p. 985.
59. R. R. Dogonadze, in *Reactions of Molecules at Electrodes,* Ed. by N. S. Hush, Wiley, New York, 1972, p. 135.
60. S. I. Pekar, *Untersuchung über die Electronentheorie der Kristalle,* Akademie Verlag, Berlin, 1954.
61. M. Lax, *J. Chem. Phys.* **20** (1952) 1752.
62. H. Fröhlich, *Adv. Phys.* **3** (1954) 325.
63. T. Holstein, *Ann. Phys.* **8** (1959) 325.
64. R. R. Dogonadze and Y. A. Chizmadznev, *Fiz. Tverd. Tela.* **3** (1961) 3712; R. R. Dogonadze, Y. A. Chizmadznev and A. A. Chernenko, *Ibid.,* **3** (1961) 3720.
65. R. R. Dogonadze, A. M. Kuznetsov, and A. A. Chernenko, *Usp. Khimii,* **34** (1965) 1779.
66. N. Sutin, *Ann. Rev. Nuclear Sci.* **12** (1962) 285.
67. N. S. Hush, *Trans. Farad. Soc.* **57** (1961) 557.
68. H. S. Johnston, *Adv. Chem. Phys.* **3** (1961) 131.
69. N. S. Hush, *Electrochim. Acta* **13** (1968) 1005.
70. R. Kubo, *Phys. Rev.* **86** (1952) 929; R. Kubo and Y. Toyozawa, *Prog. Theor. Phys.* **13** (1955) 160.
71. S. U. M. Khan and J. O'M. Bockris, *Chem. Phys. Lett.* **99** (1983) 83.
72. J. G. Kirkwood, *J. Chem. Phys.* **7** (1939) 911.
73. F. Booth, *J. Chem. Phys.* **19** (1951) 391.
74. P. George and J. S. Griffith, in *The Enzymes 1,* Ed. by P. D. Boyer, H. Lardy, and K. Myrback, Academic Press, New York, 1959, p. 347.
75. L. E. Orgel, *Proc. Solvay Conf., Brussels,* 1956, 289.

76. Refs. 5a, p. 161-3; 5c, p. 442-445.
77. Ref. 17b,p. 102.
78. M. Falk and P. A. Giguère, *Can. J. Chem.* **35** (1957) 1195; R. A. More O'Ferrall, G. W. Koeppl, and A. J. Kresge, *J. Am. Chem. Soc.* **93** (1971)1.
79. J. O'M. Bockris, K. L. Mittal, and R. K. Sen, *Nature Phys. Sci.* **234** (1971) 118.
80. A. M. Kuznetsov, *J. Electroanal. Chem.* **159** (1983) 241.
81. R. A. Marcus, *J. Phys. Chem.* **72** (1968) 892; A. O. Cohen and R. A. Marcus, *Ibid.* **72** (1968) 4249.
82. R. R. Dogonadze, A. M. Kuznetzov, and V. G. Levich, *Electrochim. Acta* **13** (1968) 1025.
83. L. I. Krishtalik, *Elecktrokhimiya* **6** (1970) 507.
84. A. M. Kuznetzov, *J. Electroanal. Chem.* **65** (1975) 545.
85. R. R. Dogonadze, J. Ulstrup, and Y. I. Kharkats, *J. Chem. Soc. Faraday Trans. 2,* **68** (1972) 744.
86. Y. I. Kharkats and J. Ulstrup, *J. Electroanal. Chem.* **65** (1975) 555.
87. R. R. Dogonadze and A. M. Kuznetsov, in *Comprehensive Treatise of Electrochemistry,* Ed. by B. E. Conway, J. O'M. Bockris , E. Yeager, S. U. M. Khan, and R. E. White, Plenum, New York, 1983, Vol. 7, p. 1.
88. A. M. Kuznetsov, in *Modern Aspects of Electrochemistry,* Ed. by J. O'M. Bockris, R. E. White, and B. E. Conway, Plenum, New York, Vol. 20, p. 95.
89. E. D. German and A. M. Kuznetsov, in *Modern Aspects of Electrochemistry,* Ed. by R. E. White, B. E. Conway and J. O'M. Bockris, Plenum, New York, Vol. 24, p. 140.
90. M. T. M. Koper and W. Schmickler, in *Electrocatalysis,* Ed. by J. Lipkowski and P. N. Ross, Wiley-VCH, New York, 1998. p. 291.
91. M. T. M. Koper and W. Schmickler, *Chem. Phys.* **211** (1996) 123.
92. D. D. Eley and M. G. Evans, *Trans. Faraday Soc.* **34** (1938) 1093.
93. E. A. Moelwyn-Hughes, *Proc. Camb. Phil. Soc.* **45** (1948) 477.
94. B. S. Brunschwig, C. Creutz, D. H. Macartney, T-K Sham, and N. Sutin, *Farad. Disc. Chem. Soc.* **74** (1982) 113.
95. J. O'M. Bockris and A. K. N. Reddy, *Modern Electrochemistry,* Plenum, New York, 1970, Vol. 1, pp. 88-108, 171-174,
96. A. D. Buckingham, *Disc. Farad. Soc.* **34** (1957) 151.

97. B. E. Conway, in *Modern Aspects of Electrochemistry,* Ed. by B. E. Conway and R. E. White, Kluwer Academic/Plenum Publishers, New York, 2002, Vol. 35, p. 295.
98. Ref. 17b, p. 881-891.
99. B. E. Conway, *Ionic Hydration in Chemistry and Biophysics,* Elsevier, New York, 1981, p. 313.
100. Ref. 99, p. 214-221.
101. L. Onsager, *J. Am. Chem. Soc.* **58** (1936) 1486.
102. Ref. 17b, p. 308.
103. J. A. Pople, *Proc. Roy. Soc. London* **A205** (1951) 134.
104. R. R. Dogonadze and A. A. Kornyshev, *J. Chem. Soc. Faraday Trans. II* **70** (1974) 1121.
105. Ref. 17b, p. 310.
106. (a) Ref. 17b, p. 363-366; (b) Ref. 99, 221-222.
107. P. Debye, *Phys. Z.* **13** (1912) 97.
108. H. Frölich, (a) *Trans. Faraday Soc.* **44** (1948) 238; (b) *Theory of Dielectrics,* Oxford University Press, 1949.
109. G. Oster and J. G. Kirkwood, *J. Chem. Phys.* **11** (1943) 175.
110. F. E. Harris and B. J. Alder, *J. Chem. Phys.* **21** (1953) 1031.
111. G. H. Haggis, J. B. Hasted, and T. J. Buchanan, *J. Chem. Phys.* **20** (1952)1452.
112. J. Malsch, *Physik. Z.* **29** (1928) 770; **30** (1929) 837.
113. Ref. 99, p. 290.
114. J. Van Vleck, *J. Chem. Phys.* **5** (1937) 556.
115. C. Böttcher, *Theory of Electric Polarization,* Elsevier, New York, 1952.
116. A. Schellman, *J. Chem. Phys.* **26** (1957) 1225.
117. D. C. Grahame, *J. Chem. Phys.* **18** (1950) 903.
118. H. Sack, *Phys. Z.* **27**, 206 (1926); **28** (1927) 299.
119. T. J. Webb, *J. Am. Chem. Soc.* **48** (1926) 2589.
120. B. E. Conway, J. O'M. Bockris and I. A. Ammar, *Trans. Faraday Soc.* **47** (1951) 746.
121. A. D. Buckingham, *J. Chem. Phys.* **25** (1956) 428.
122. D. M. Ritson and J. B. Hasted, *J. Chem. Phys.* **16** (1948) 11.
123. C. A. Coulson and D. Eisenberg, *Proc. Roy. Soc. London* **A291** (1966) 445, 454.
124. F. Booth, *J. Chem. Phys.* **19** (1951) 1327, 1615.
125. F. Booth, *J. Chem. Phys.* **23** (1955) 453.
126. Ref. 17b, p. 696.
127. Ref. 17b, p. 577.

128. A. D. Buckingham and J. A. Pople, *Proc. Phys. Soc.* **A68** (1955) 905; A, D. Buckingham, *Ibid.* **A68** (1955) 910.
129. P. Debye, *Marx Handbuch der Radiologie (Leipzig)* **6** (1925) 777.
130. D. C. Grahame, *J. Chem. Phys.* **21** (1953) 1054.
131. K. J. Laidler and C. Pegis, *Proc. Roy. Soc.* **A241** (1957) 80.
132. J. A. Schellman, *J. Chem. Phys.* **24** (1956) 912.
133. J. A. Stratton, *Electromagnetic Theory,* § 2.8, McGraw-Hill, New York, 1941.
134. H. S. Frank and P. T. Thompson, in *The Structure of Electrolytic Solutions,* Ed. by W. Hamer, Wiley, New York, 1960.
135. M. Mandel and P. Mazur, *Physica* **24** (1958) 116.
136. W. F. Brown, *Encyclopedia of Physics,* Springer-Verlag, Berlin, 1956, Vol. 17, p. 1; *Physica* **24** (1958) 695.
137. Ref. 17b, pp. 316,338.
138. J. Morgan and B. E. Warren, *J. Chem. Phys.* **6** (1938) 666.
139. Ref. 17b, p. 306.
140. C. W. Kern and M. Karplus, in *Water, a Comprehensive Treatise,* Ed. by F. Franks, Plenum, NY, 1972, Vol. 1, Chap. 2.
141. J. S. Rowlinson,*Trans.Faraday Soc.* **47** (1951) 120.
142. H. L. Lemberg and F. H. Stillinger, *J. Chem. Phys.* **62** (1975) 1667.
143. (a). A. B. F. Duncan and J. A. Pople, *Trans. Faraday Soc.* **49** (1953) 217; (b). Ref. 17b, p. 479.
144. F. H. Stillinger and A. Rahman, *J. Chem. Phys.* **60** (1974) 1545.
145. A. Raman, F. H. Stilinger, and H. L. Lemberg, *J. Chem. Phys.* **63** (1975) 5223.
146. B. E. Conway and J. O'M. Bockris, *Electrochim. Acta* **3** (1961) 340.
147. Ref. 99, p. 584.
148. J. E. Desnoyers, R. E. Verrall, and B. E. Conway, *J. Chem. Phys.* **43** (1965) 243.
149. L. Pauling, *Phys. Rev.* **36** (1930) 430.
150. H. H. Nielsen, *Phys. Rev.* **40** (1932) 445.
151. Ref. 17b, p. 85-86.
152. J. O'M. Bockris and P. P. S. Saluja, *J. Phys. Chem.* **76** (1972) 2298.
153. L. E. Orgel, *J. Chem. Soc.* (1952) 4756.
154. J. O'M. Bockris and P. P. S. Saluja, *J. Phys. Chem.* **76** (1972) 2140.

155. J. O'M. Bockris and P. P. S. Saluja, *J. Electrochem. Soc.* **119** (1972) 1060.
156. Ref. 99, pp. 88-116.
157. F. H. Stilinger and A. Raman, *J. Chem. Phys.* **61** (1974) 4973; R. W. Impey, M. L. Klein, and I. R. McDonald, *J. Chem. Phys.* **74** (1981)647.
158. (a) P. Bopp, G. Jancsó, and K. Heinzinger, *Chem. Phys. Lett.* **98** (1983) 129; (b) G. Pálinkás, P. Bopp, G. Janscó, and K. Heinzinger, *Z. Naturforsch.* **39a** (1984) 179; (c) G. Heinje, W. A. P. Luck, and K. Heinzinger, *J. Phys. Chem.* **91** (1987) 331; (d) E. Spohr, G. Pálinkás, K. Heinzinger, P. Bopp, and M. M. Probst, *J. Phys. Chem.* **92** (1988) 6754.
159. Ref. 99, p. 5.
160. Ref. 17b, p. 555.
161. E. J. W. Verwey, (a) *Rec. Trav. Chim. Pays Bas* **61** (1942) 127; (b) *Rec. Trav. Chim. Pays Bas* **60** (1941) 887.
162. P. Delahay, *Chem. Phys. Letters* **87** (1982) 607; **99** (1983) 87.
163. L. Pauling, *J. Am. Chem. Soc.* **49** (1927) 765.
164. S. R. Milner, *Phil. Mag.* **23** (1912) 551; **25** (1913) 742.
165. A. J. Appleby, to be published.
166. J. C. Ghosh, *J. Chem.Soc.* **113** (1918) 449, 707.
167. Ref. 95, pp. 267-272.
168. R. A. Robinson and R. H. Stokes, *Electrolyte Solutions,* 2nd Revised Edition, Butterworth, London, 1970.
169. N. Sutin, *Farad. Disc. Chem. Soc.* **74** (1982) 113.
170. B. E. Conway, in *Modern Aspects of Electrochemistry,* Ed. by J. O'M. Bockris and B. E. Conway, Butterworth, London, 1964, Vol. 3, p. 63-64.
171. B. E. Conway, J. O'M. Bockris, and H. Linton, *J. Chem. Phys.* **24** (1956) 834.
172. H. F. Halliwell and S. C. Nyburg, *Trans. Farad. Soc.* **59** (1963) 1126.
173. Ref. 17b, p. 337.
174. S. H. Lih, in *Physical Chemistry, An Advanced Treatise,* Ed. by H. Eyring, D. Henderson, and Y. Jost, Academic Press, New York, 1970, Vol. X, p. 439.
175. H.-P. Cheng, R. N. Barnett, and U. Landman, *Chem. Phys. Lett.* **237** (1995) 161.
176. N. S. Hush, *J. Electronal. Chem.* **460** (1999) 5.
177. L. A. Curtiss, J. W. Halley, N. C. Hung, Z. Nagy, Y. J. Rhee, and R. M. Yonco, *J. Electrochem. Soc.* **138** (1991) 2033.

178. W. Schmickler, *J. Electroanal. Chem.* **100** (1978) 277; **204** (1986) 31; *Chem. Phys. Lett.* **237** (1995) 152; *Electrochim. Acta* **41**(1996)2329.
179. S. U. M. Khan, in *Modern Aspects of Electrochemistry,* Ed. by R. E. White, B. E. Conway and J. O'M. Bockris, Plenum, New York, 1993, Vol. 31, p. 71.
180. P. W. Anderson, *Phys. Rev.* **124** (1961) 41.
181. D. M. Newns, *Phys. Rev.* **178** (1969) 1123; J. P. Muscat and D. M. Newns, *Prog. Surf. Sci.* **9** (1978) 1.
182. H. A. Kramers, *Physica* **40** (1940) 284.
183. A. J. Appleby, in B. E. Conway, *Comprehensive Treatise of Electrochemistry,* Ed. by J. O'M. Bockris, E. Yeager, S. U. M. Khan, and R. E. White, Plenum, New York, 1983. Vol. 7, p. 173.
184. W. R. Fawcett and C. A. Foss, *J. Electroanal. Chem.* **250** (1988) 225.
185. W. R. Fawcett, *Langmuir* **5** (1989) 661.
186. N. M. Marković and P. N. Ross, in *Interfacial Electrochemistry, Theory, Experiment and Applications,* Ed. by A. Wieckowski, Marcel Dekker, New York, 1999, p. 821; *Surf. Sci. Repts.* **45** (2002)117.
187. J. O'M. Bockris, R. K. Sen, and B. E. Conway, *Nature Phys. Sci.* **240** (1972) 143.
188. B. E. Conway, *Faraday Disc. Chem. Soc.* **74** (1982) 267.
189. Ref. 17b, p. 667-685.
190. *Handbook of Chemistry and Physics,* 70th Edition., Ed. by R. C. Weast, CRC Press Inc., Boca Raton, FL, 1989, p. D41.
191. Ref. 170, p. 59 (footnote).
192. W. M. Latimer, K. S. Pitzer, and W. V. Smith, *J. A. C. S.* **60** (1938) 1829.
193. Ref. 17b, p. 1240 et sequ.
194. C. N. Hinshelwood, *Proc. Roy. Soc. (London),* **A113** (1927) 320; G. N. Lewis and D. F. Smith, *J. A. C. S.* **47** (1925) 1508; R. H. Fowler and E. K. Rideal, *Proc. Roy. Soc. (London),* **A113** (1927) 570.
195. K. J. Laidler, *Theories of Chemical Reaction Rates,* McGraw-Hill, New York, 1969, pp. 106-129.
196. R. Parsons, in *Advances in Electrochemistry and Electrochemical Engineering,* Ed. by P. Delahay and C. W. Tobias, Interscience, New York, 1961, Vol. 1, p. 1; W. R. Fawcett, in *Electrocatalysis,* Ed. by J. Lipkowski and P. N. Ross,

Wiley-VCH, New York, 1998 p. 323; W. R. Fawcett, *J. Phys. Chem.* **93** (1989) 2675.
197. J. O'M. Bockris and S. Srinivasan, *J. Electrochem, Soc.* **111** (1964) 844, 853, 858.
198. S. Glasstone, K. J. Laidler, and H. Eyring, *The Theory of Rate Processes,* McGraw-Hill, New York, 1941.
199. Ref. 17b, p. 1177.
200. Ref. 170, p. 119.
201. R. P. Auty and R. H. Cole, *J. Chem. Phys.* **20** (1952) 1309; B. E. Conway, *Can. J. Chem.* **37** (1959) 613; M. Eigen, L. de Mayer, and H. C. Spatz, *Berichte Bunsengesell* **68** (1964) 19.
202. B. E. Conway and J. O'M. Bockris, in *Modern Aspects of Electrochemistry,* J. O'M. Bockris and B. E. Conway, Butterworth, London, 1954, Vol. 1, p. 47.
203. Ref. 170, p. 66 (footnote).
204. B. E. Conway, in *Interfacial Electrochemistry, Theory, Experiment and Applications,* Ed. by A. Wieckowski, Marcel Dekker, New York, 1999, p. 131.
205. J. Barber, S. Morin, and B. E. Conway, *J. Electroanal. Chem.* **446** (1998) 125.
206. L. I. Krishtalik, *Electrochim. Acta* **13** (1968) 1045.
207. B. Kabanow, *Acta Physicochim. U. R. S. S.,* **5** (1936) 193.
208. H. A. Leibhavsky and E. J. Cairns, *Fuel Cells and Fuel Batteries,* Wiley, New York, 1968, p. 138,
209. J. O'M. Bockris and A. M. Azzam, *Trans. Faraday Soc.* **48** (1952) 145.
210. Ref. 3, p. 21; Ref. 5a, p. 228.
211. F. P. Bowden and K. W. Grew, *Discuss. Faraday Soc.* **2** (1947) 81,91.
212. H. Nürnberg, *Studien mit Modernen Technik zur Kinetik Schneller Chemischer und Elektrochemischer Schritte von Protonen Transferprozessen,* Bonn, 1969, quoted by Levich, Ref. 58.
213. S. Trassatti. *J. Electroanal. Chem.* **39** (1977) 183.
214. A. R. Despic and J. O'M. Bockris, *J. Chem. Phys.* **32** (1960) 389.
215. J. O'M. Bockris and D. B. Matthews, *J. Chem. Phys.* **44** (1966) 298.
216. S. Fischer, quoted in P. P. Schmidt and J. Ulstrup, *Nature Phys. Sci.* **245** (1972)126.
217. H. Bauer, *J. Electroanal Chem.* **16** (1968) 419.

218. R. Parsons, *Trans. Faraday Soc.* **47** (1951) 1332; I. H. Plonski, *Rev. Roumaine de Chimie* **14** (1969) 569.
219. K. J. Vetter, Z. *Naturforsch.* **7a** (1952) 328; *Z. Elektrochem.* **59** (1955) 596; *Elekrochemischer Kinetik,* Springer-Verlag, Berlin, 1961, p. 101.
220. R. Audubert and S. Cornevin, *J. Chim. Phys.* **38** (1941) 46.
221. J. O'M. Bockris and Z. Nagy, *J. Chem. Education* **50**(1973)839.
222. V. Harff, *C. R. Acad. Sci. Paris Ser. C* **268** (1969) 1657; **269** (1969) 1352; **270** (1970) 1695.
223. A. J. Appleby, in *Modern Aspects of Electrochemistry,* Ed. by J. O'M. Bockris and B. E. Conway, Plenum, New York, 1974. Vol. 9, p. 369.
224. R. Parsons, *Surface Science* **2** (1964) 418; A. N. Frumkin, *Elektrokhimya* **1** (1965) 394.
225. Ref. 17b, p. 652.
226. H. J. Gardiner and L. E. Lyons, *Rev. Pure Appl. Chem.* **3** (1953) 134.
227. H. Eyring, S. Glasstone, and K. J. Laidler, *J. Chem. Phys.* **7** (1939) 1053.
228. R. Parsons and E. Passeron, *J. Electroanal. Chem.* **12** (1966) 524.
229. V. Marecek, Z. Samec, and J. Weber, *J. Electroanal. Chem.* **94** (1978) 169.
230. J. E. B. Randles, *Can. J. Chem.* **37** (1959) 238.
231. B. E. Conway, B. MacKinnon, and B. V. Tilak, *Trans. Faraday Soc.* **66** (1970) 1203; B. E. Conway, in *Modern Aspect of Electrochemistrey,* Ed. by B. E. Conway, J. O'M. Bockris, and R. E. White, Plenum, New York, 1986, Vol. 16, p. 103.
232. J. O'M. Bockris and A. Gochev, *J. Electroanal. Chem.* **214** (1986) 655.
233. B. E. Conway and J. O'M. Bockris, *Electrochim. Acta* **3** (1961) 140.
234. A. J. Appleby, *J. Electroanal. Chem.* **51** (1974) 1; **357** (1993) 117.